

Hydrocarbon staple constructing highly efficient α -helix cell-penetrating peptides for intracellular cargos delivery

Shu Li^{ab}, Xingjiao Zhang^b, Chen Guo^b, Yali Peng^b, Xiaojing Liu^b, Bo Wang^b, Ran Zhuang^b, Min Chang^{*b}, Rui Wang^{*a}

^aKey Laboratory of Preclinical Study for New Drugs of Gansu Province, School of Basic Medical Sciences, Lanzhou University, Lanzhou 730000, China

^bInstitute of Biochemistry and Molecular Biology, School of Life Sciences, Lanzhou University, Lanzhou 730000, China

***Corresponding author:**

Rui Wang

E-mail addresses: wangrui@lzu.edu.cn

Min Chang

E-mail addresses: changmin@lzu.edu.cn

Electronic Supplementary Information (ESI)

Table of contents

I. Experimental procedure

Stapled Peptide Synthesis and Characterization

Molecular Modeling

Circular Dichroism (CD) Spectroscopy.

LogD_{7.4} Value of the Peptide Measurement.

Cell Culture.

Flow cytometry.

Confocal Microscopy.

Cell viability.

Hemolysis Assay

Resistance to serum

Investigation of Cellular Endocytosis Mechanism

Isothermal Titration Calorimetry and Dynamic Light Scattering.

Quantitation of Endosomal Escape.

Delivery of cargoes into living cells.

II. Supporting Table:

Table S1. Mass spectrometry data for the FITC labeled peptides.

Table S2. Mass spectrometry data for the peptides.

Table S3. LogD_{7.4} for peptides.

Table S4. Results of ITC Binding Studies between HS and Stapled CPPs and Size of HS clusters.

III. Supporting Figure:

Fig. S1 CD spectra of stapled peptides in water.

Fig. S2 Molecular three-dimensional models of stapled CPPs structures.

Fig. S3 Live-cell confocal microscopy images of FITC labeled A1, A2, A3, A4, A5, A6, A12 and A14 uptake by Hela cells.

Fig. S4 Cellular uptake of FITC-labeled A1-A14 in MCF-7 cells.

Fig. S5 Flow cytometry and Cytotoxicity.

Fig. S6 Cellular uptake of FITC-labeled Tat₄₈₋₆₀, SAH-Tat-1, SAH-Tat-2, A1, A4 and A6

Fig. S7 Live-cell confocal microscopy images of Tat₄₈₋₆₀, SAH-Tat-2 and A4 uptake

Fig. S8 Plots of total fluorescence intensity versus retention times and Log D_{7.4} value of peptides measured versus cell permeability

Fig. S9 Comparison of the serum stabilities of A1, A4, A6, A4u, A6u, and A11.

Fig. S10 Cellular uptake of A1, A4 and A6 in the presence of Trypan blue or Trypan blue and Triton-X100.

Fig. S11 Effect of Heparinase III and heparin treatment on uptake of A1 and A4.

Fig. S12 Cellular uptake of Rho-labeled CPPs or NF-labeled CPPs in Hela cells.

Fig. S13 Investigation of cellular endocytosis mechanism.

Fig. S14 LDH assay, Cytotoxicity and Hemolysis.

Fig. S15 Live-cell confocal microscopy images of FITC labeled AGpTALF (B1), B2, B3 and B4 uptake by Hela cells.

Fig. S16 Co-localization of B2, B3 or B4 and lysosome in Hela cells

Fig. S17 Cellular uptake of fluorescence-labeled AGpTALF(B1), fluorescence-labeled B2, B3 and B4 and co-localization with lysosome in MCF-7 cells.

Fig. S18 Live-cell confocal microscopy images of fluorescently labeled C1, C2 and C3 uptake by Hek293 cells.

Fig. S19 Live-cell confocal microscopy images of avidin, D1-avidin conjugate, D2-avidin conjugate and D3-avidin conjugate uptake by Hela cells.

Fig. S20 Co-localization of FITC-labelled D1-avidin conjugates, D2-avidin conjugates or D3-avidin conjugates and lysosome in Hela cells

Fig. S21 Cellular uptake of avidin, D1-avidin conjugate, D2-avidin conjugate and D3-avidin conjugate and co-localization with lysosome in MCF-7 cells.

IV. HPLC Traces and MS Spectra

EXPERIMENTAL SECTION

Stapled Peptide Synthesis and Characterization. Peptides synthesis was performed by using Fmoc solid-phase peptide synthesis (SPPS) method on Rink Amide MBHA resin (loading capacity: 0.55 mmol/g). Rink Amide MBHA resin was purchased from Tianjin Nankai and Technology Co (Tianjin, China). Fmoc-protected amino acids were purchased from GL Biochem Ltd (Shanghai, China). Rink Amide MBHA resin commonly was pre-swelled with dichloromethane (DCM) for 0.5 h. DCM has been replaced with N,N-dimethylformamide (DMF) for 3 min. 20 % piperidine in DMF was prepared to remove Fmoc for 10 min \times 2. Then Fmoc-protected amino acids (4 equiv loading of the resin), coupling reagents (HBTU/HOBt, 4 equiv) and N,N-Diisopropylethylamine (DIEA, 8 equiv) was dissolved in DMF and proceed at RT with shaking for 60 min. Hydrocarbon stapled peptides were performed using the previously published protocol^{1, 2}. (R)-2-(7'-octenyl) alanine (R₈, Aldrich) and (S)-2-(4'-pentenyl)-alanine (S₅, Aldrich) were loaded via Fmoc-SPPS method. Ring-closing olefin metathesis was synthesized using Grubbs' first-generation catalyst (0.2 equiv loading of the resin) in 1,2-dichloroethane (DCE) for 4 h, and then Fmoc was removed to introduce fluorescent dyes. In order to label peptides, the resin was incubated with a mixture of fluorescein isothiocyanate, Lissamine rhodamine B sulfonyl chloride or naphthofluorescein succinimidyl ester (3 equiv) and DIEA (6 equiv) dissolved in DMF in dark overnight. Subsequently, the crude peptides were dissolved in water/acetonitrile, which was purified by reversed phase-HPLC (RP-HPLC). The final compounds were further characterized by analytical RP-HPLC and ESI-TOF mass spectrometry.

Molecular Modeling. The folding process: All linear models with standard residues of the peptides (A1 to A6) were constructed in the tleap module of amber 14 software. Then, the standard residues were mutated to the nonstandard residues (S5 and S8) at specific positions for A2, A3, A4 and A6. Geometry and partial charges of S5 and S8 were optimized at an B3LYP 6-31G (d, p) level of theory and assigned partial charges based on the restrained electrostatic potential (RESP) methodology³. The force field parameters for S5 and S8 and other standard residues in the peptides (A1 to A6) were built using the ff99SB force field in antechamber module. The folding process of the peptides (A1 to A6) were performed referring to the protocol of tutorials 5.5 in the Amber project⁴ and produced 10 ns trajectories with 10000 snapshots for each system. The snapshots were clustered by k-mean methods in MMTSB Toolset⁵.

The sampling process: the representative conformations in all the clusters of A1 and A5 were applied to perform the conventional molecular dynamics systems. The complex proteins were neutralized with counterions (Na⁺/Cl⁻) and solvated in a rectangular box of TIP3P water box. The periodic boundary conditions were setup with all the solvents at least 10 Å away from the complex and the solvated systems were parameterized using the ff99SB force field. The molecular dynamics simulations were performed in four steps. Firstly, energy minimization was performed to remove the local atomic collision in the systems. Both the descent steepest method and the conjugated gradient method with 5000 steps were adopted in the energy minimization. Then in the

heat step, each system was gradually heated from 0 K to 300 K in the NVT ensemble with all the solute atoms constrained with a force constant of 2.0 kcal mol⁻¹ Å⁻². After that, each system was equilibrated with the force constant decreasing from 2.0 to 0 kcal mol⁻¹ Å⁻² in 1 ns. Finally, a production run of 50 ns was performed for each replica in the NPT ensemble at 300 K with 1.0 atm pressure. The representative conformations of A22, A3, A4 and A6 were applied to perform the adaptive steered molecular dynamics (ASMD) systems^{6,7}. The complex proteins were neutralized with counterions (Na⁺/Cl⁻) and solvated in a rectangular box of TIP3P water box. The periodic boundary conditions were setup with all the solvents at least 10 Å away from the complex and the solvated systems were parameterized using the ff99SB force field. The molecular dynamics simulations were performed in four steps. Firstly, energy minimization was performed to remove the local atomic collision in the systems. Both the descent steepest method and the conjugated gradient method with 5000 steps were adopted in the energy minimization. Then in the heat step, each system was gradually heated from 0 K to 300 K in the NVT ensemble with all the solute atoms constrained with a force constant of 2.0 kcal mol⁻¹ Å⁻². After that, each system was equilibrated with the force constant decreasing from 2.0 to 0 kcal mol⁻¹ Å⁻² in 1 ns. Finally, the conformational sampling was performed by decreasing the distance of the bonding atoms of the stapled peptides, mimicking the formation of the covalent bond of the stapled peptides. The initial distance between the bonding atoms of the stapled peptides were measured from the last snapshot in the equilibration step and gradually decreased to 1.5 Å with sampling bins of 0.5 Å. The molecular dynamics simulation for each bin was under a force constant of 10.0 kcal mol⁻¹ Å⁻² and produced a trajectory of 1 ns. The snapshots for all the trajectories were saved per 2 ps. The secondary structures of all residues in peptides (from A1 to A6) were further analyzed for each replica (AmberTools15) as shown in Fig. 1 and Fig. S2.

Circular Dichroism (CD) Spectroscopy. Stapled peptides were prepared for concentrations of 40 μM in H₂O. The CD spectroscopy was obtained at room temperature. The spectroscopy was obtained wavelengths from 190 to 260 nm at a 50 nm/s scanning speed (Olis DSM 1000 CD, USA). The α-helical content of peptides was determined by K2D2 tool in the range of 190-240 nm.

LogD_{7.4} Value of the Peptide Measurement. LogD_{7.4} measurement was performed using previously reported procedure⁸. All peptides have been prepared as stock peptide solution (10 mM) in DMSO. The peptide solution is diluted in the aqueous pH 7.4 phosphate buffer in a 1:100 volume ratio. This solution is used as standard solution. From it, different partitions are made with different octanol/water ratios according to approximate logD_{7.4} value of the peptide. Partitions are shaken for 1 hour at room temperature. Both the standard solution (conveniently diluted, r, if necessary) and the aqueous phase of each partition after equilibration are chromatographed for analysis. LogD_{7.4} was performed using equation:

$$\text{LogD}_{7.4} = \text{Log}((A_{st}/A_o - 1) V_w/V_o)$$

Where Ast and Aw are, respectively, the peak areas of the standard and the aqueous

phase of the partition and V_w and V_o the volumes of water and octanol of the partition.

Cell Culture. HeLa cells, MCF-7 cells and Hek 293 cells grown in medium consisting of Dulbecco's modified Eagle's medium (DMEM, Gibco, Carlsbad, CA, USA), 10% fetal bovine serum (Gibco) and 100 U/mL penicillin/ 100 μ g/mL streptomycin at 37 °C in presence of 5% CO₂.

Flow cytometry. HeLa cells, MCF-7 cells or Hek293 cells were seeded for 1×10^5 cells/well in 24-well plates overnight. The medium was substituted with fresh DMEM with 2 μ M fluorescein isothiocyanate (FITC) and 5 μ M rhodamine B (Rho) or naphthofluorescein (NF)-labelled peptides. After incubated at 37 °C for 2 h, PBS was used to wash the cells for 3 times and the samples were collected with 0.25% trypsin for 15 min. The fluorescence intensity was measured using flow cytometry. For the rhodamine-labelled peptides and naphthofluorescein-labelled peptides, fluorescence was measured and analyzed by previously reported procedure⁹. Data was analyzed using the Flowjo software. In addition, to quench extracellular fluorescence, Trypan Blue was utilized and the cellular uptake was performed by a previously reported procedure¹⁰. In short, the cells were incubated with FITC-labeled peptides in the conditions described above. After that, for one group, Trypan Blue (0.05 % w/v) was used to treat the cells for 3 min. For another group, 0.05% (v/v) TritonX100 was prepared to treat the cells before treated with Trypan Blue. Finally, the cellular uptake respectively was carried out using flow cytometry for Each sample and fluorescence was analyzed.

Confocal Microscopy. 1 ml of HeLa cells, MCF-7 cell or Hek293 cells suspension (5×10^4 cells) were seeded in a Fluorodish overnight. DMEM containing 2 μ M FITC, 5 μ M Rho or 5 μ M NF-labeled compounds was added for 2 h. PBS was used to wash the cells for 3 times and DMEM was added. Cells were observed by ZEN 2009 (Carl Zeiss, Oberlochen, Germany). Before imaging, nuclei were marked by Hoechst33342 for 10 min the late endosomes/lysosomes were marked by LysoTracker Red for 30 min. The images were further processed via Photoshop.

Cell viability. The cytocompatibility of stapled peptides were measured using MTT and LDH assays in MCF-7 cells and HeLa cells. Cells were seeded at a density of 4×10^3 cells/well in 96-well plates with increasing concentrations of indicated peptides for 24 h in MTT assay. Then MTT solution (2 mg/ml, 10 μ l) was added to each well and cultured for another 4 h. The MTT solution was substituted with 150 μ l DMSO at 37 °C for 10 min before measured using Microplate reader (MOLECULAR M5). In the LDH assay, HeLa cells or MCF-7 cells were seeded for 15,000 cells /well in 96-well plates at 37 °C for 24 h. After incubation, stapled peptides were added at various concentrations and incubated for 2 h, then, which was carried out using CytoTox-ONE™ Homogeneous Membrane Integrity Assay (Promega) and measured with Microplate reader.

Hemolysis Assay. The hemolytic activity of stapled peptides was determined by using fresh mouse the red blood cells (RBCs, LOT NO. KJ-0044R, purchased from Biological Technology Co., Ltd. Jiangsu, China). RBCs were prepared by centrifuging (800rpm, 10min). A range concentration of A1, A4 or A6 was incubated with RBCs (4.0×10^8 cells/ml) at 37 °C for 2 h. After incubation, the samples were obtained by centrifuging (1000 rpm, 15 min) and were measured at 490 nm.

Resistance to serum. The serum stability test was performed using previously reported procedure¹¹. Briefly, the mouse serum (LOT NO. KJ-S-0031M, purchased from Biological Technology Co., Ltd. Jiangsu, China) was diluted into 25 % serum. Then 25% serum was prepared by centrifuging (15,000 rpm, 15 min). Indicated peptides were treated with 25% serum at 37 °C for a final concentration of 50 μ M. At various time points, 200- μ l of sample were withdrawn and mixed with 50 μ l of 15 % trichloroacetic acid and incubated at 4 °C overnight. Then the final sample was obtained by centrifuging (15,000 rpm, 20 min) and was analyzed by RP-HPLC.

Investigation of Cellular Endocytosis Mechanism. To identify possible internalization mechanism of the stapled peptide, the Hela cells were treated with inhibitors respectively at 37 °C for 1 h, followed by 5 μ M FITC-labeling peptide treating in the presence of inhibitors at 37 °C for another 1 h. The concentration of inhibitors was 10 μ g/ml chlorpromazine (CPZ, a clathrin-mediated pathway inhibitor), 0.5 mM 5-(N-ethyl-N-isopropyl) amiloride (EIPA, a micropinocytosis inhibitor), 2.5 mM methyl- β -cyclodextrin (M- β -CD, lipid raft inhibitor) and heparin 50 units/ml (heparan sulfate proteoglycan inhibitor)¹². For experiments that were conducted at 4 °C, the cells were pre-incubated in serum-free DMEM at 4 °C for 1 hours. The cells were then incubated in serum-free DMEM containing 5 μ M FITC-labeling peptide for 1 hours before flow cytometry analysis. The cellular uptake of 5 μ M FITC-labeling peptide was used as the positive control, which was measured by flow cytometry and set as 100 %.

Isothermal Titration Calorimetry and Dynamic Light Scattering. The binding of the peptides to HS was measured using an ITC200 Microcap at 25 °C by a previously reported procedure¹³. Briefly, HS and peptides were dissolved in HBSS, respectively. After degassed all solutions, the sample cell was filled with the peptide solution (50 μ M) and 39 times 1 μ l of the HS solution (30 μ M) was injected into the sample cell. Data was analyzed with the ITC200 Microcal software. The binding of the peptides to HS led to cluster formation. The size of HS clusters was measured using dynamic light scattering (90Plus PALS, Brookhaven, USA).

Quantitation of Endosomal Escape. The endosomal escape efficiency (γ) was performed by a previously reported procedure⁹. γ of each peptide, relative to Tat, was performed using equation:

$$\gamma = (\text{MFI}_{\text{ID}}^{\text{NF}}/\text{MFI}_{\text{ID}}^{\text{Rho}})/(\text{MFI}_{\text{Tat}}^{\text{NF}}/\text{MFI}_{\text{Tat}}^{\text{Rho}}) \times 100\%.$$

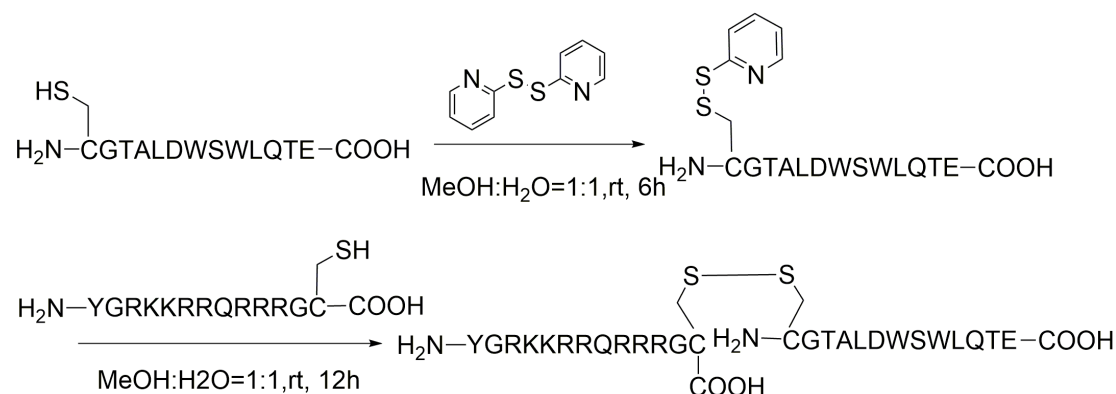
Delivery of cargoes into living cells.

1. Phosphopeptide synthesis and Cellular Uptake.

Phosphopeptide, was covalent connected into the N-terminus of A1, A4 and A6 through aminocaproic acid spacer. Phosphopeptide synthesis was performed by using SPPS method. Then cellular uptake and the intracellular distribution were performed by described above.

2.1. Representative synthetic scheme of C1 and Cellular Uptake.

C1, C2 and C3 were synthesized as showed in follow. A1-Gly-Cys, A4-Gly-Cys, A6-Gly-Cys and Cys-Gly-NBD (NEMO-binding domain NBD, TALDWSWLQTE) were synthesized with SPPS method. To synthesis of C1, C2 and C3, Cys-Gly-NBD reacted with 8equiv of 2,2'-dipyridyldisulfide in MeOH/H₂O (1:1) for 6 h to generate the thiolpyridine peptide. The reaction mixture was purified by RP-HPLC. The purified



Scheme S1. Synthesis procedures of C1.

thiolpyr-Cys-Gly-NBD was reacted with 2equiv of purified A1-Gly-Cys, A4-Gly-Cys, or A6-Gly-Cys in MeOH/H₂O (1:1) for 12 h to generate C1, C2 or C3. The reaction mixture was purified by RP-HPLC. Then cellular uptake and the intracellular distribution were performed by described above.

2.2. NF- κ B Luciferase Assay.

For luciferase assays, NF- κ B reporter (Luc)-Hek293 cells were seeded for 1.5×10^4 cells/well in 96-well plates under 37 °C overnight. The media was substituted with fresh DMEM containing 5 μ l C1-C3. Then the cells were treated for 2 h. 5 μ l of recombinant TNF- α of the final concentration of 5 ng/ml was added to the cells. After an additional 4 h incubation time, the medium was replaced with and 60 μ l passive lysis buffer (Promega) for 15 min. Then luciferase was measured as reported¹⁴.

3. Streptavidin.

The FITC labeled streptavidin (Strep, 1 equiv) was pre-complexed with a biotinylated version of D1, D2 or D3 (1 equiv) at 37 °C for 0.5 h, forming peptide-avidin complex through biotin avidin interactions. The cellular uptake of the FITC labeled peptide-avidin complex was performed by flow cytometer (BD Biosciences, USA). In addition, the complex was added to the dish and analyzed by Live-cell confocal microscopy according to the above protocol. The cellular uptake of the fluorescent D1-avidin conjugates was used as the positive control, which was measured by flow cytometry and set as 100 %.

Supporting Figures

Table S1. Mass spectrometry data for the peptides

NO.	Sequence	Stapled	MS (calcd)	MS (obsd)
A1	FITC-AcpYGRKKRRQRRR-NH ₂	None	2059.09	2060.45
A2	FITC-AcpS ₅ GRKS ₅ RRQRRR-NH ₂	S ₅ -S ₅	2019.13	2020.13
A3	FITC-AcpR ₈ GRKKRRS ₅ RRR-NH ₂	R ₈ -S ₅	2061.21	2062.20
A4	FITC-AcpYGRKS ₅ RRQS ₅ RR-NH ₂	S ₅ -S ₅	2026.06	2027.10
A5	FITC-AcpYGRKERRQKRR-NH ₂	Glu-Lys	2015.03	2016.03
A6	FITC-AcpYGRAS ₅ RRQS ₅ RR-NH ₂	S ₅ -S ₅	1969.03	1969.91
A7	FITC-AcpYGRAS ₅ RRQS ₅ RA-NH ₂	S ₅ -S ₅	1883.97	1884.82
A8	FITC-AcpYGRAS ₅ ARQS ₅ RA-NH ₂	S ₅ -S ₅	1798.90	1799.77
A3u	FITC-AcpR ₈ GRKKRRS ₅ RRR-NH ₂	None	2089.21	2090.29
A4u	FITC-AcpYGRKS ₅ RRQS ₅ RR-NH ₂	None	2054.45	2055.13
A6u	FITC-AcpYGRAS ₅ RRQS ₅ RR-NH ₂	None	1996.90	1997.17
A9	FITC-AcpYGRKR ₈ RRQS ₅ RR-NH ₂	R ₈ -S ₅	2068.17	2069.12
A10	FITC-AcpYGRKR ₈ RRQXRR-NH ₂	R ₈ -X	2026.09	2027.08
A11	FITC-AcpYGRKS ₅ RRQXRR-NH ₂	S ₅ -X	1984.05	1985.01
A1 ^{Rho}	Rho-AcpYGRKKRRQRRR-NH ₂	None	2211.19	2212.20
A4 ^{Rho}	Rho- AcpYGRKS ₅ RRQS ₅ RR-NH ₂	S ₅ -S ₅	2177.19	2178.27
A6 ^{Rho}	Rho- AcpYGRAS ₅ RRQS ₅ RR-NH ₂	S ₅ -S ₅	2120.13	2121.11
A1 ^{NF}	NF- AcpYGRKKRRQRRR-NH ₂	None	2129.13	2130.15
A4 ^{NF}	NF- AcpYGRKS ₅ RRQS ₅ RR-NH ₂	S ₅ -S ₅	2095.13	2096.12
A6 ^{NF}	NF- AcpYGRAS ₅ RRQS ₅ RR-NH ₂	S ₅ -S ₅	2038.08	2039.04
B1	FITC-AcpAGpTALF-NH ₂	None	1159.34	1160.41
B2	FITC-AcpAGpTALF-AcpYGRKKRRQRRR-NH ₂	None	2813.37	2814.45
B3	FITC- AcpAGpTALF-AcpYGRKS ₅ RRQS ₅ RR- NH ₂	S ₅ -S ₅	2779.59	2780.45
B4	FITC- AcpAGpTALF-AcpYGRAS ₅ RRQS ₅ RR- NH ₂	S ₅ -S ₅	2722.17	2723.39
C1	FITC-AcpYGRKKRRQRRRGC-(S-S)- CGTALDWSWLQTE	None	3226.64	3727.77
C2	FITC-AcpYGRKS ₅ RRQS ₅ RRGC-(S-S)- CGTALDWSWLQTE	S ₅ -S ₅	3692.89	3693.75
C3	FITC-AcpYGRAS ₅ RRQS ₅ RRGC-(S-S)- CGTALDWSWLQTE	S ₅ -S ₅	3636.58	3636.66

All mass spectrometric data correspond to [M+H]⁺ peaks.

Table S2. Mass spectrometry data for the peptides

NO.	Sequence	Stapled	MS (calcd)	MS (obsd)
A1	YGRKKRRQRRR-NH ₂	None	1557.97	1558.99
A2	S ₅ GRKS ₅ RRQRRR-NH ₂	S ₅ -S ₅	1517.01	1518.01
A3	R ₈ GRKKRRS ₅ RRR-NH ₂	R ₈ -S ₅	1559.05	1560.04
A4	YGRKS ₅ RRQS ₅ RR-NH ₂	S ₅ -S ₅	1523.91	1524.95
A5	YGRKERRQKRR-NH ₂	Glu-Lys	1512.91	1513.90
A6	YGRAS ₅ RRQS ₅ RR-NH ₂	S ₅ -S ₅	1466.91	1467.89
A7	YGRAS ₅ RRQS ₅ RA-NH ₂	S ₅ -S ₅	1381.85	1382.71
A8	YGRAS ₅ ARQS ₅ RA-NH ₂	S ₅ -S ₅	1296.78	1297.66
A3u	R ₈ GRKKRRS ₅ RRR-NH ₂	None	1587.05	1588.13
A4u	YGRKS ₅ RRQS ₅ RR-NH ₂	None	1551.97	1553.03
A6u	YGRAS ₅ RRQS ₅ RR-NH ₂	None	1494.91	1495.92
A9	YGRKR ₈ RRQS ₅ RR-NH ₂	R ₈ -S ₅	1566.02	1567.00
A10	YGRKR ₈ RRQXRR-NH ₂	R ₈ -X	1524.97	1524.95
A11	YGRKS ₅ RRQXRR-NH ₂	S ₅ -X	1481.92	1482.90
A12	FITC-Acp-YGRKS ₅ RR Φ S ₅ RR-NH ₂	S ₅ -S ₅	2095.32	2096.12
A13	FITC-Acp-Y Φ RKS ₅ RRQS ₅ RR-NH ₂	S ₅ -S ₅	2166.57	2167.14
C1	YGRKKRRQRRRGC-(S-S)-CGTALDWSWLQTE	None	3224.64	3225.73
C2	YGRKS ₅ RRQS ₅ RRGC-(S-S)-CGTALDWSWLQTE	S ₅ -S ₅	3190.65	3191.40
C3	YGRAS ₅ RRQS ₅ RRGC-(S-S)-CGTALDWSWLQTE	S ₅ -S ₅	3133.59	3134.56
D1	Biotin-miniPEG ₂ -Acp-YGRKKRRQRRR-NH ₂	None	2187.15	2188.28
D2	Biotin-miniPEG ₂ -Acp-YGRKS ₅ RRQS ₅ RR-NH ₂	S ₅ -S ₅	2153.38	2154.29
D3	Biotin-miniPEG ₂ -Acp-YGRAS ₅ RRQS ₅ RR-NH ₂	S ₅ -S ₅	2096.29	2097.23

All mass spectrometric data correspond to [M+H]⁺ peaks.

Table S3. LogD_{7.4} for peptides.

Peptide	logD _{7.4}	Average
A1	-2.327	-2.159±0.359
	-2.403	
	-1.746	
A2	-1.367	-1.180±0.191
	-0.985	
	-1.188	
A3	-0.359	-0.397±0.0806
	-0.343	
	-0.490	
A4	-0.239	-0.144±0.117
	-0.180	
	-0.013	
A5	-0.91	-1.33±0.364
	-1.561	
	-1.519	
A12	1.079	0.936±0.184
	1.000	
	0.729	
A13	1.026	0.690±0.292
	0.534	
	0.509	

Table S4. Results of ITC Binding Studies between HS and Stapled CPPs and Size of HS clusters.

Peptide	K_D (μM)	ΔH (kcal/ mol)	ΔG (kcal/ mol)	$-T\Delta S$ (kcal/ mol)	Size(nm)
A1	0.137 \pm 0.0249	-38.4 \pm 1.10	-9.37	29.0	236 \pm 9.1
A2	0.116 \pm 0.0223	-55.8 \pm 2.91	-9.47	46.3	329 \pm 20.7
A4	0.065 \pm 0.0077	-51.3 \pm 21.13	-9.80	56.7	88 \pm 3.6
A5	0.114 \pm 0.314	-56.9 \pm 9.83	-8.11	48.8	331 \pm 35.2
A6	0.416 \pm 0.431	-51.6 \pm 1.74	-8.71	56.1	102 \pm 8.8
A4u	1.61 \pm 0.158	-46.4 \pm 5.51	-8.58	37.8	192 \pm 13.4
A6u	1.58 \pm 0.167	-50.6 \pm 6.62	-7.91	42.7	121 \pm 5.6
A9	1.07 \pm 0.236	-80.0 \pm 10.1	-8.15	71.6	185 \pm 35.4
A11	1.36 \pm 0.99	-80.0 \pm 1.0	-8.01	72	248 \pm 15.1

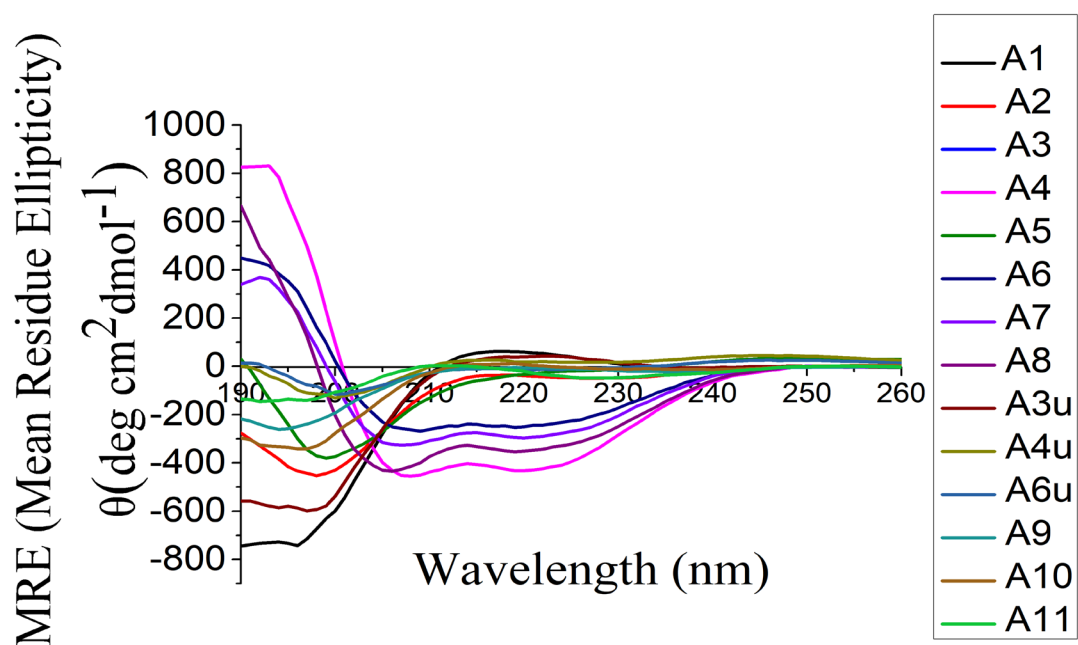


Fig. S1 CD spectra of peptides at 40 μM in H_2O .

Fig. S3 Live-cell confocal microscopy images of FITC labelled A1, A2, A3, A4, A5, A6, A9 and A11 uptake by Hela cells (2 μ M, 2 h). Scale bar=20 μ m.

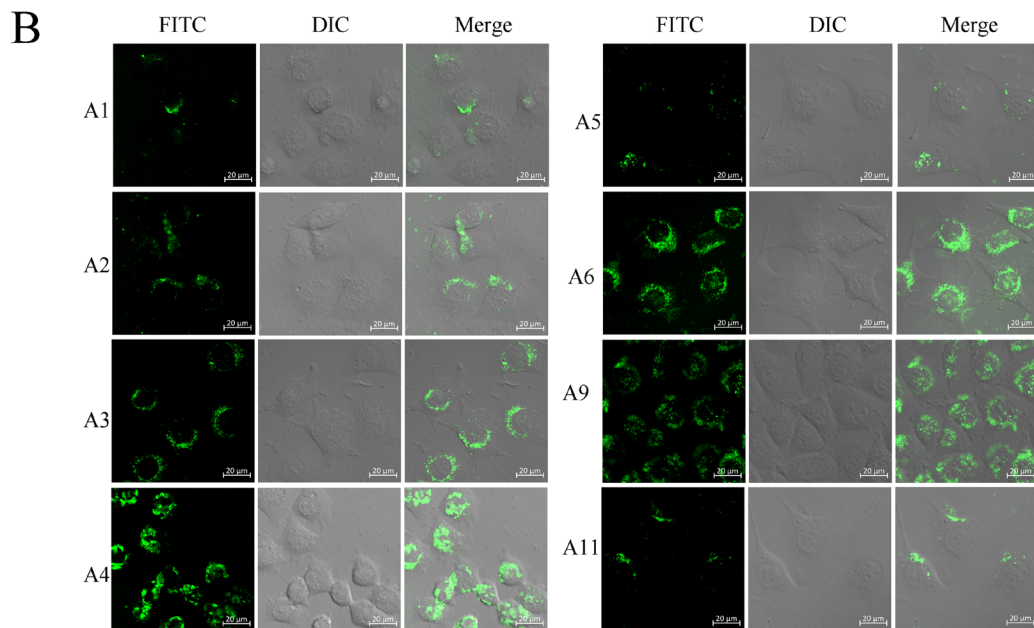
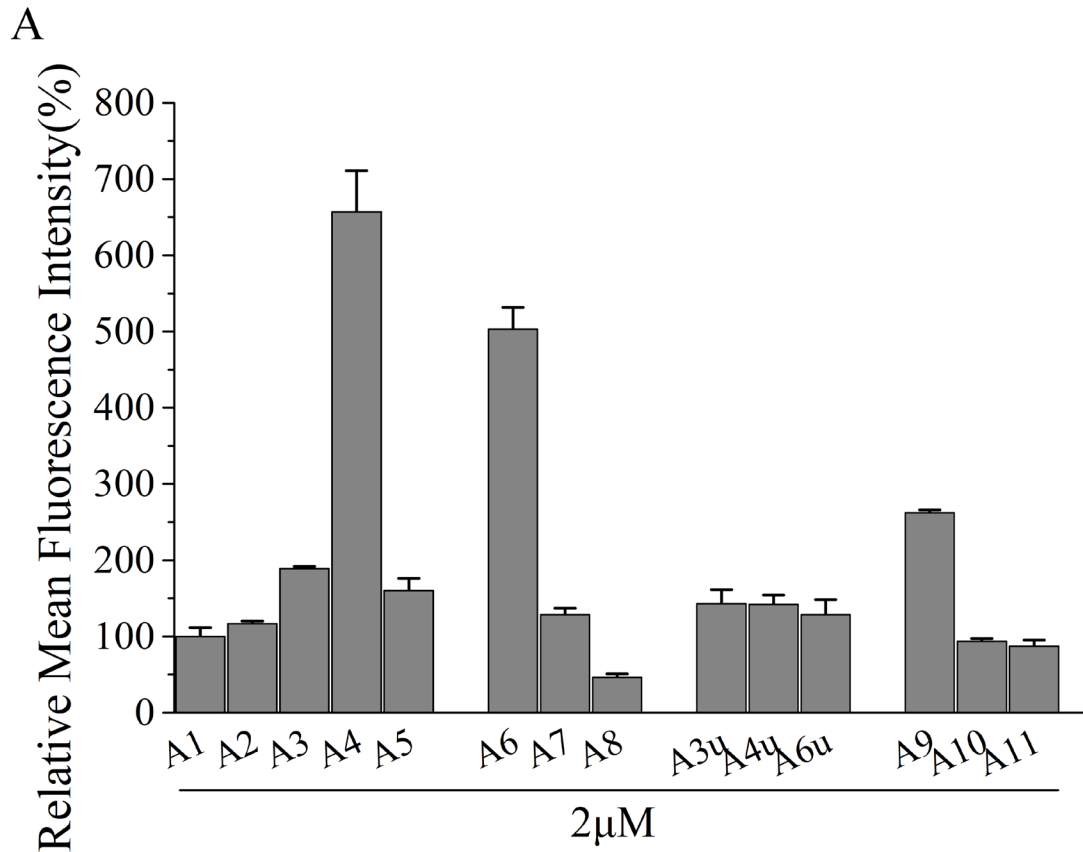


Fig. S4 (A) Cellular uptake of FITC-labelled A1-A11 in MCF-7 cells (2 μ M, 2 h). Results are the mean \pm SEM (n=4). (B) Live-cell confocal microscopy images of FITC labelled A1, A2, A3, A4, A5, A6, A9 and A11 uptake by MCF-7 cells (2 μ M, 2 h). Scale bar=20 μ m.

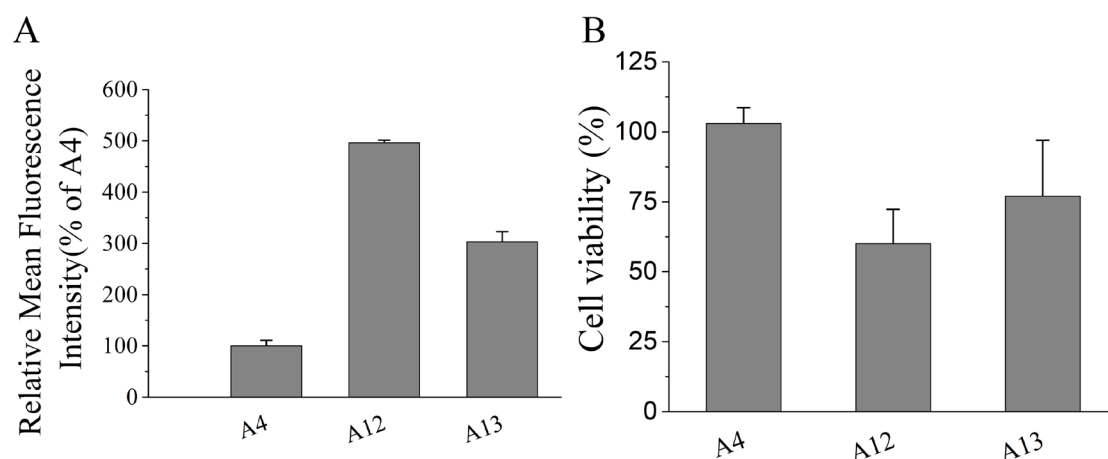


Fig. S5 (A) Cellular uptake of FITC-labelled A4, A12 and A13 in HeLa cells (2 μ M, 2 h). Results are the mean \pm SEM (n=4). (B) Cytotoxicity of A4, A12 and A13 in HeLa cells (10 μ M, 24 h). Results are the mean \pm SEM (n=4).

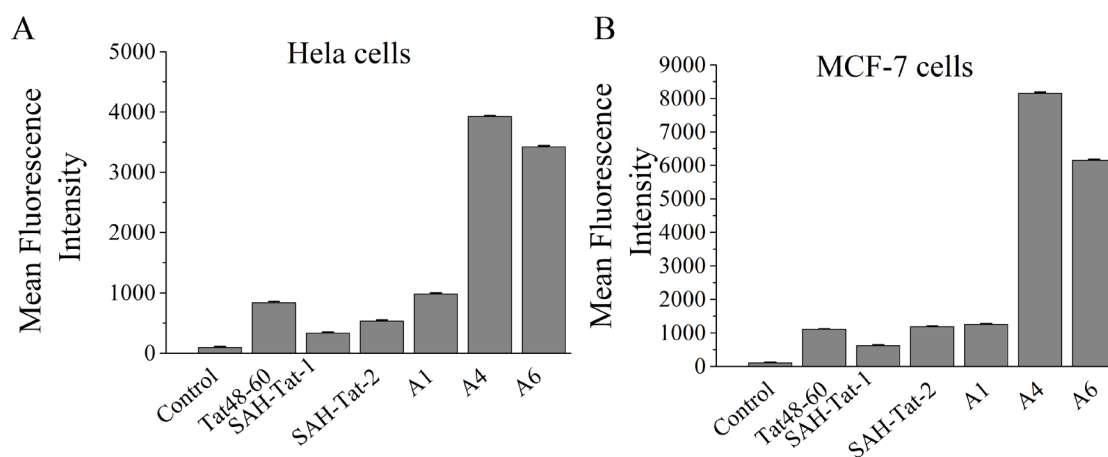


Fig. S6 Cellular uptake of FITC-labelled Tat₄₈₋₆₀, SAH-Tat-1, SAH-Tat-2, A1, A4 and A6 in HeLa cells (A) and MCF-7 cells (B, 2 μ M, 2 h). Results are the mean \pm SEM (n=4).

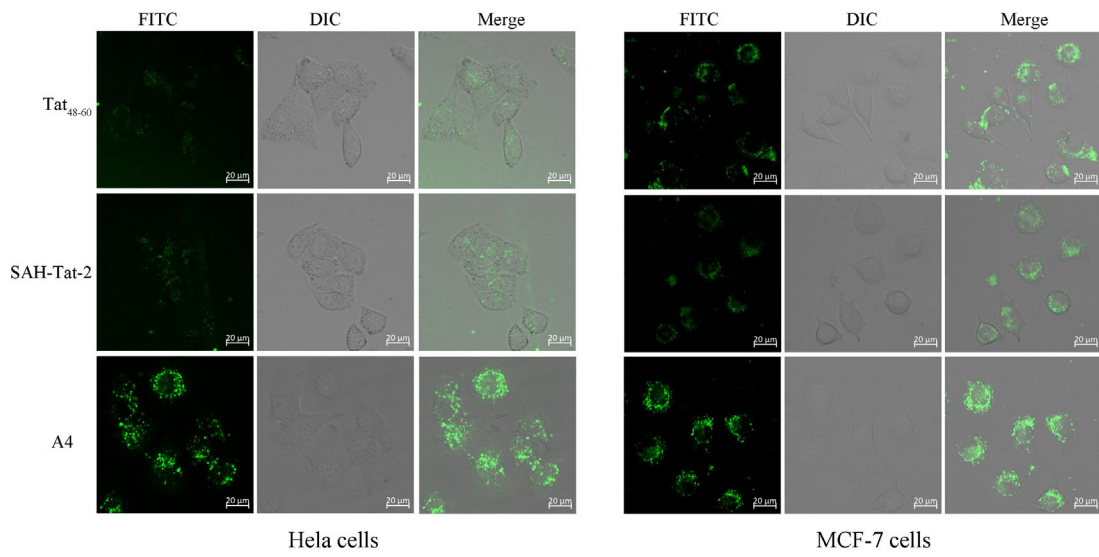


Fig. S7 Live-cell confocal microscopy images of FITC-labelled Tat₄₈₋₆₀, SAH-Tat-2 and A4 uptake by HeLa cells or MCF-7 cells (5 μ M, 2 h). Scale bar, 20 μ m.

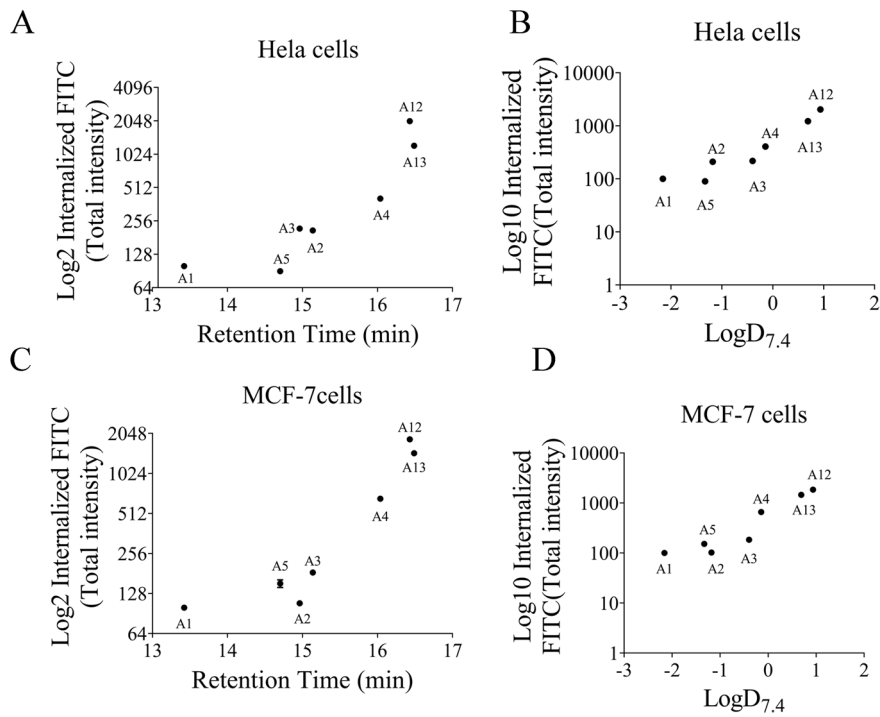


Fig. S8 The results of cell penetration in HeLa and MCF-7 cells treated with

2 μM FITC-labeled stapled peptides using FACS analysis. (A) Plots of total fluorescence intensity versus retention times in HeLa cells. Results are the mean \pm SEM (n=4). (B) Log $D_{7.4}$ value of peptides measured versus cell permeability in HeLa cells. (C) Plots of total fluorescence intensity versus retention times in MCF-7 cells. Results are the mean \pm SEM (n=4). (D) Log $D_{7.4}$ value of peptides measured versus cell permeability in MCF-7 cells.

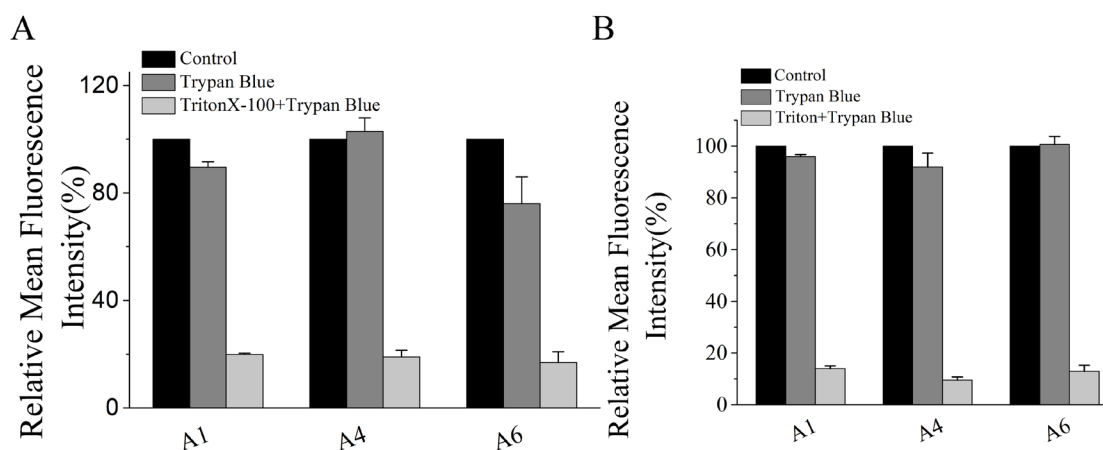


Fig. S9 Cellular uptake of A1, A4 and A6 (2 μM , 2 h) in the presence of Trypan blue or Trypan blue and Triton-X100 in HeLa cells (A) and MCF-7 cells (B). Results are the mean \pm SEM (n=4).

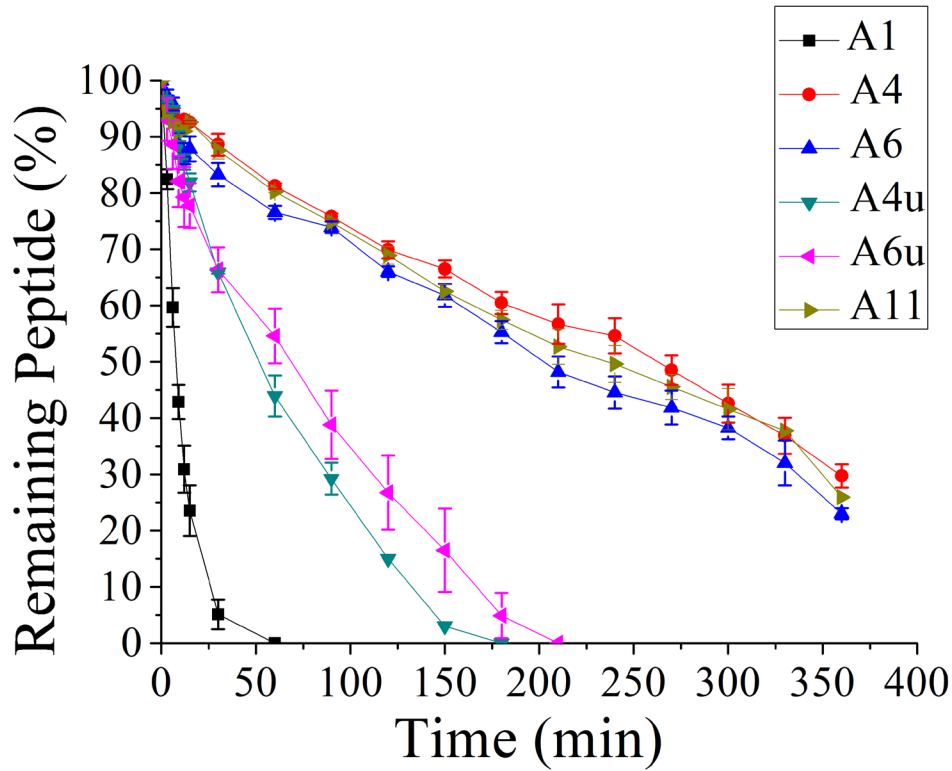


Fig. S10 Comparison of the serum stabilities of A1, A4, A6, A4u, A6u, and A11.

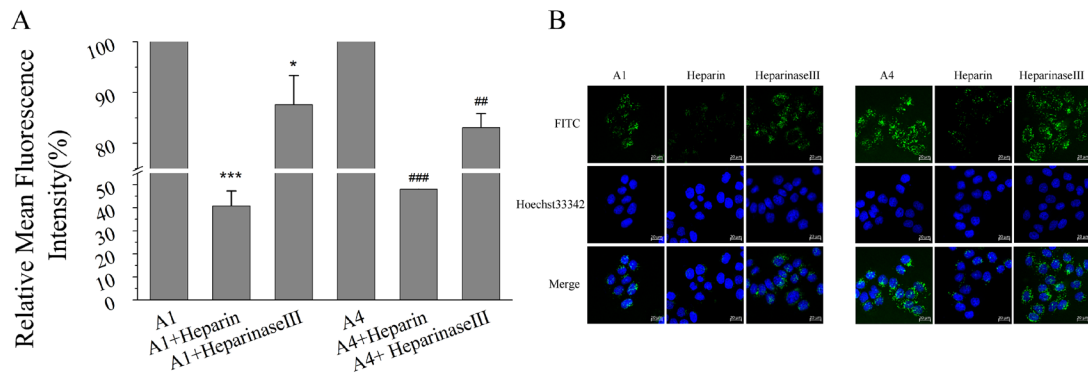


Fig. S11 Effect of heparinase III and heparin treatment on uptake of A1 and A4. (A) Cellular uptake of FITC labelled A1 and A4 (5 μ M, 1 h) in HeLa cells after incubated with 3 mIU/ml Heparinase III or 50 U/ml heparin for 1 h. Results are the mean \pm SEM (n=4). ***p < 0.001, 0.001 \leq **p < 0.01,

0.01 ≤ *p < 0.05 vs A1 or A4. (B) HeLa cells were treated with heparinase III (3 mIU/ml) or heparin (50 U/ml) for 1 h, after which they were incubated for 1 h with 5 μM of A1 or A4. Nucleus was stained with Hoechst33342. Images were obtained with Confocal microscopy. Scale bar=20 μm.

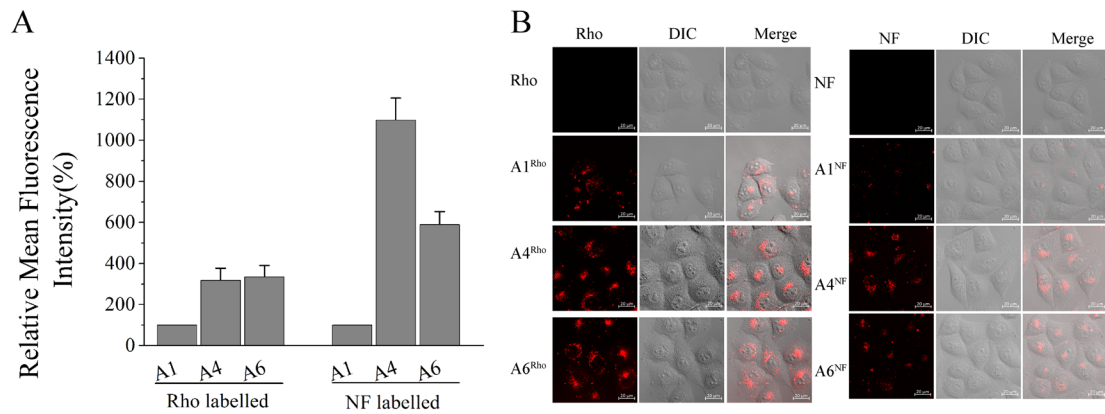


Fig. S12 (A) Cellular uptake of Rho-labelled CPPs or NF-labelled CPPs in HeLa cells (5 μM, 2 h). Results are the mean ± SEM (n=4). (B) Live-cell confocal microscopy images of Rho-labeled CPPs or NF-labeled CPPs uptake by HeLa cells (5 μM, 2 h). Scale bars indicate 20 μm.

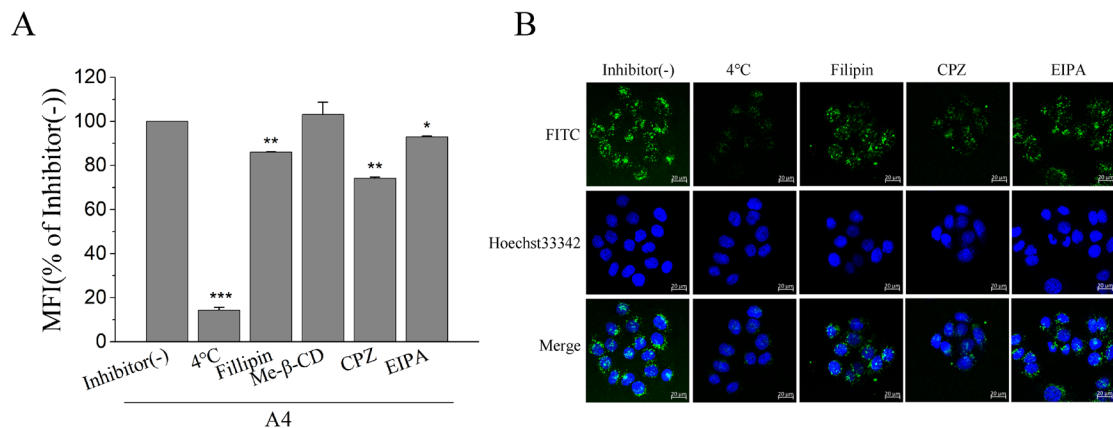


Fig. S13 (A) Cellular uptake of FITC labelled A4 in HeLa cells (5 μM, 1 h) after incubated with endocytosis-inhibitors or 4 °C for 1 h. Results are the

mean \pm SEM (n=4). *** $p < 0.001$, $0.001 \leq **p < 0.01$, $0.01 \leq *p < 0.05$ vs inhibitor (-). (B) 4 °C, Filipin, EIPA and CPZ respectively inhibits cellular internalization of A4. Nucleus marker Hoechst33342 (blue) was used to counterstain nuclei. Scale bars indicate 20 μ m.

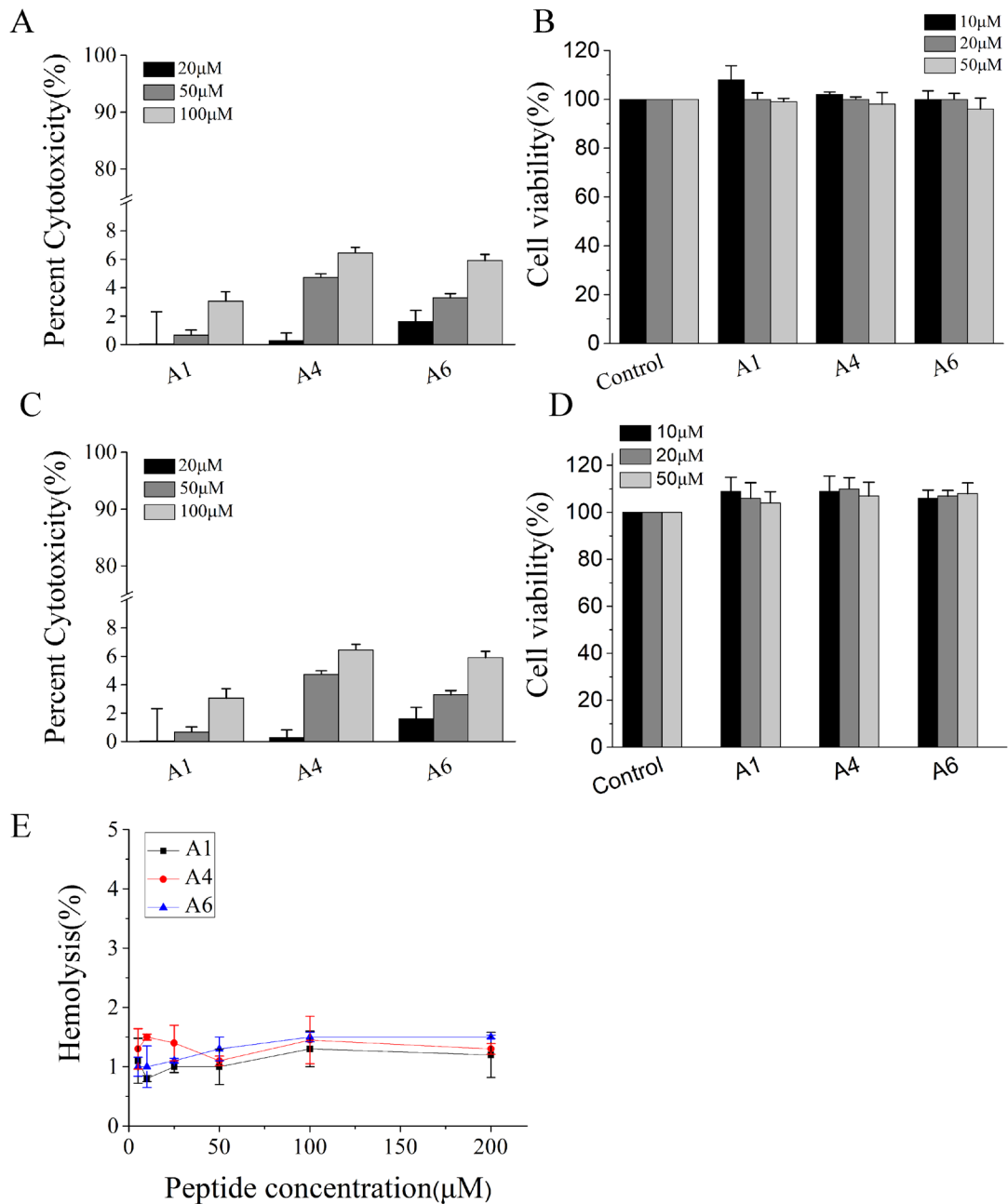


Fig. S14 (A) LDH assay data of A1, A4 and A6 in HeLa cells (2 h). Results

are the mean \pm SEM (n=4). (B) Cytotoxicity of A1, A4 and A6 in MCF-7 cells. The cells were treated with DMSO (control) or A1, A4 and A6 at 10, 20, and 50 μ M for 24 h. Results are the mean \pm SEM (n=4). (C) LDH assay data of A1, A4 and A6 in MCF-7 cells (2 h). Results are the mean \pm SEM (n=4). (D) Cytotoxicities of A1, A4, and A6. Hela cells were treated with PBS (control) or A1, A4 and A6 under concentrations of 10, 20, and 50 μ M for 24 h. Results are the mean \pm SEM (n=4). (E) Hemolysis of A1, A4 and A6 in human red blood cells (2h). Results are the mean \pm SEM (n=4).

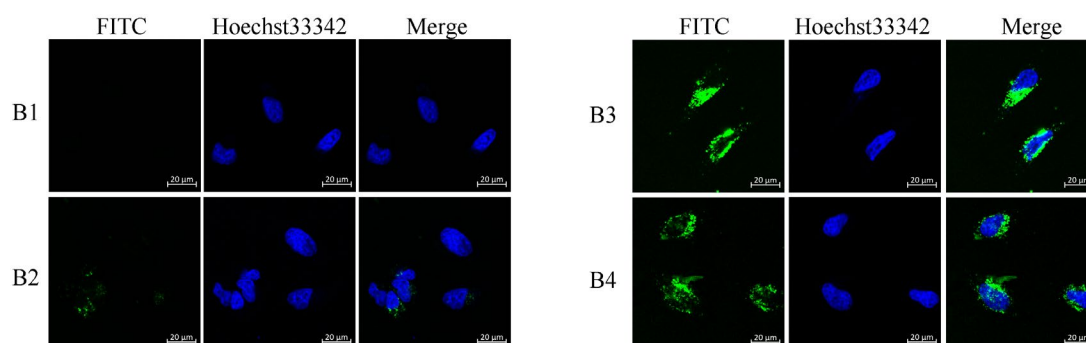


Fig. S15 Live-cell confocal microscopy images of FITC labelled AGpTALF (B1), B2, B3 and B4 uptake by HeLa cells (5 μ M, 2 h). Nucleus was stained with Hoechst33342 (middle). Scale bars indicate 20 μ m

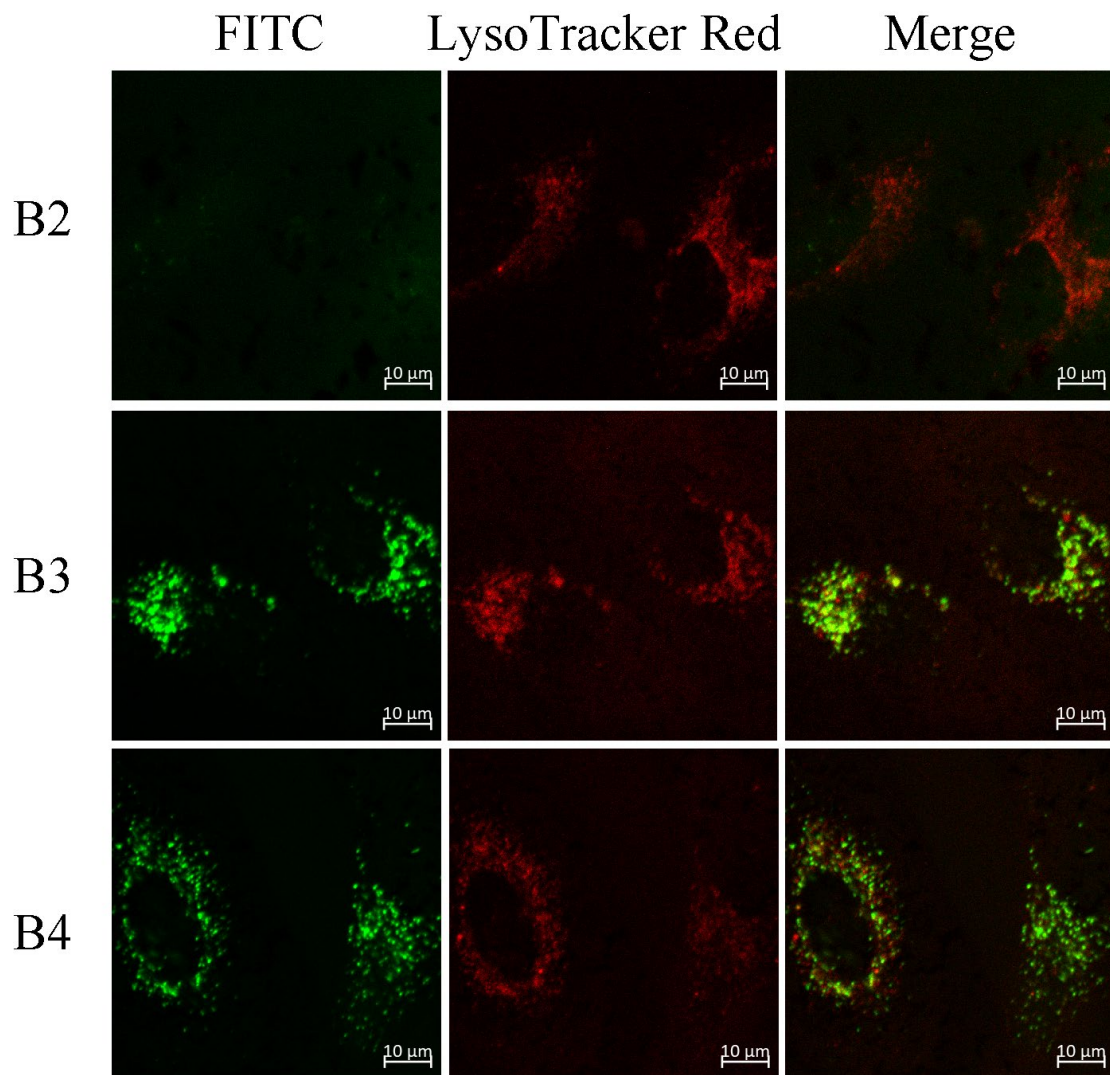


Fig. S16 Co-localization of B2, B3 or B4 and lysosome in Hela cells. Cells were incubated with FITC-labelled B2, B3, and B4 (5 μ M each) for 2 h, followed by LysoTracker Red counterstaining. The images were captured by live-cell confocal microscopy.

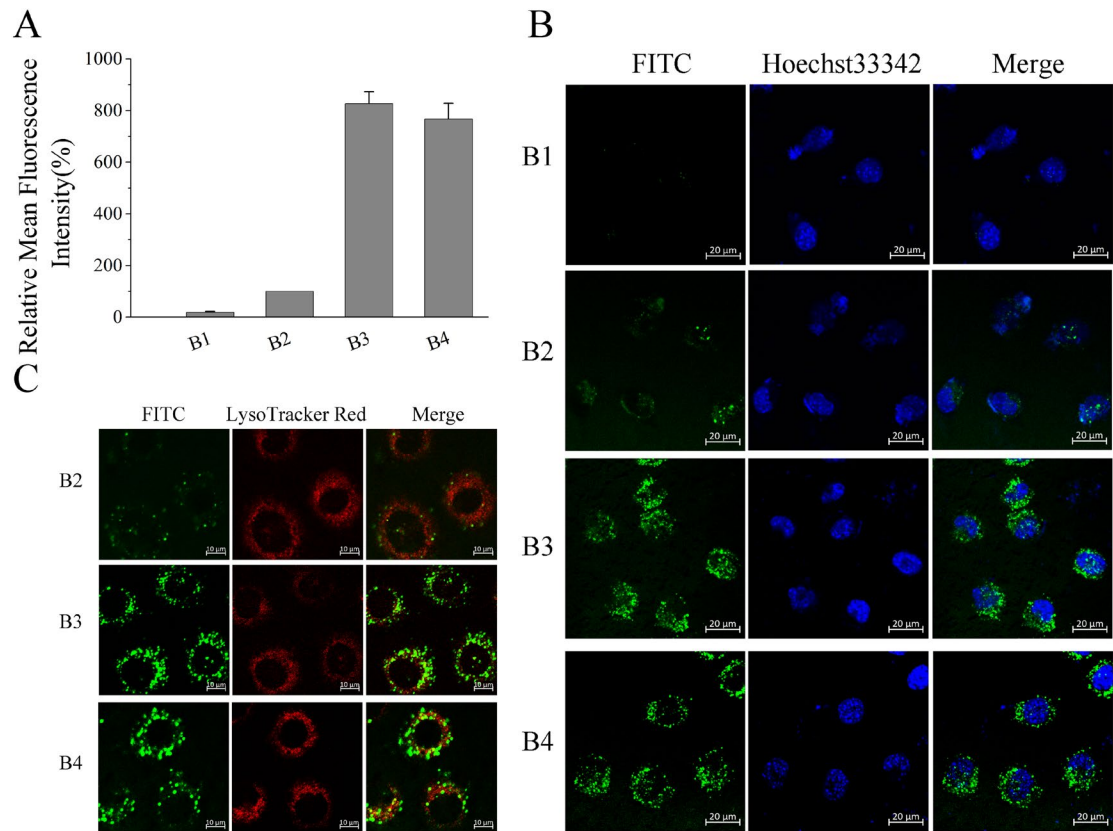


Fig. S17 (A) Cellular uptake of FITC-labelled AGpTALF(B1), FITC-labelled B2, B3 and B4 in MCF-7 cells (5 μ M, 2 h). Results are the mean \pm SEM (n=3). (B) Live-cell confocal microscopy images of FITC labelled B1, B2, B3 and B4 uptake by HeLa cells (5 μ M, 2 h). Nucleus was stained with Hoechst33342 (middle). Scale bar = 20 μ m. (C) Co-localization of FITC-labelled B2, B3 or B4 and lysosome in MCF-7 cells. MCF-7 cells were treated with 5 μ M FITC-labeled B2, B3 and B4 for 2 h, follow by LysoTracker Red counterstaining.

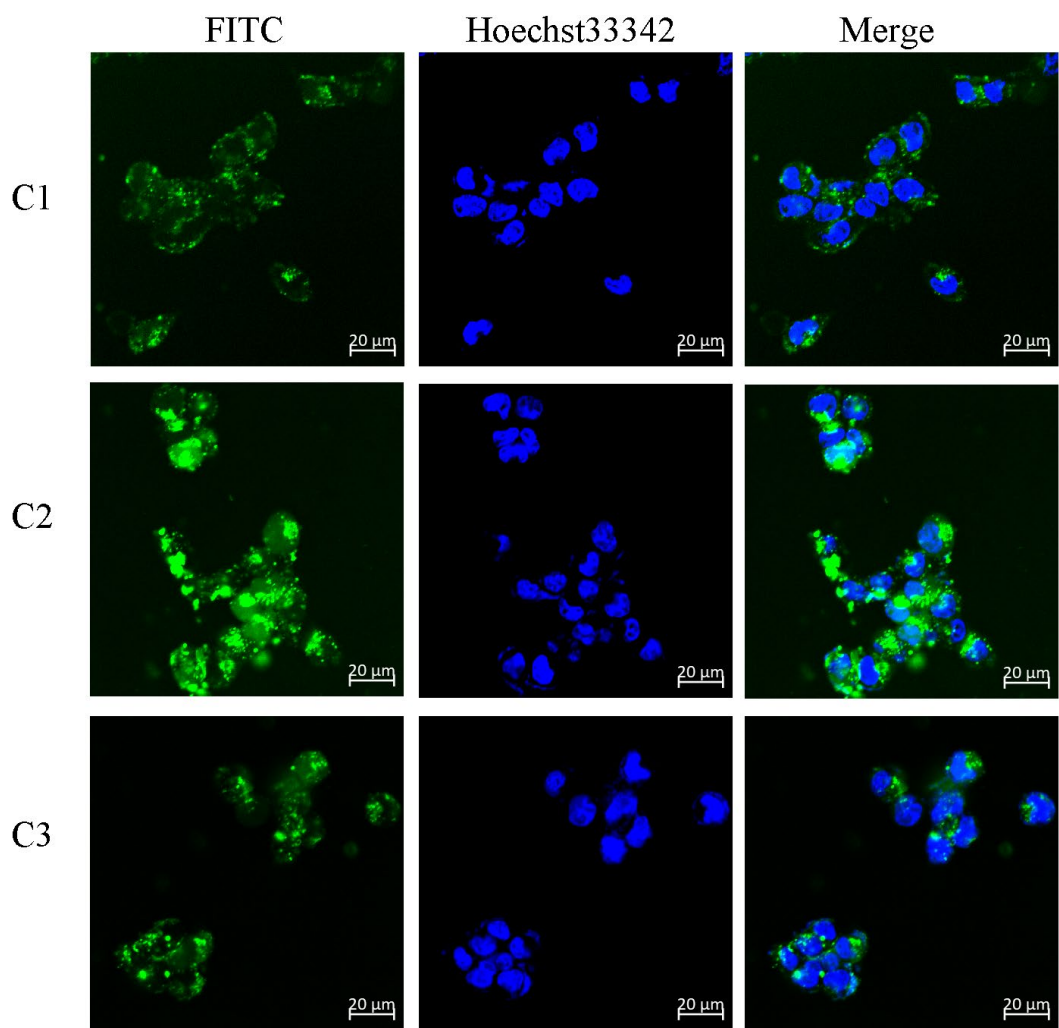


Fig. S18 Live-cell confocal microscopy images of fluorescently labelled C1, C2 and C3 uptake by Hek293 cells (5 μ M, 2 h). Nucleus was stained with Hoechst33342 (middle). Scale bar = 20 μ m.

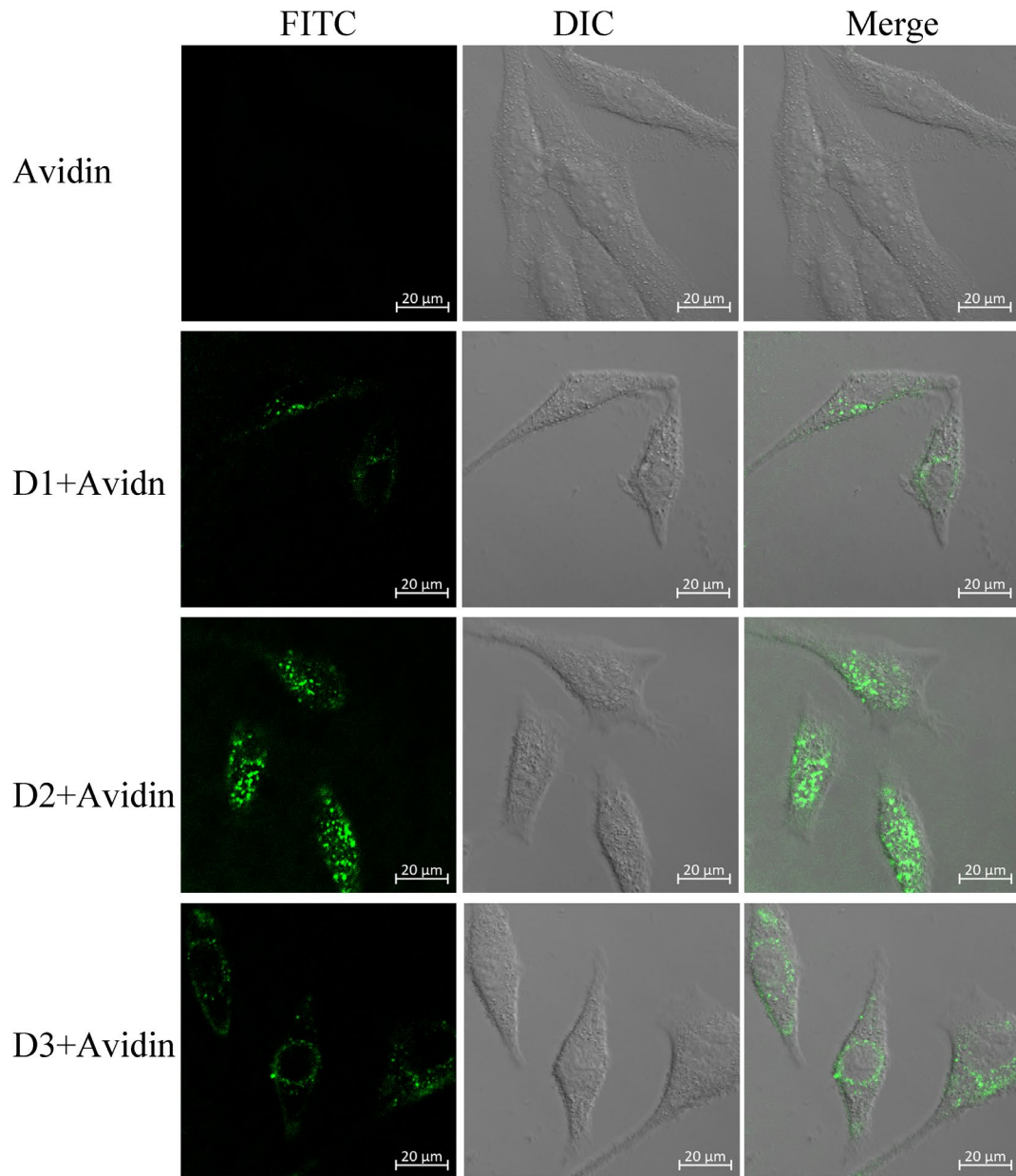


Fig. S19 Live-cell confocal microscopy images of avidin, D1-avidin conjugate, D2-avidin conjugate and D3-avidin conjugate uptake by HeLa cells (5 μ M, 2 h). Scale bar, 20 μ m.

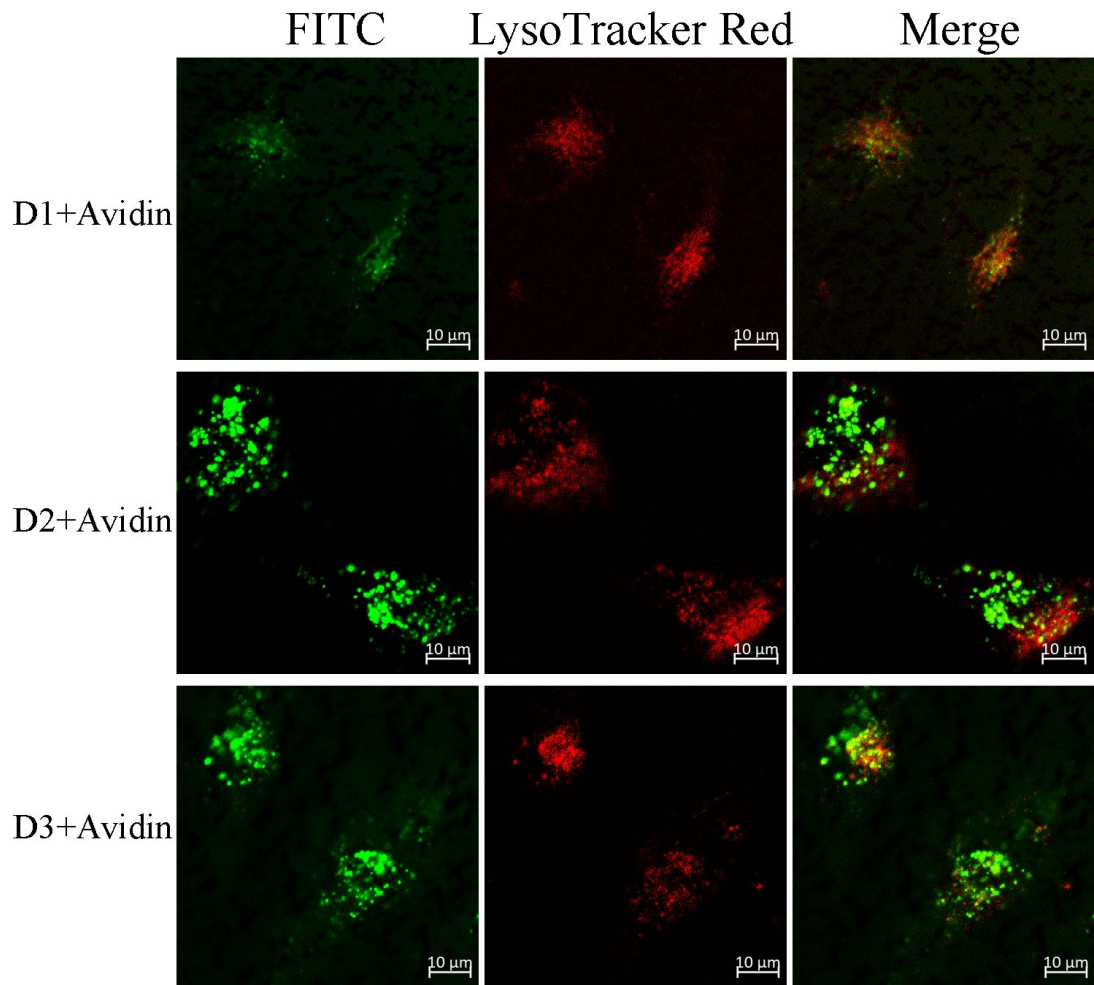


Fig. S20 Co-localization of FITC-labelled D1-avidin conjugates, D2-avidin conjugates or D3-avidin conjugates and lysosome in Hela cells. Cells were treated with FITC-labelled D1-avidin conjugates, D2-avidin conjugates and D3-avidin conjugates for 2 h, followed by LysoTracker Red counterstaining. The images were obtained by live-cell confocal microscopy. Scale bar = 20 μm .

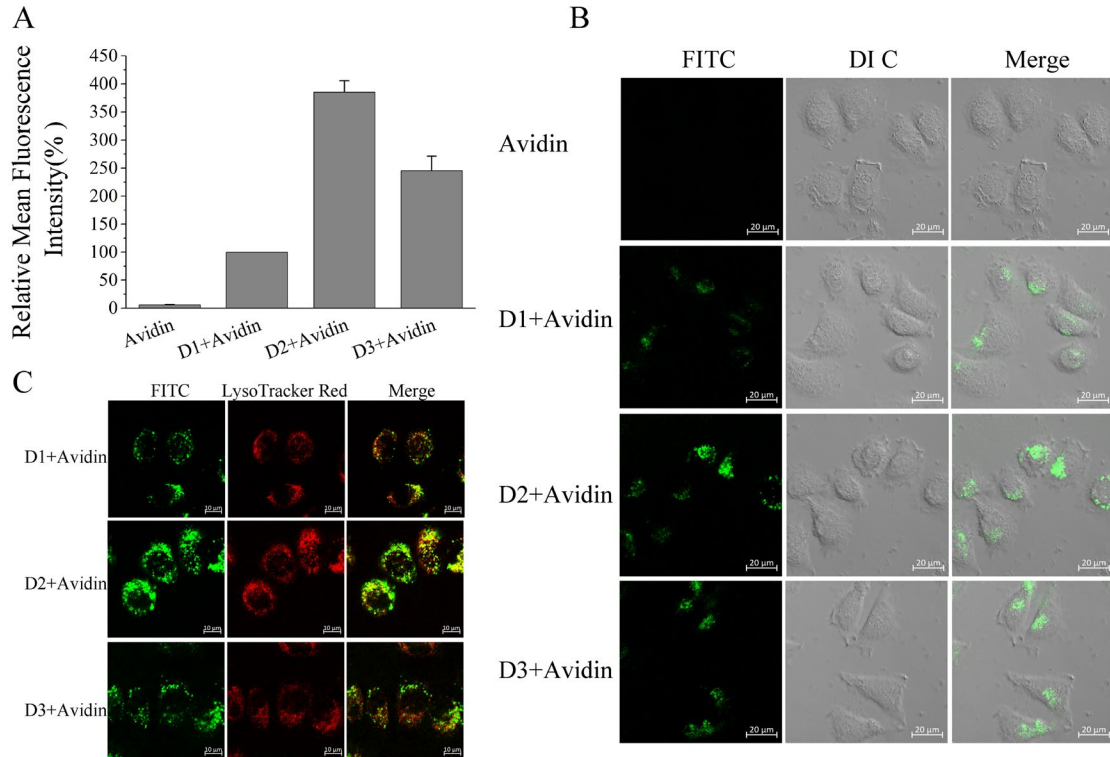
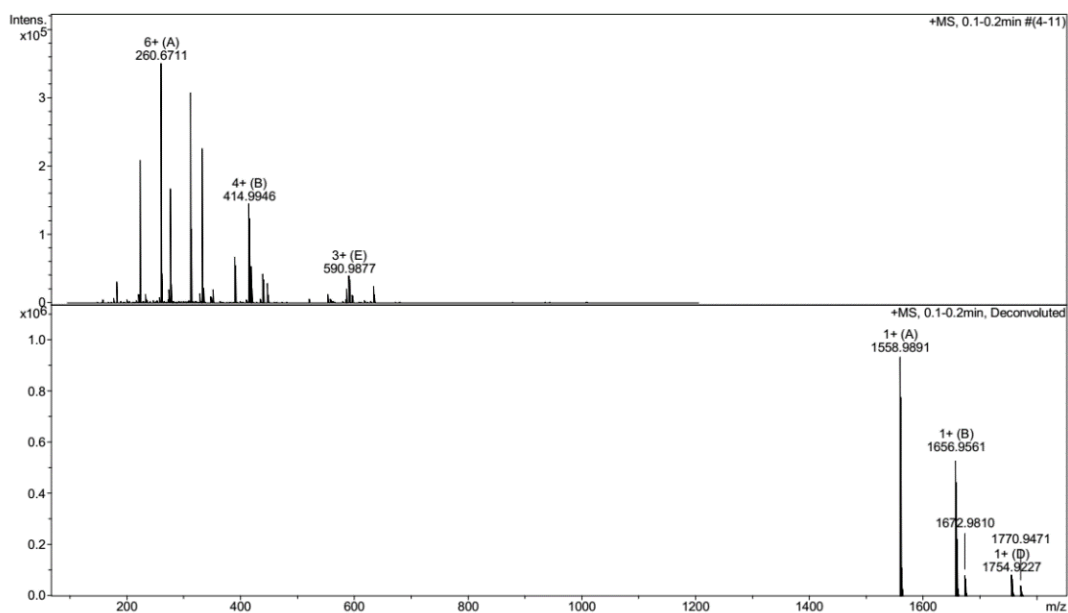
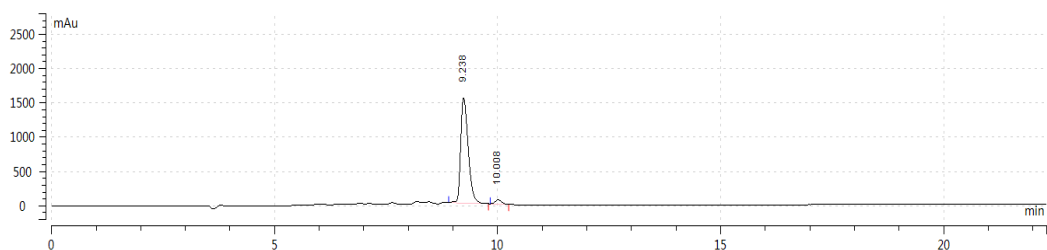


Fig. S21 (A) Cellular uptake of avidin, D1-avidin conjugate, D2-avidin conjugate and D3-avidin conjugate (5 μ M, 2 h) in MCF-7 cells. Results are the mean \pm SEM (n=4). (B) Confocal microscopy imaging of avidin, D1-avidin conjugate, D2-avidin conjugate and D3-avidin conjugate uptake by MCF-7 cells (5 μ M, 2 h). Scale bar = 20 μ m. (C) Co-localization of FITC-labeled D1-avidin conjugate, D2-avidin conjugate or D3-avidin conjugate and lysosome in MCF-7 cells. MCF-7 cells were treated with 5 μ M FITC-labeled D1-avidin conjugate, D2-avidin conjugate and D3-avidin conjugate for 2 hours, follow by LysoTracker Red staining. Images were obtained by live-cell confocal microscopy. Scale bar = 20 μ m.

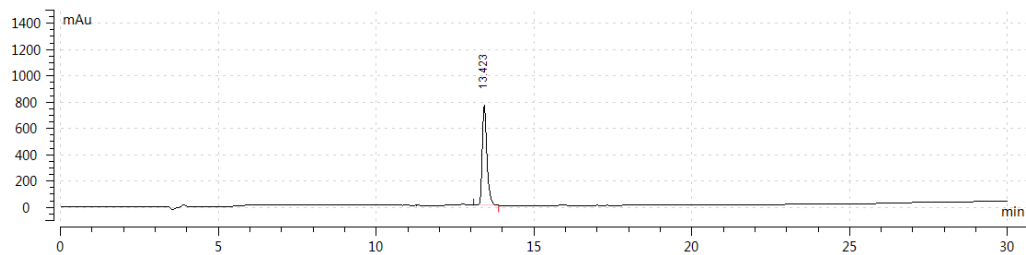
Appendix

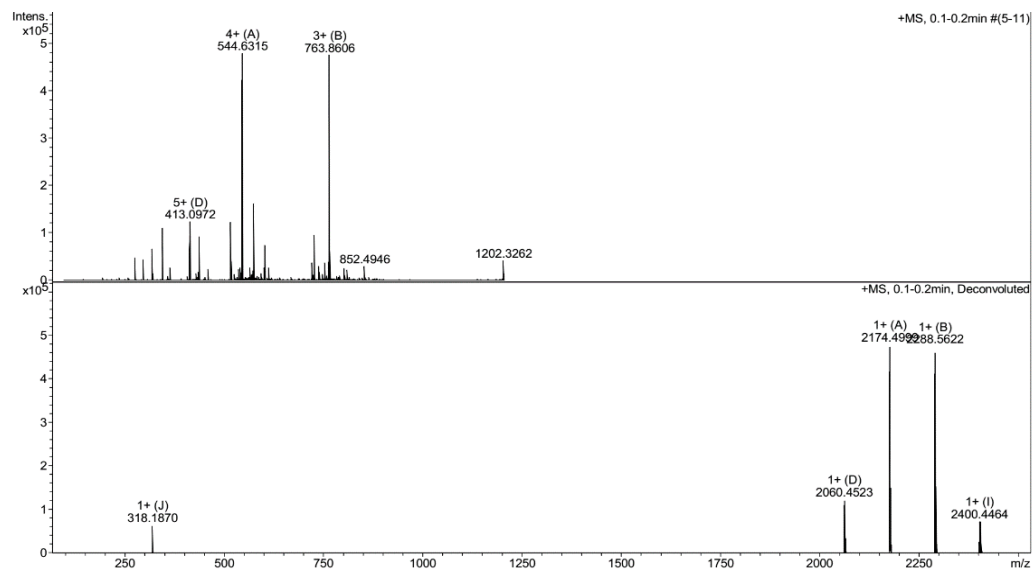
HPLC Traces and MS Spectra

A1: YGRKKRRQRRR-NH₂, C₆₄H₁₁₈N₃₂O₁₄

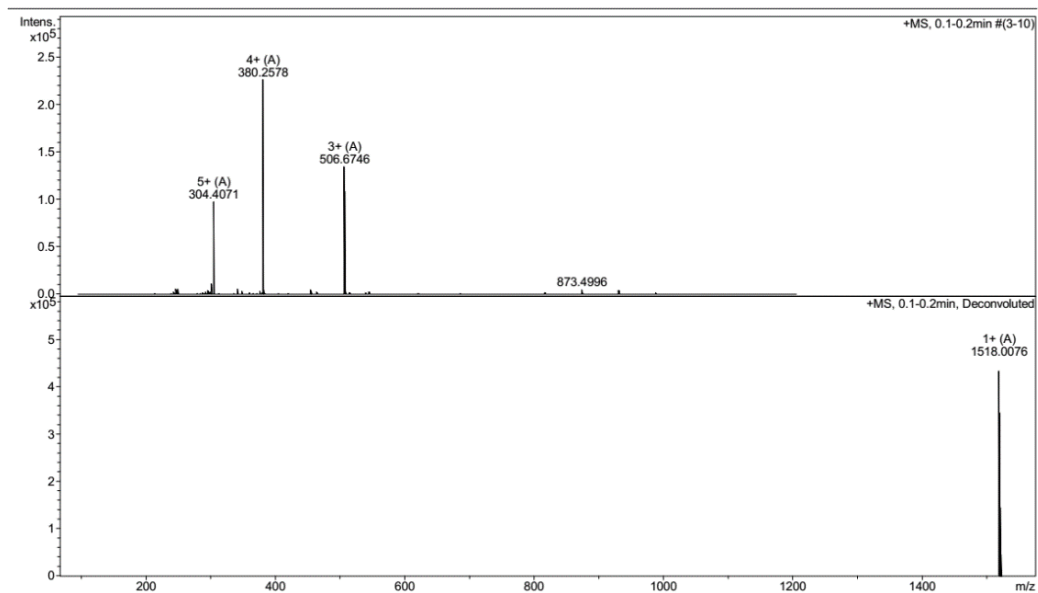
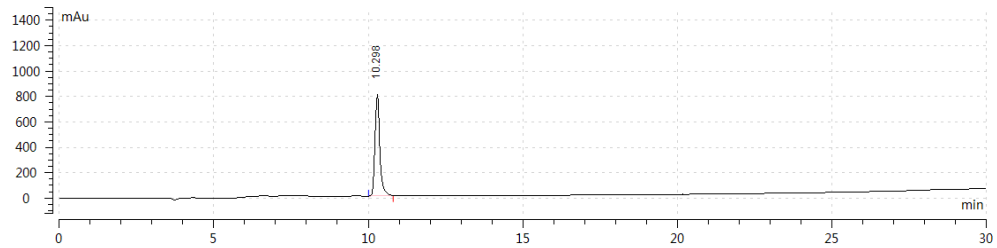


FITC labelling A1: FITC-AcpYGRKKRRQRRR-NH₂, C₉₁H₁₄₁N₃₅O₁₉S

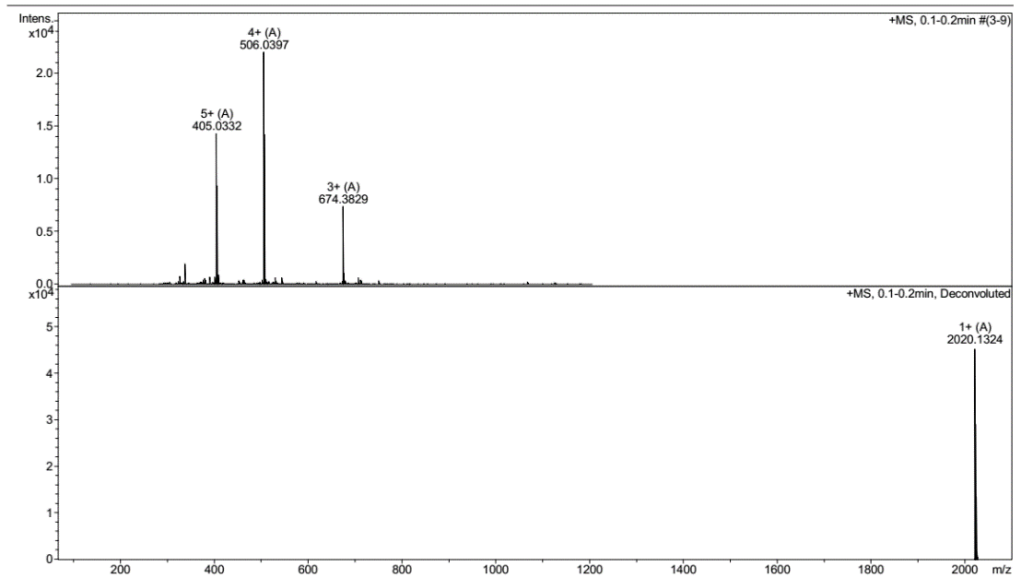
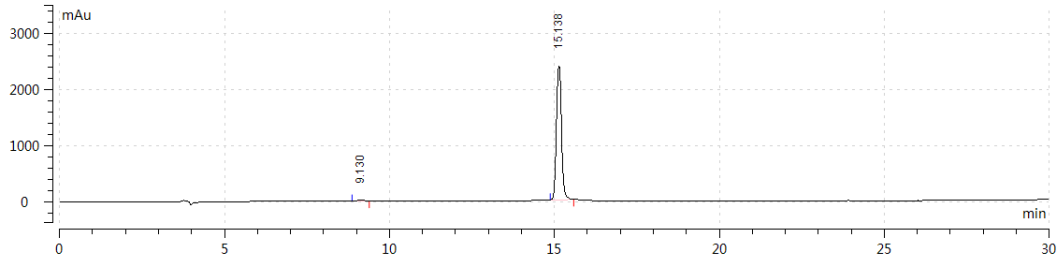




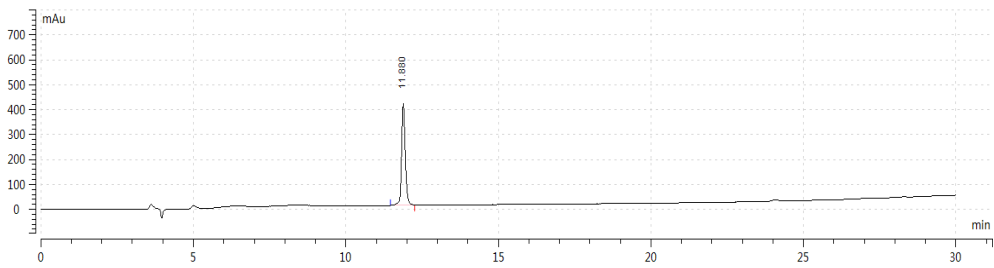
A2: Stapled S₅GRKS₅RRQRRR-NH₂, C₆₃H₁₂₀N₃₂O₁₂

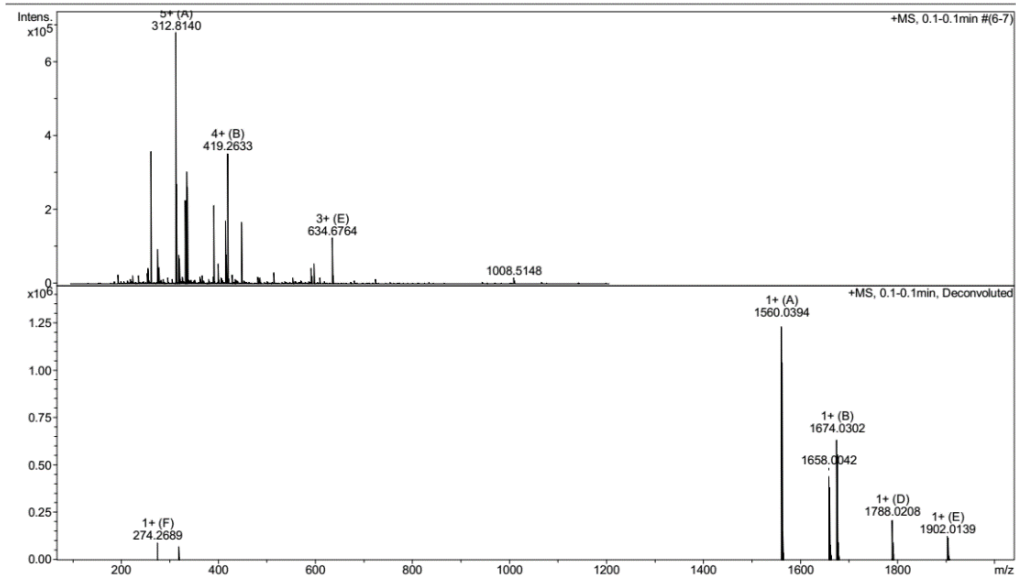


FITC labelling A2: Stapled FITC-AcpS₅GRKS₅RRQRRR-NH₂,
C₉₀H₁₄₂N₃₄O₁₈S

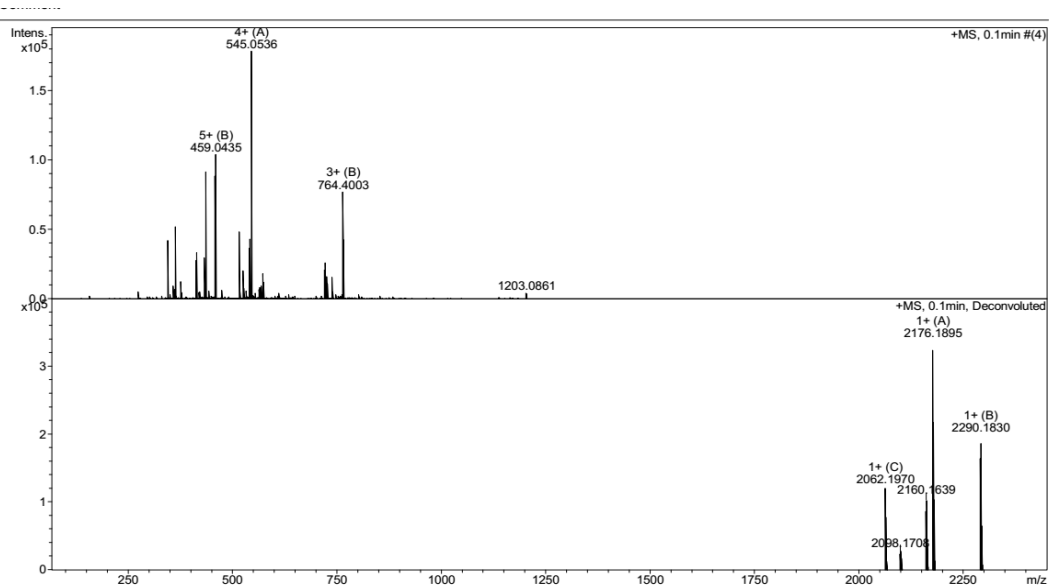
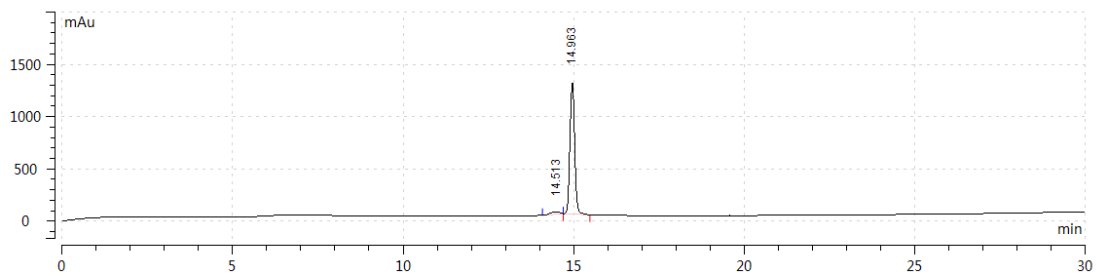


A3: Stapled R₈GRKKRRS₅RRR-NH₂, C₆₆H₁₂₆N₃₂O₁₂

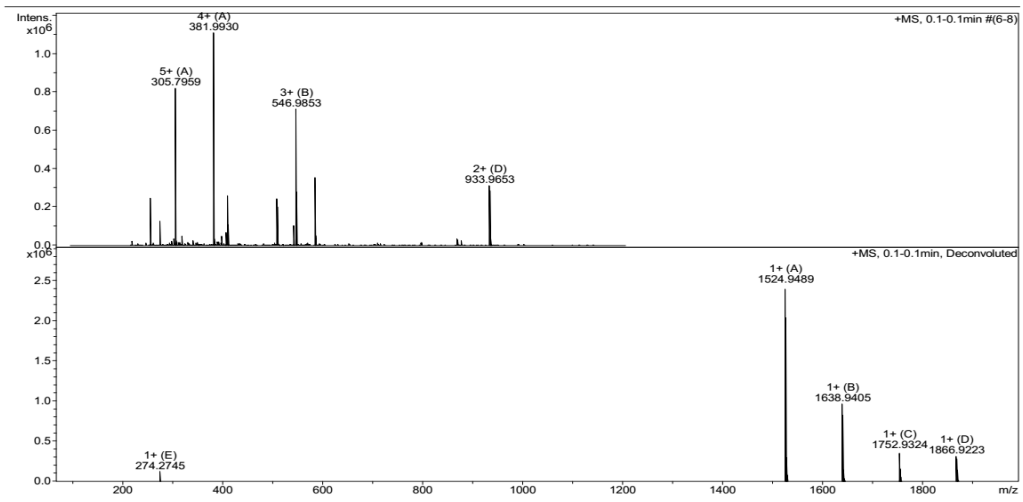
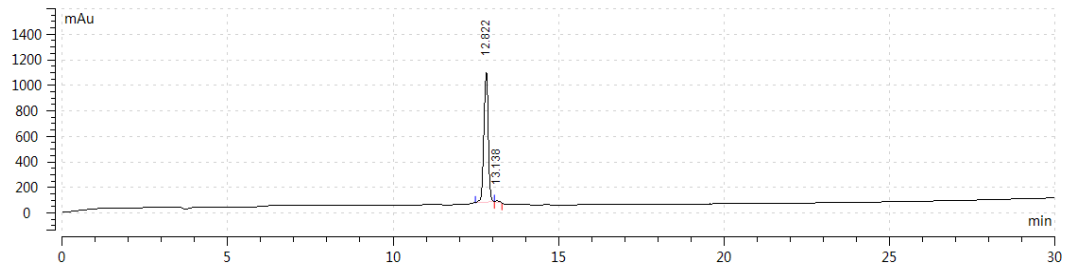




FITC labelling A3: Stapled FITC-AcpR₈GRKKRRS₅RRR-NH₂,
 $C_{93}H_{148}N_{34}O_{18}S$

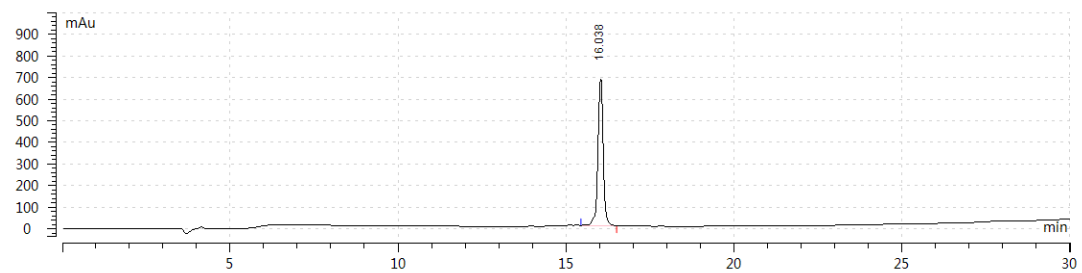


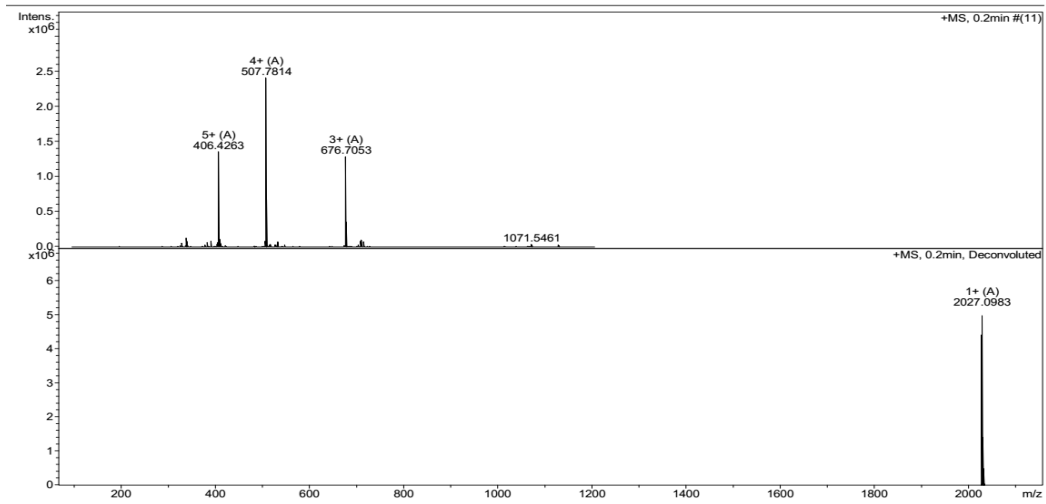
A4: Stapled YGRKS₅RRQS₅RR-NH₂, $C_{66}H_{117}N_{29}O_{13}$



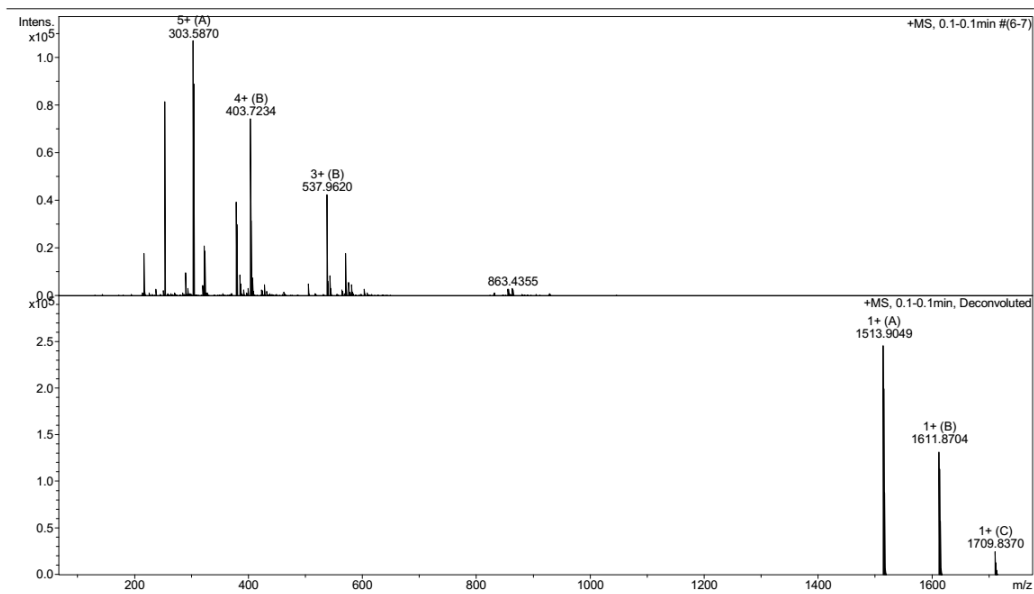
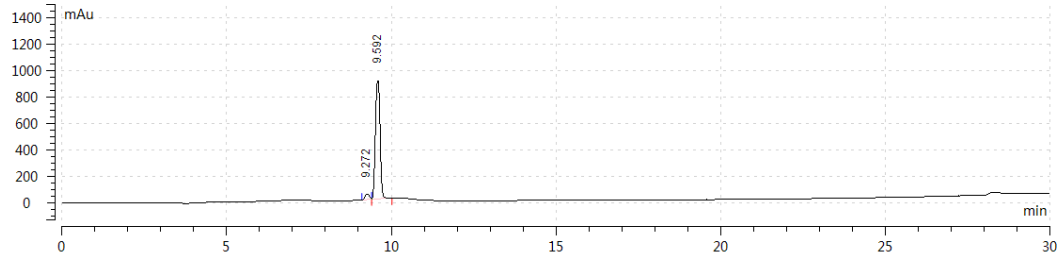
FITC labelling A4: Stapled FITC-AcpYGRKS₅RRQS₅RR-NH₂,

C₉₃H₁₃₉N₃₁O₁₉S



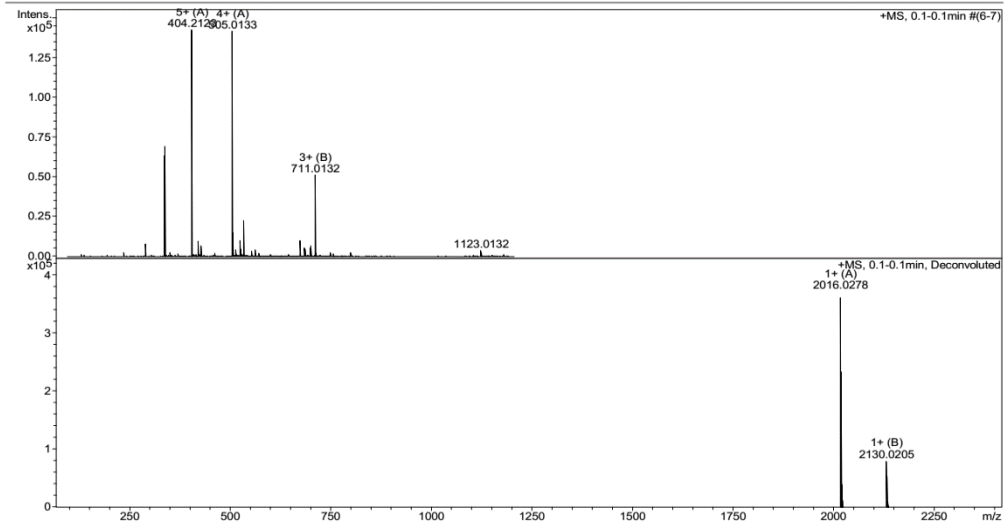
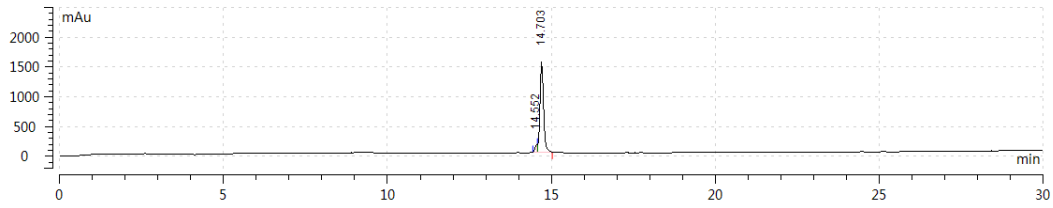


A5: Cyclized YGRKERRQKRR-NH₂, C₆₃H₁₁₁N₂₉O₁₅

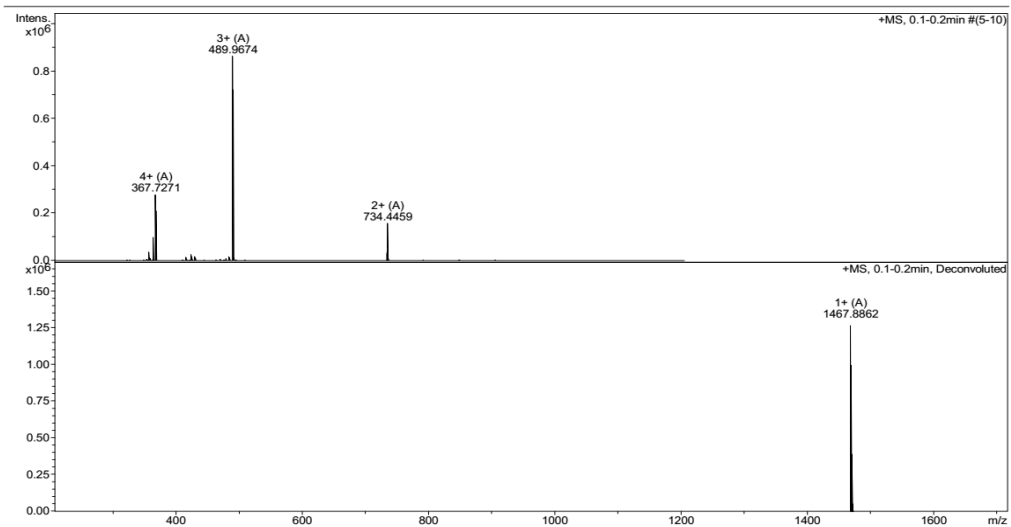
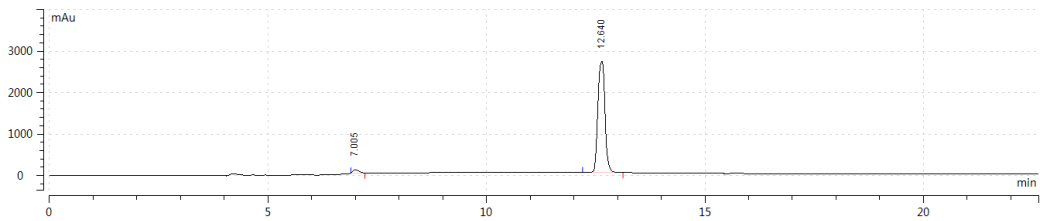


FITC labelling A5: Cyclized FITC-AcpYGRKERRQKRR-NH₂,

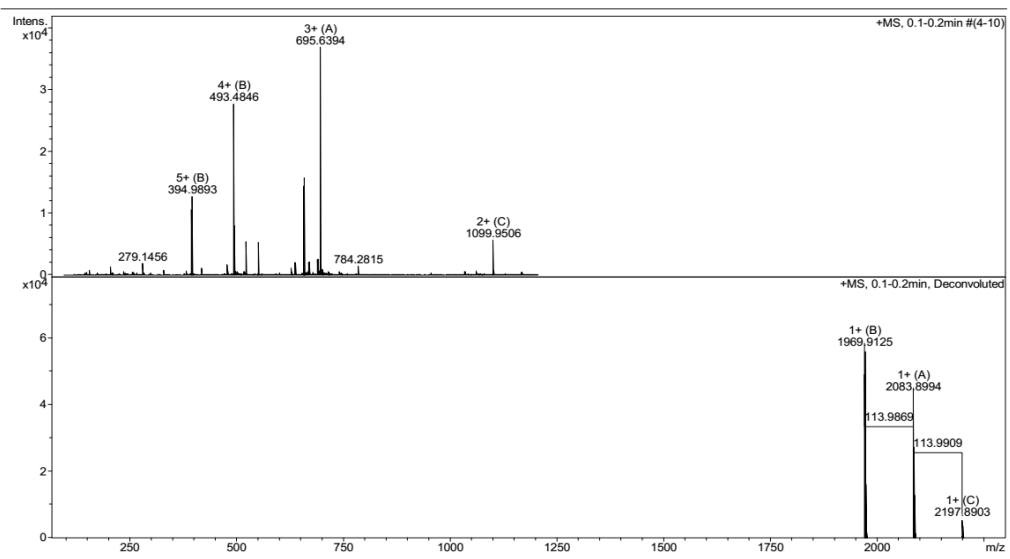
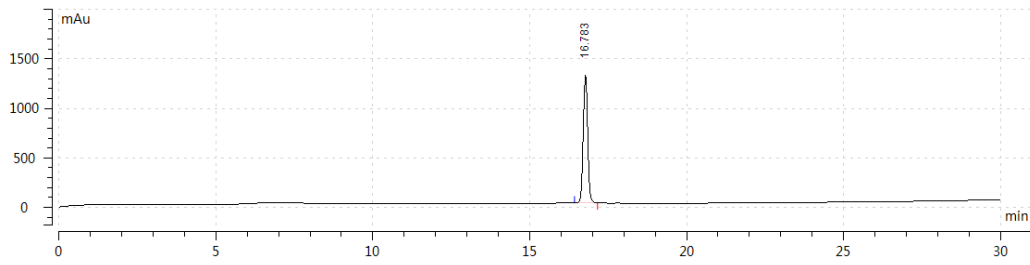
C₉₀H₁₃₃N₃₁O₂₁S



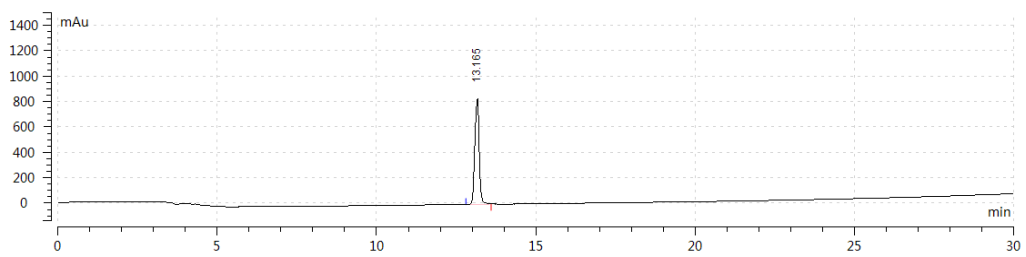
A6: Stapled YGRAS₅RRQS₅RR-NH₂, C₆₃H₁₁₀N₂₈O₁₃

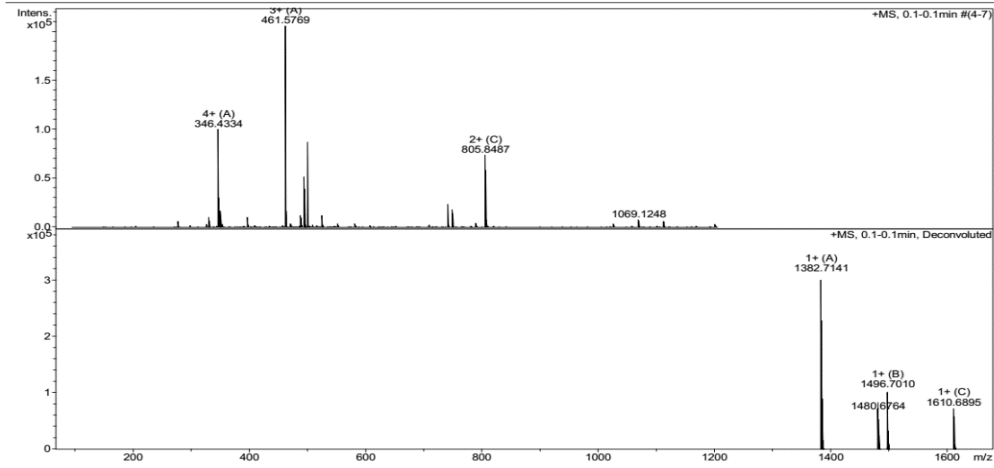


FITC labelling A6: Stapled FITC-AcpYGRAS₅RRQS₅RR-NH₂,
C₉₀H₁₃₂N₃₀O₁₉S

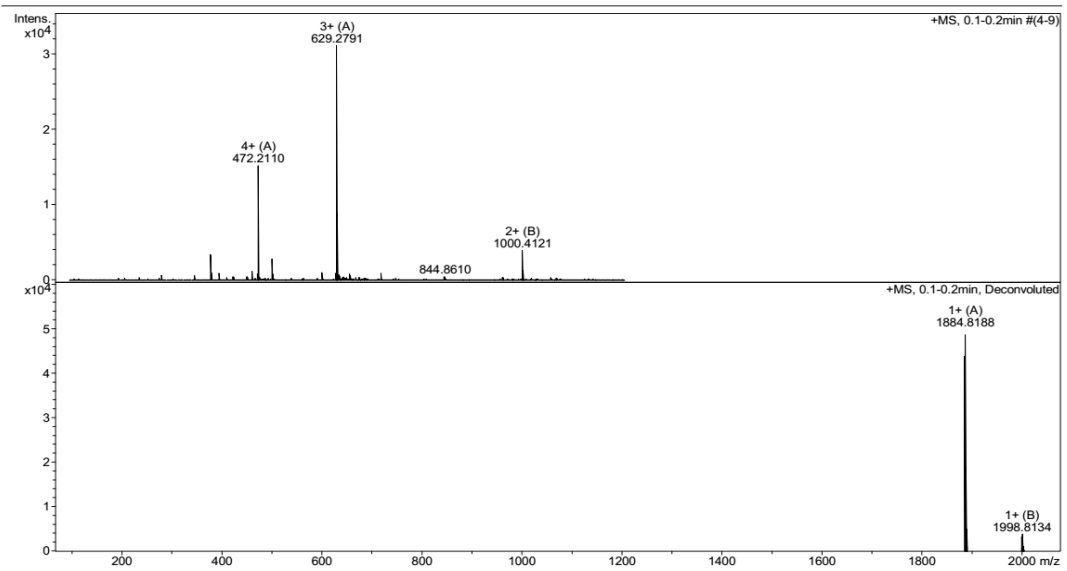
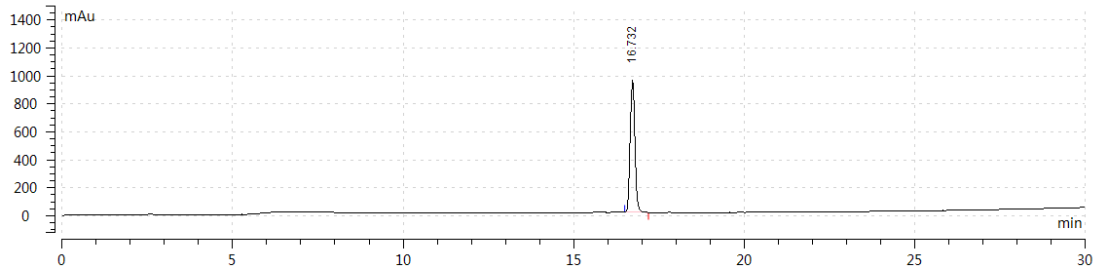


A7: Stapled YGRAS₅RRQS₅RA-NH₂, C₆₀H₁₀₃N₂₅O₁₃

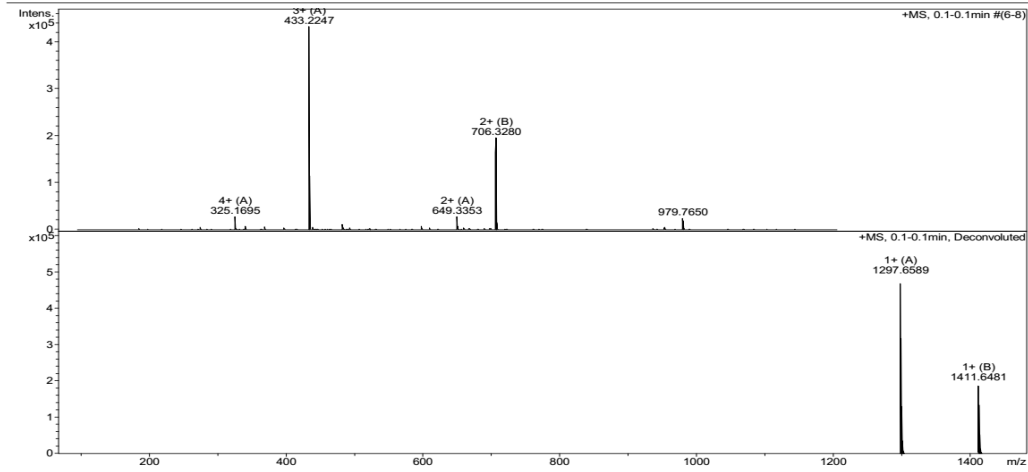
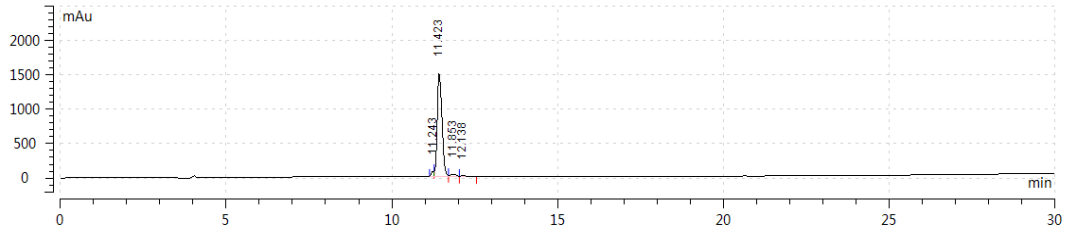




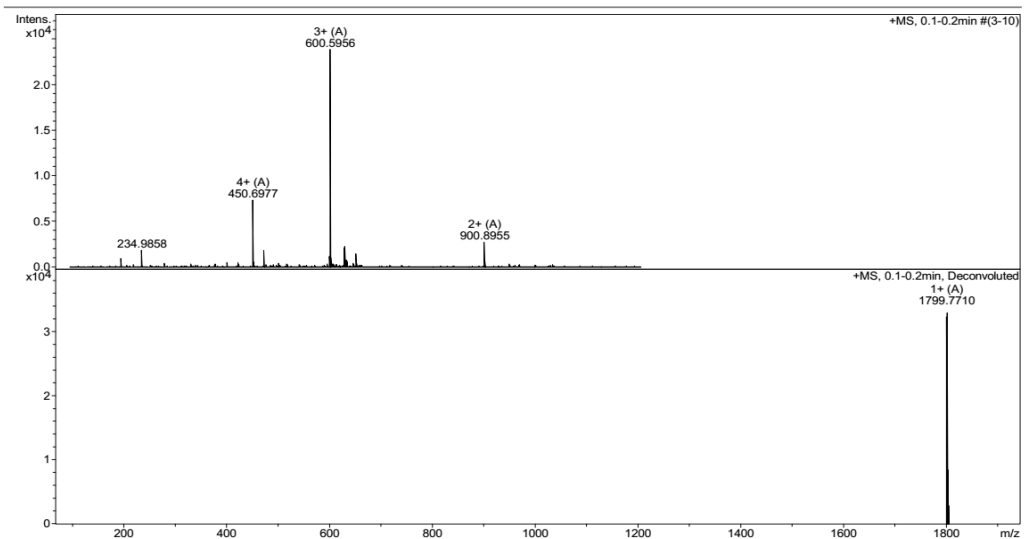
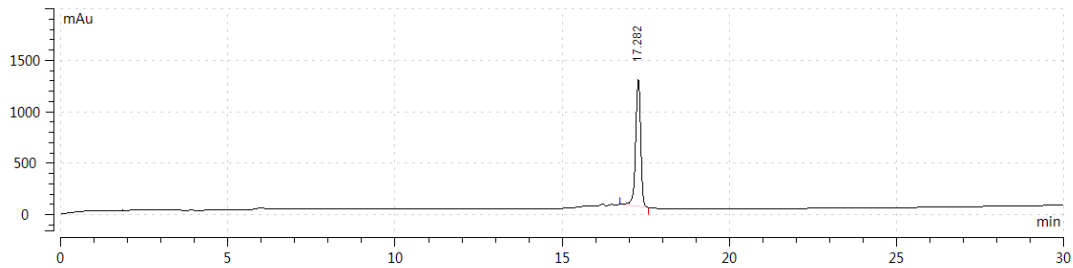
FITC labelling A7: Stapled FITC-AcpYGRAS₅RRQS₅RA-NH₂,
 C₈₇H₁₂₅N₂₇O₁₉S



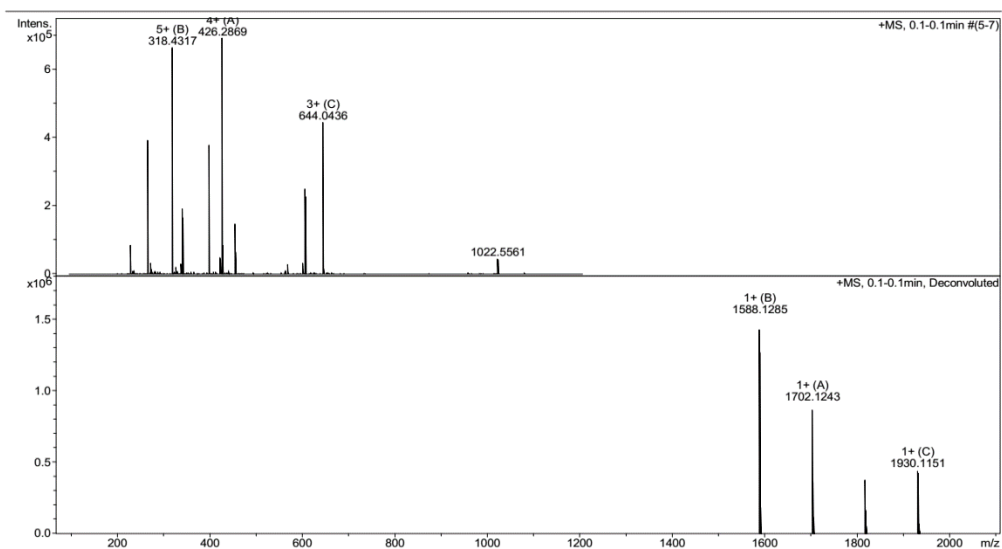
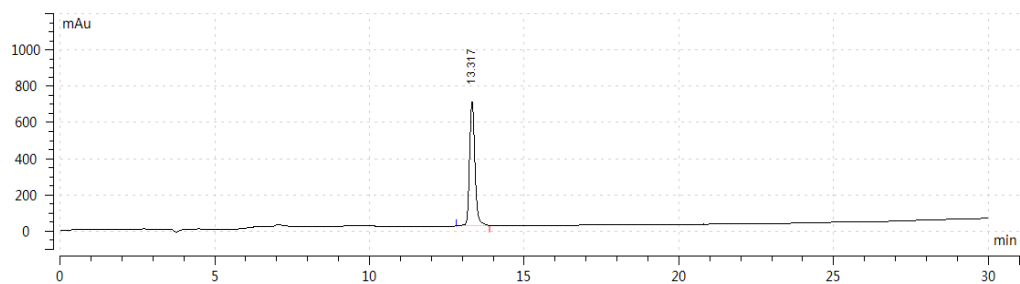
A8: Stapled YGRAS₅ARQS₅RA-NH₂, C₅₇H₉₆N₂₂O₁₃



FITC labelling A8: Stapled FITC-AcpYGRAS₅ARQS₅RA-NH₂,

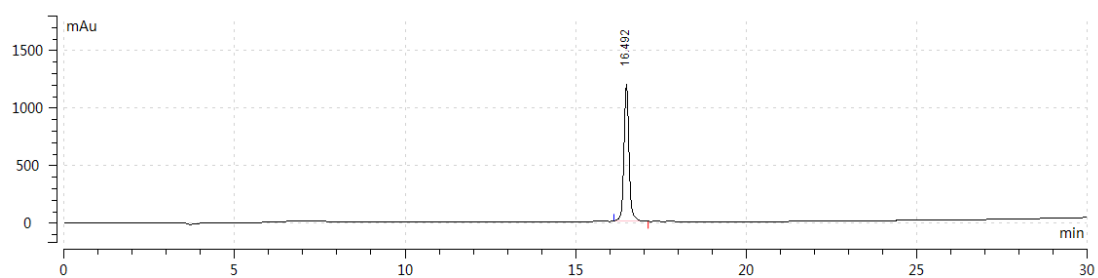


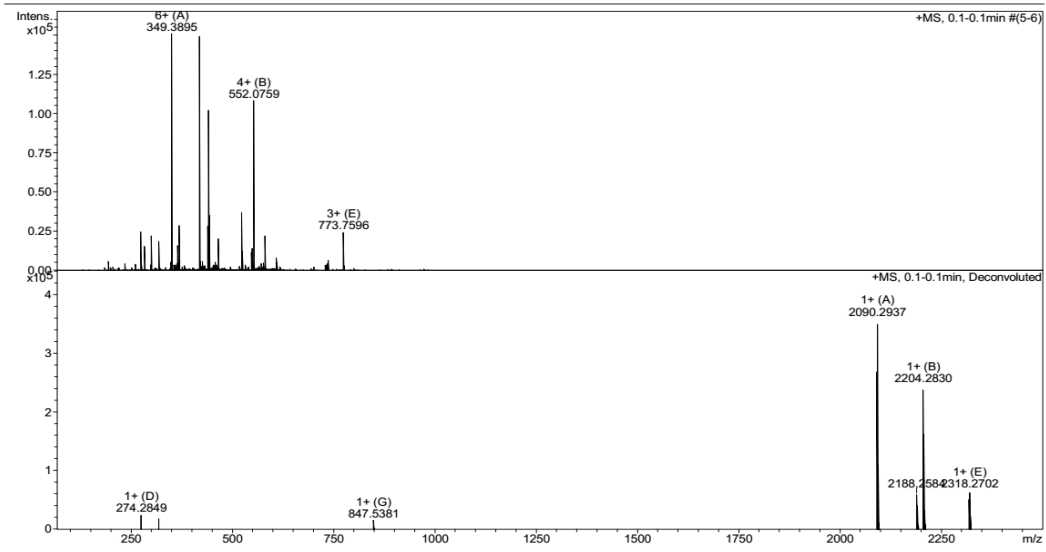
A3u: Non-Stapled R₈GRKKRRS₅RRR-NH₂, C₆₉H₁₃₄N₃₂O₁₁



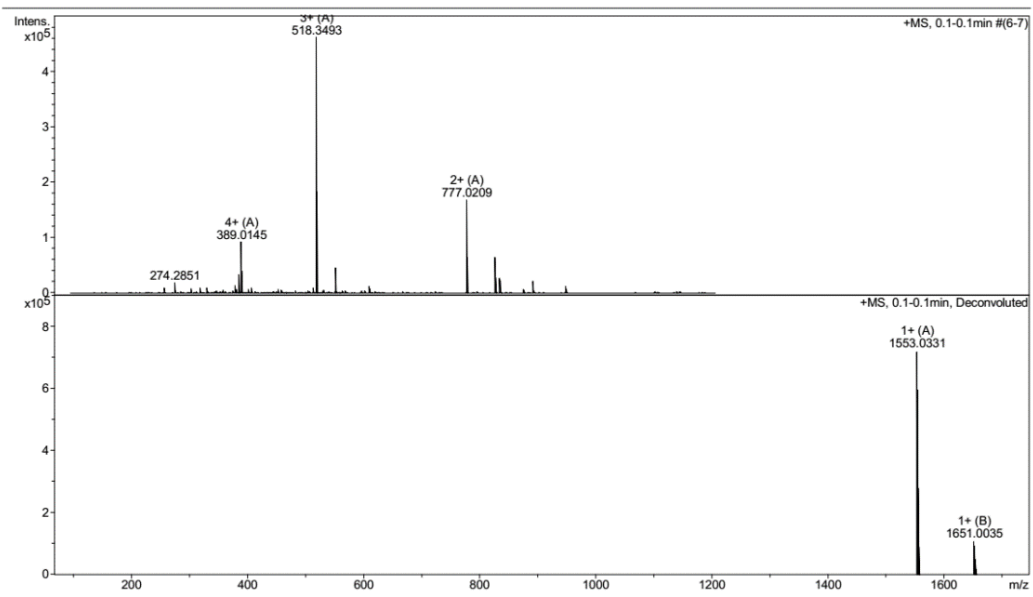
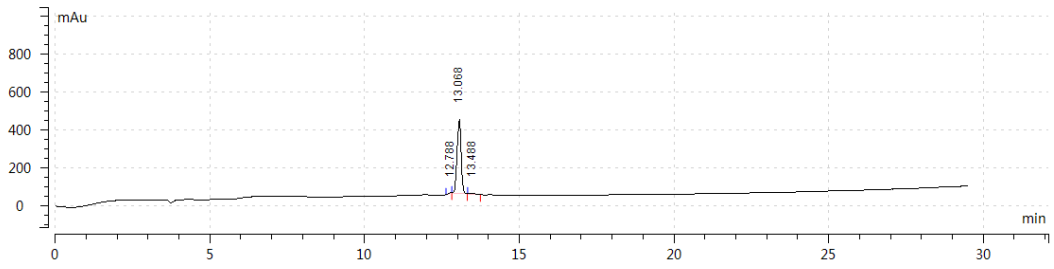
FITC labelling A3u: Non-Stapled FITC-AcpR₈GRKKRRS₅RRR-NH₂,

C₉₆H₁₅₆N₃₄O₁₇S

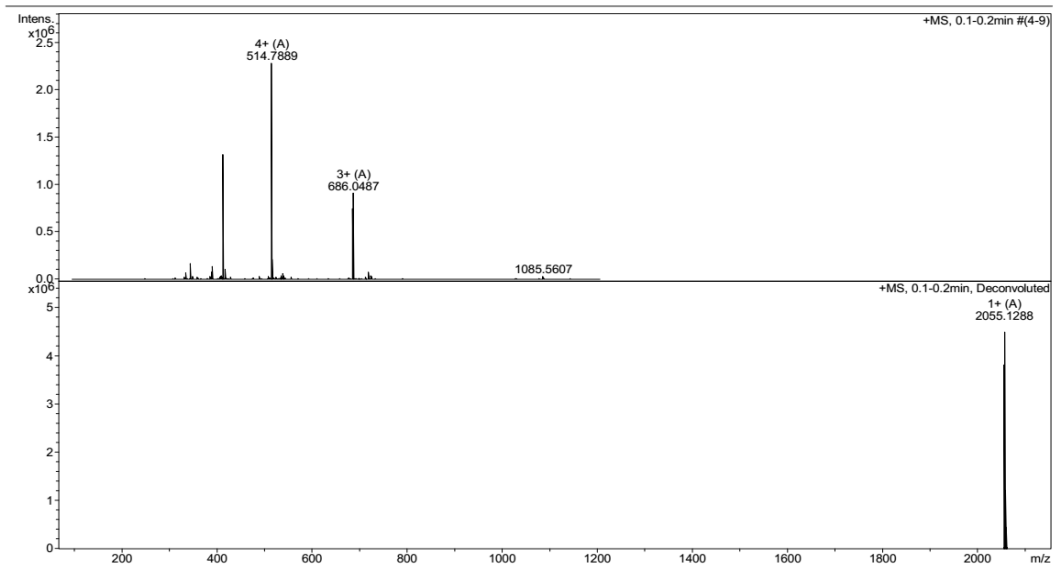
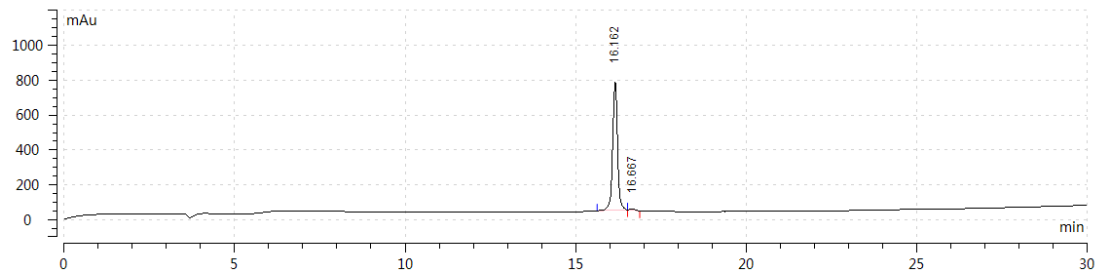




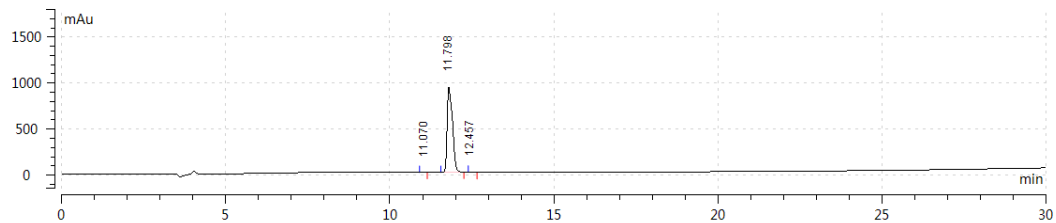
A4u: Non-Stapled YGRKS₅RRQS₅RR-NH₂, C₆₈H₁₂₁N₂₉O₁₃

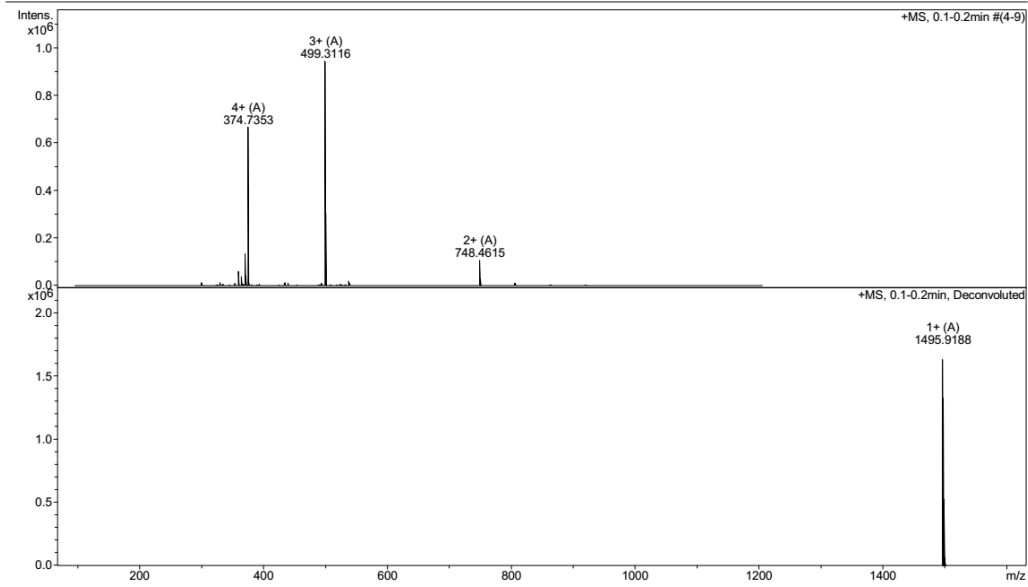


FITC labelling A4u: Non-Stapled FITC-AcpYGRKS₅RRQS₅RR-NH₂,
C₉₅H₁₄₃N₃₁O₁₉S

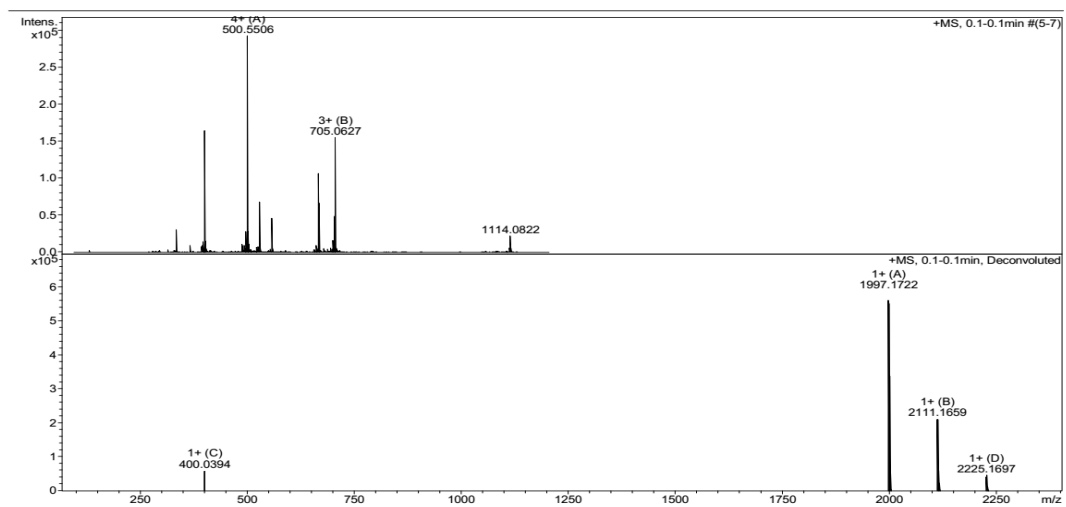
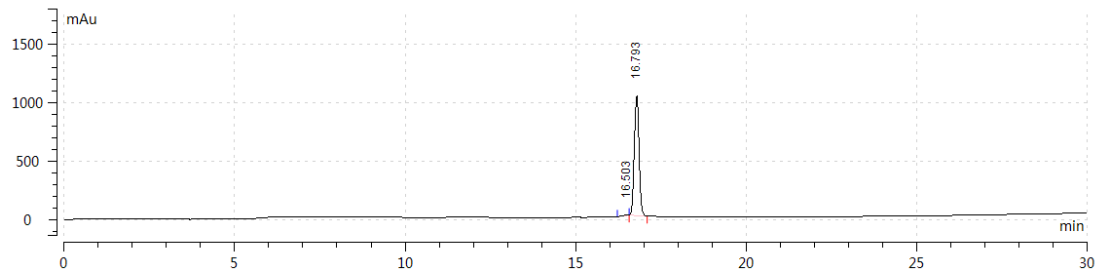


A6u: Non-Stapled YGRAS₅RRQS₅RR-NH₂, C₆₅H₁₁₄N₂₈O₁₃

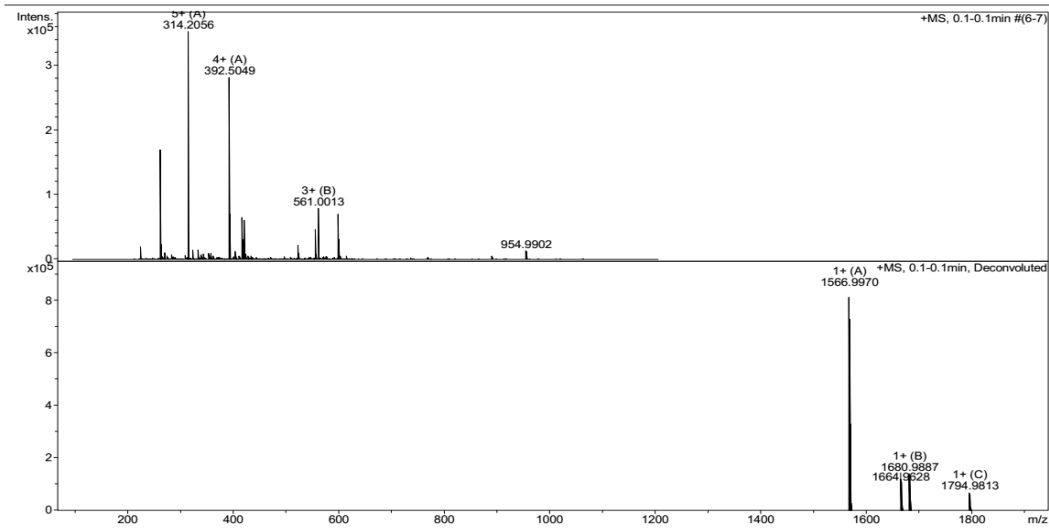
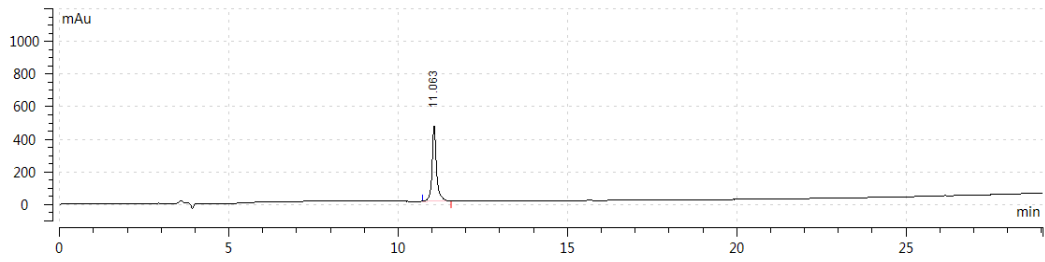




FITC labelling A6u: Non-Stapled FITC-AcpYGRAS₅RRQS₅RR-NH₂,
 $C_{92}H_{136}N_{30}O_{19}S$

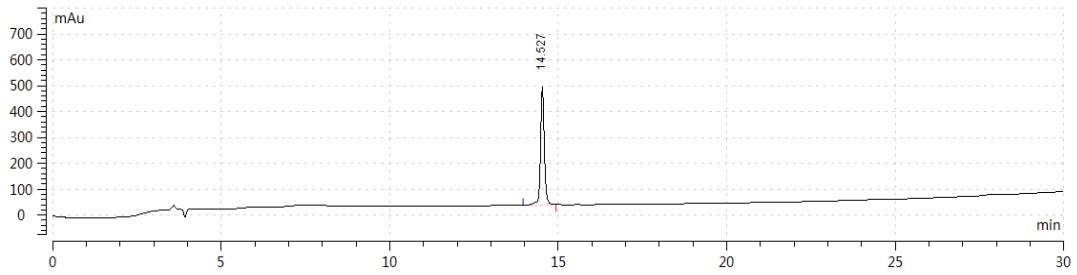


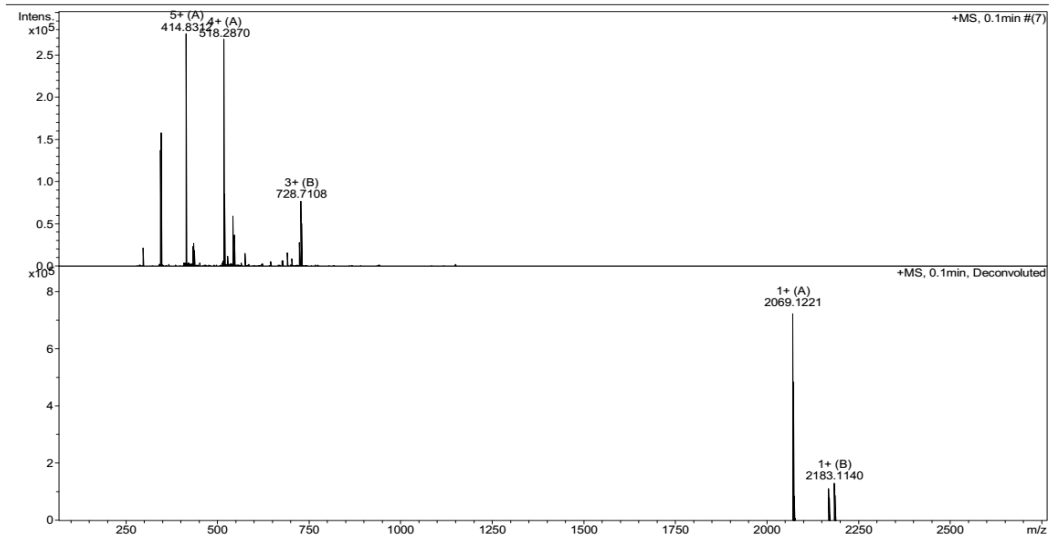
A9: Stapled YGRKR₈RRQS₅RR-NH₂, C₆₉H₁₂₃N₂₉O₁₃



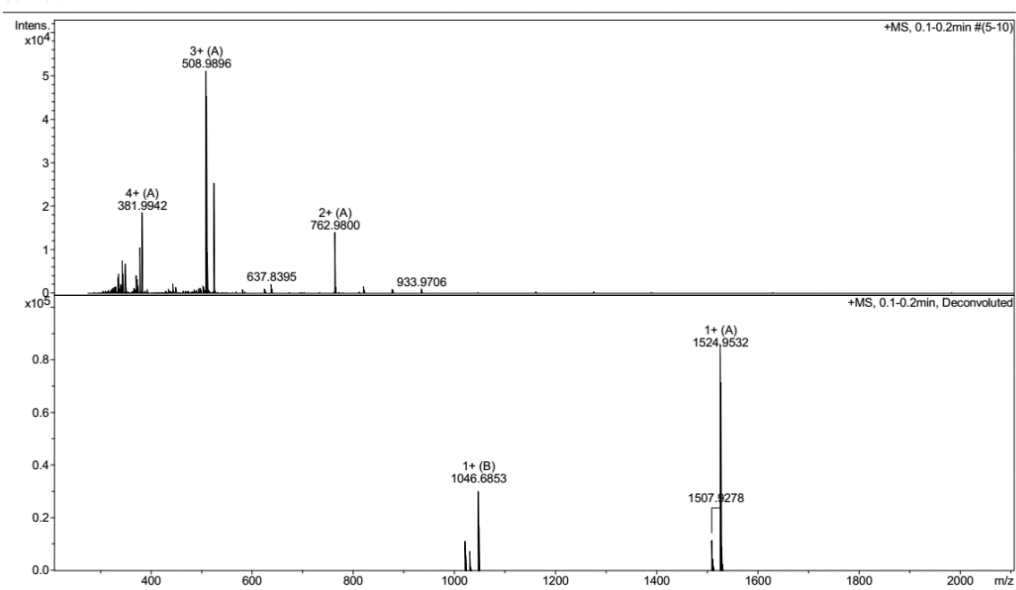
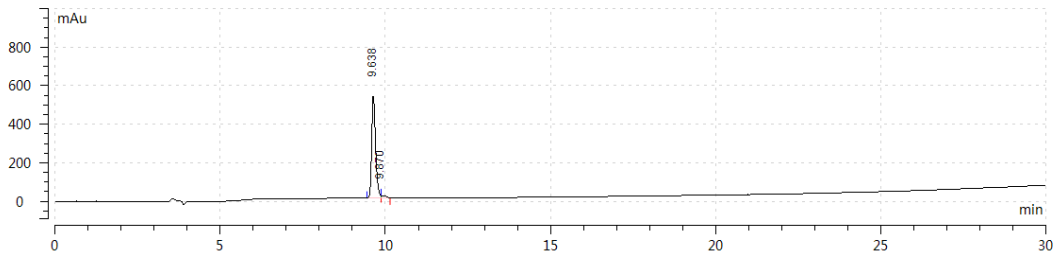
FITC labelling A9: Stapled FITC-AcpYGRKR₈RRQS₅RR-NH₂,

C₉₆H₁₄₅N₃₁O₁₉S

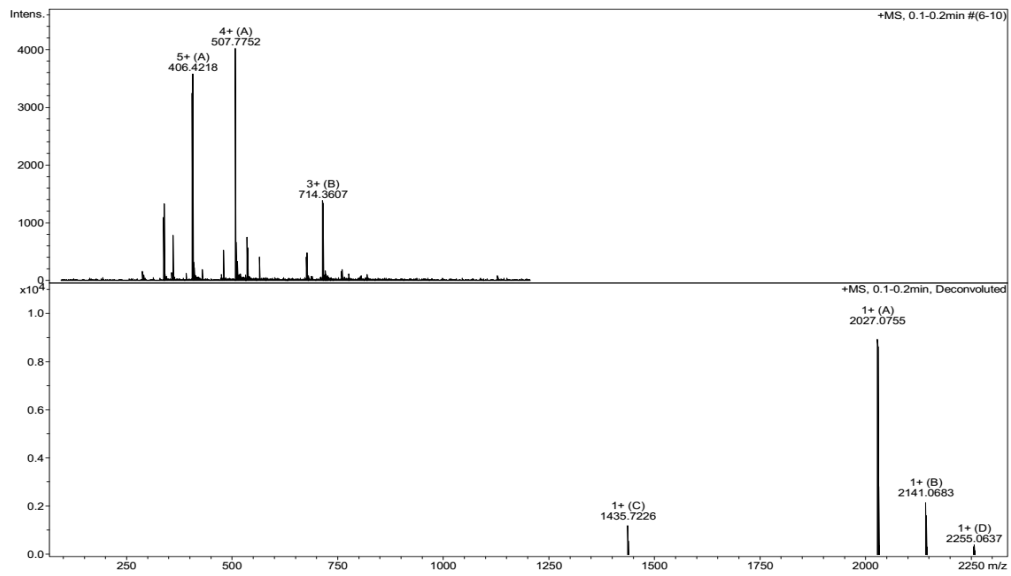
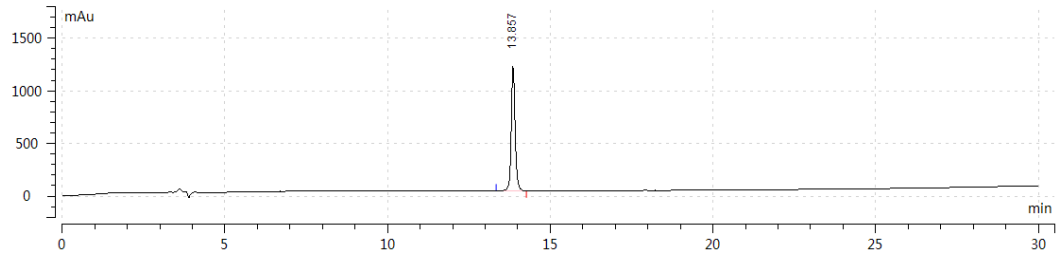




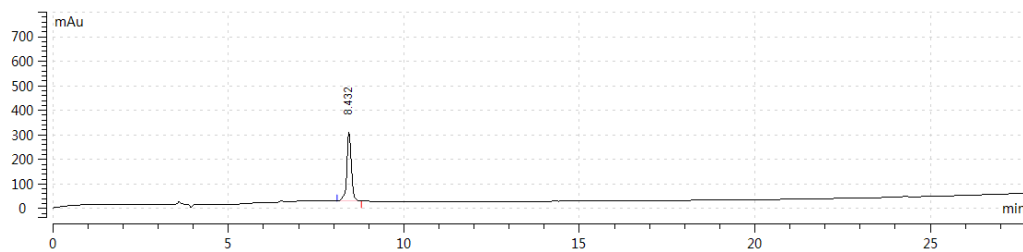
A10: Staple YGRKR₈RRQXRR-NH₂, C₆₆H₁₁₇N₂₉O₁₃

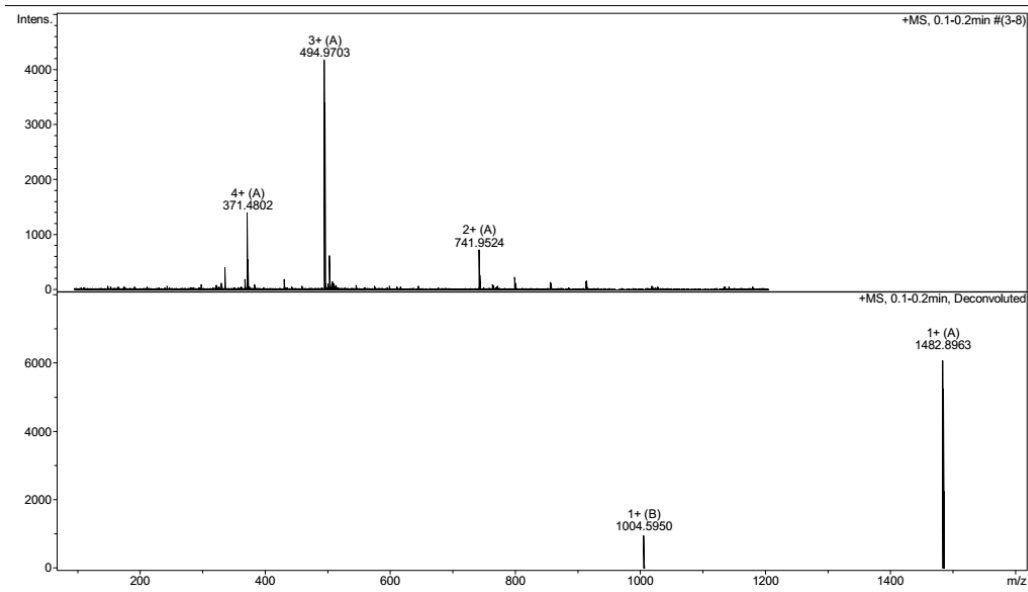


FITC labelling A10: Stapled FITC-AcpYGRKR₈RRQXRR-NH₂,
C₉₃H₁₃₉N₃₁O₁₉S

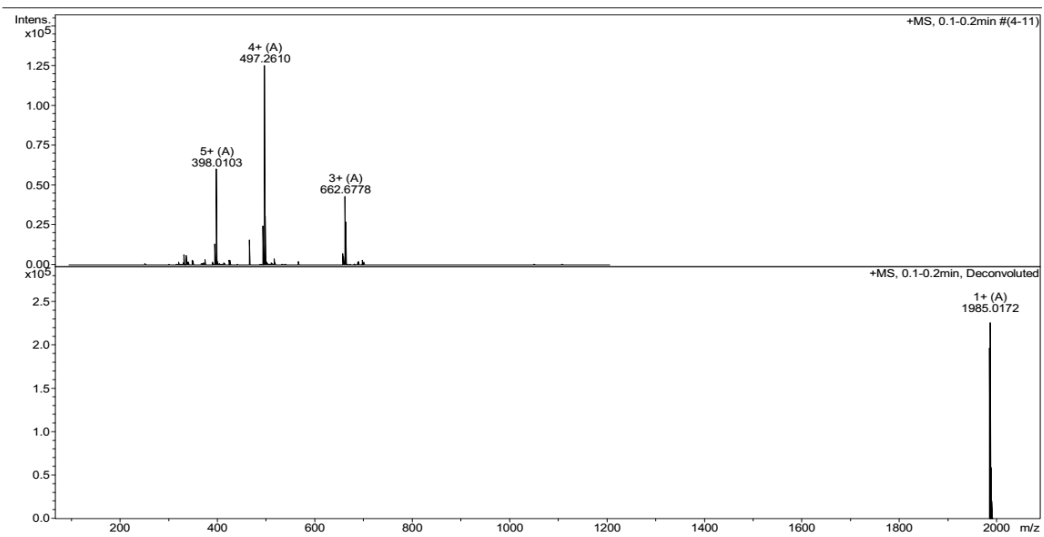
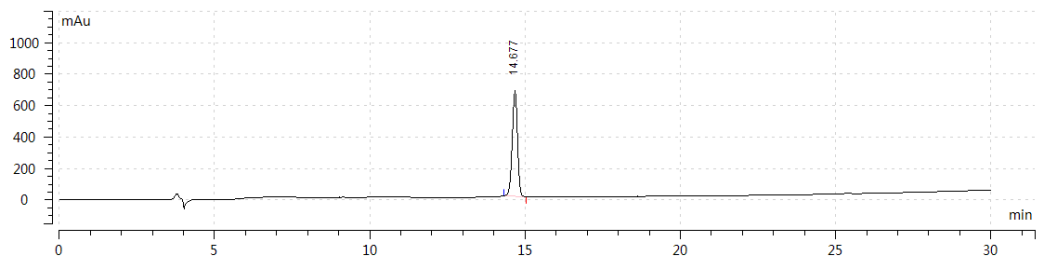


A11: Stapled YGRKS₅RRQXRR-NH₂, C₆₃H₁₁₁N₂₉O₁₃

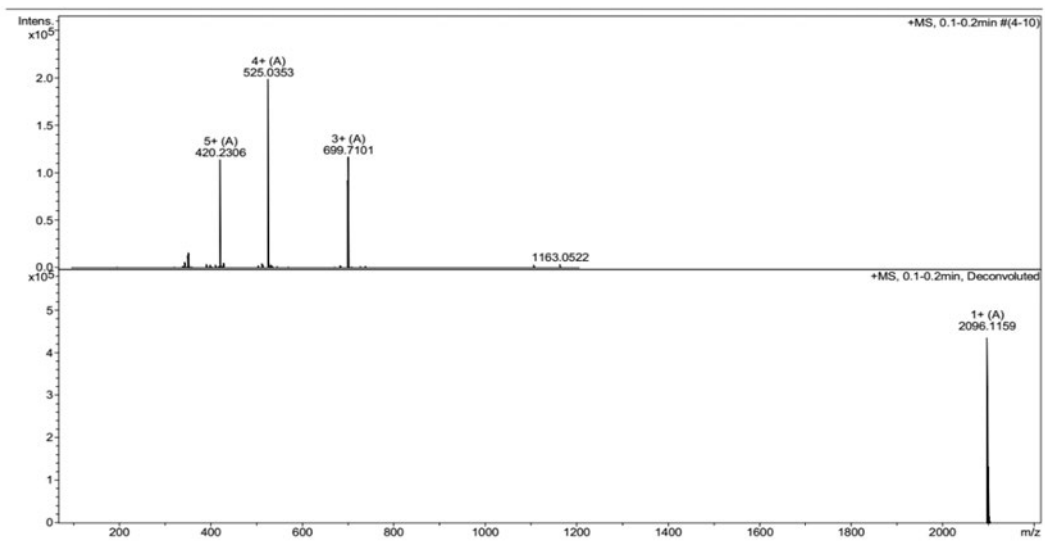
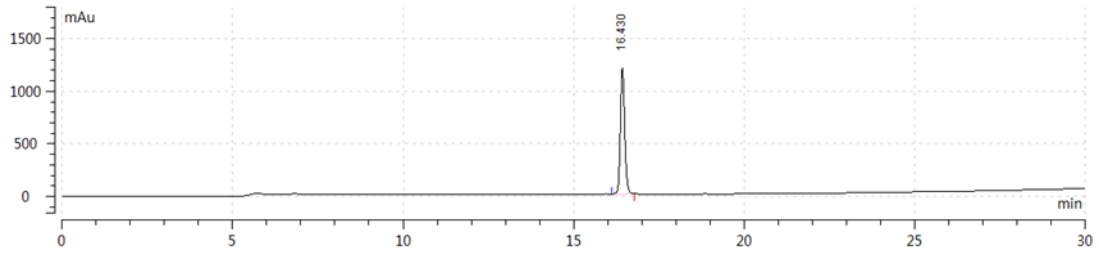




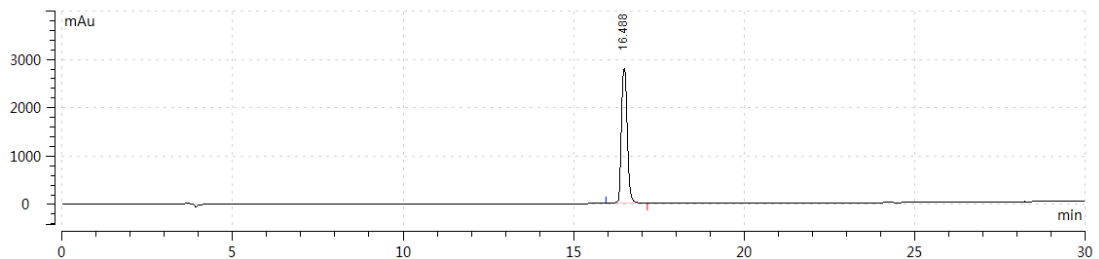
FITC labelling A11: Stapled FITC-AcpYGRKS₅RRQXRR-NH₂,
 $C_{90}H_{133}N_{31}O_{19}S$

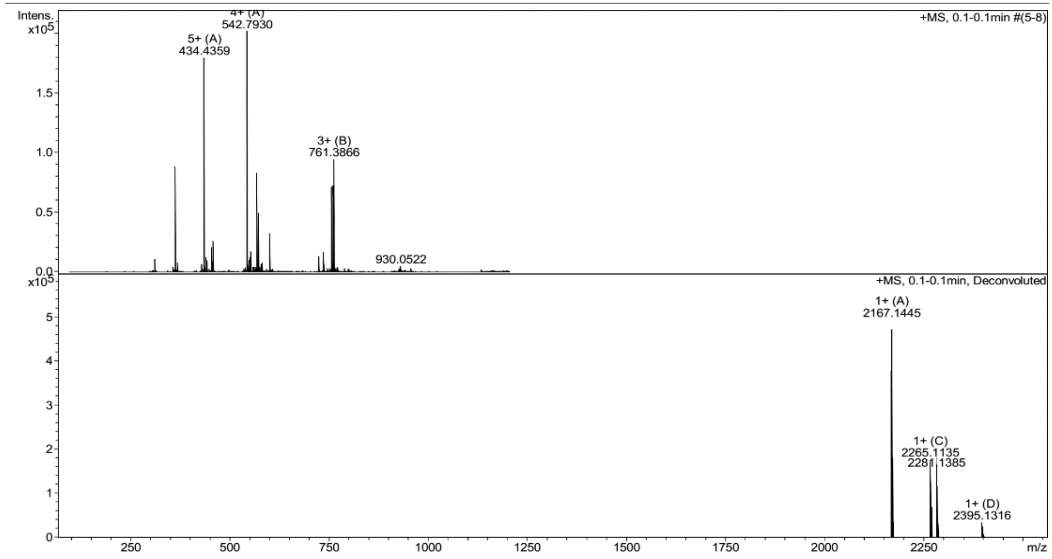


FITC labelling 12: Stapled FITC-Acp-YGRKS₅RRΦS₅RR-NH₂,
C₁₀₁H₁₄₂N₃₀O₁₈S

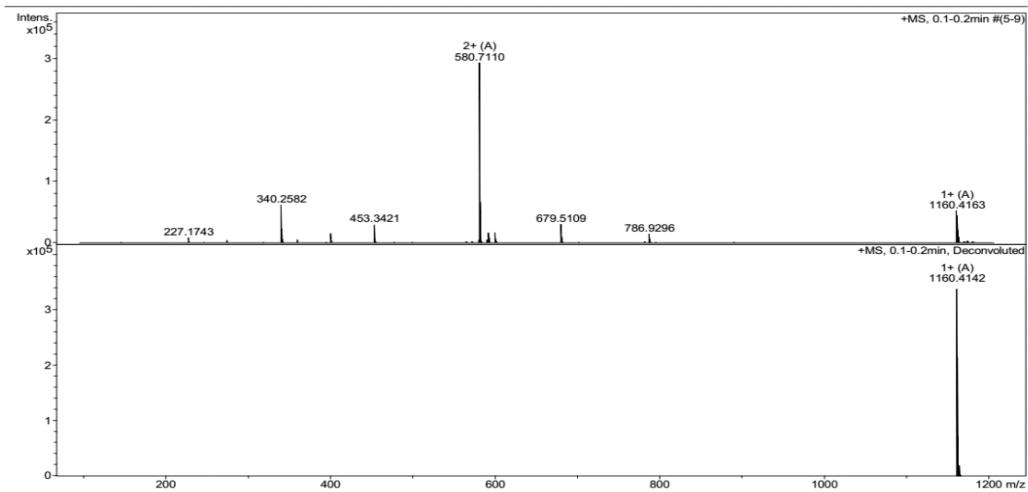
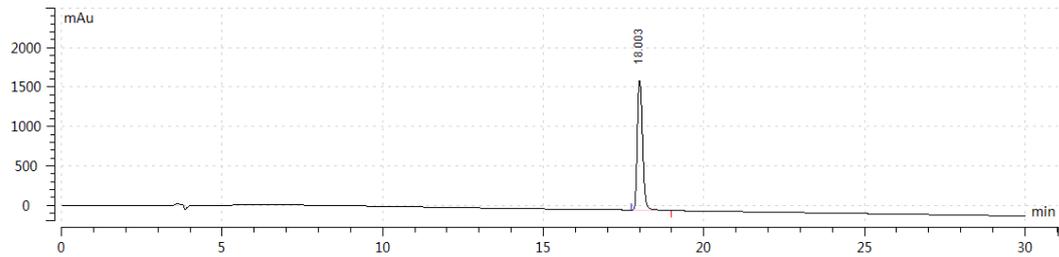


FITC labelling A13: FITC-Acp-YΦRKS₅RRQS₅RR-NH₂,
C₁₀₄H₁₄₇N₃₁O₁₉S



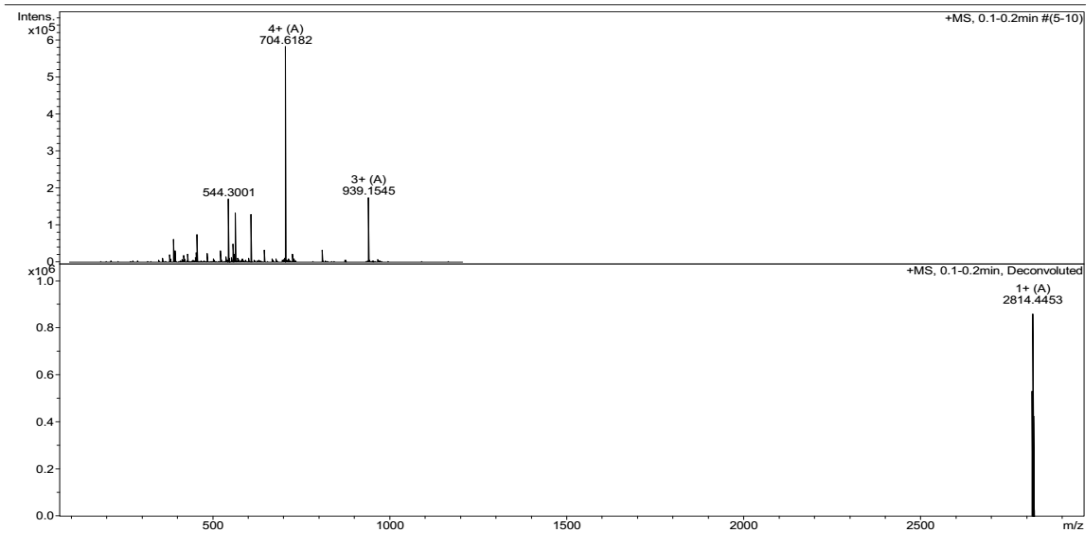
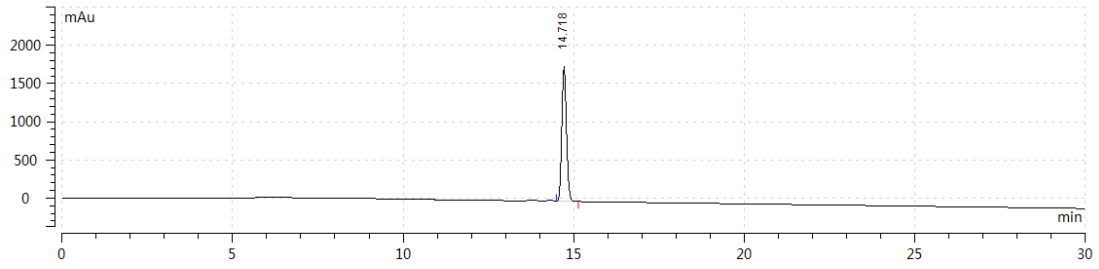


FITC labelling B1: FITC-AcpAGpTALF-NH₂, C₅₄H₆₆N₉O₁₆PS

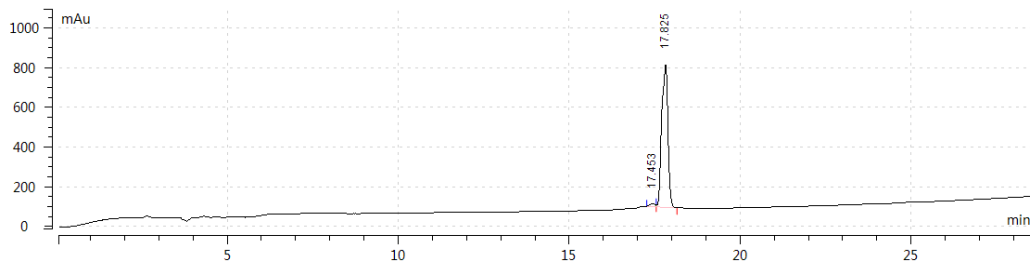


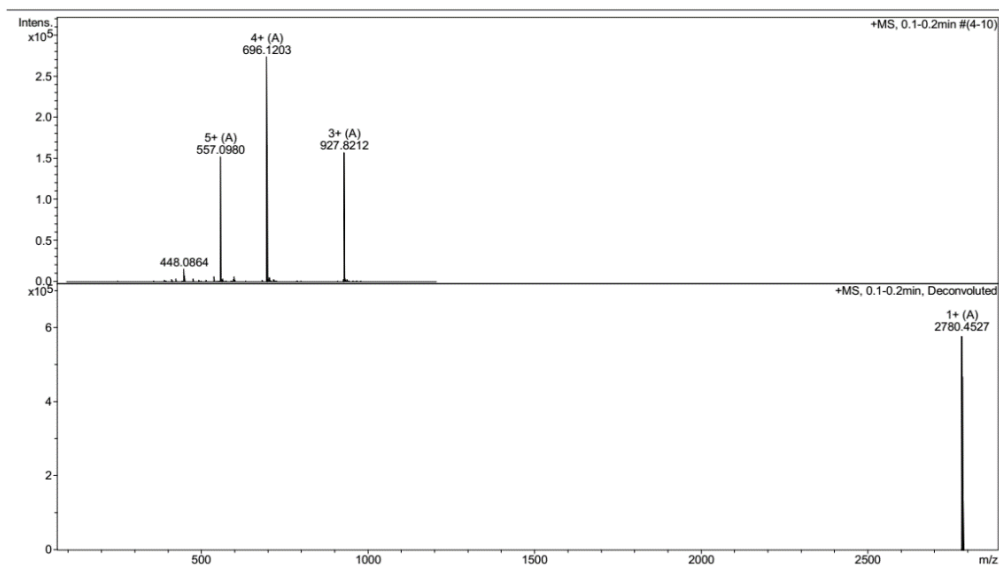
FITC labelling B2: FITC-AcpAGpTALF-AcpYGRKKRRQRRR-NH₂,

C₁₂₄H₁₉₂N₄₁O₃₁PS



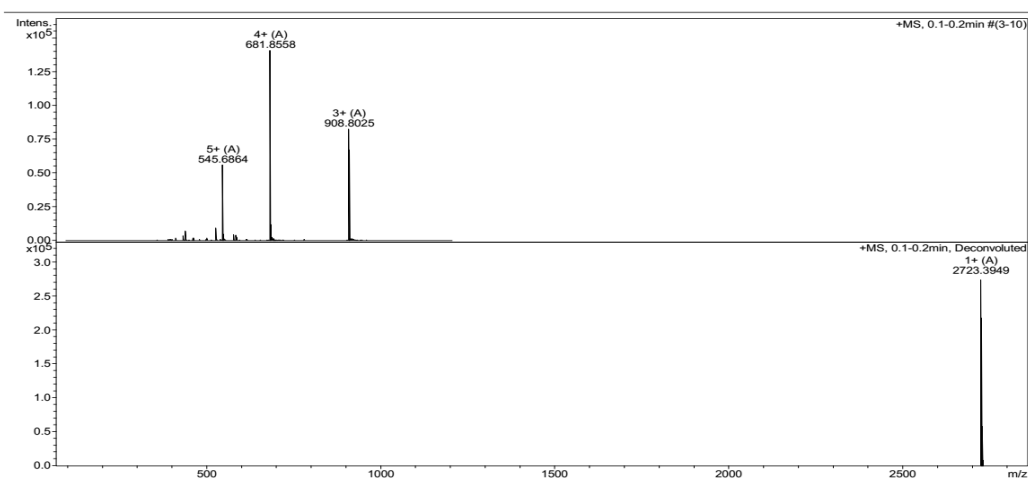
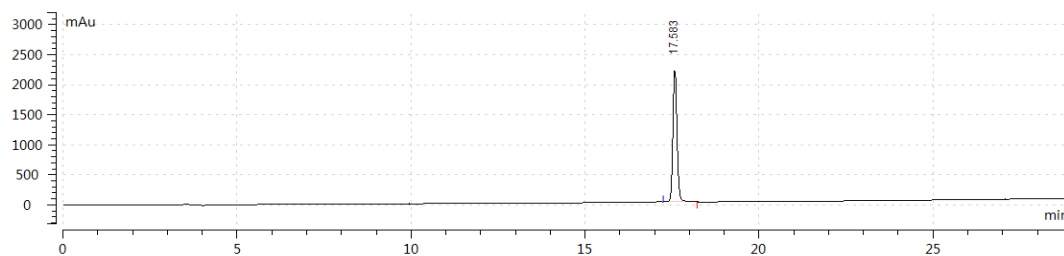
FITC labelling B3: Stapled FITC-AcpYGRKS₅RRQS₅RR-
 AcpAGpTALF-NH₂ C₁₂₆H₁₉₀N₃₇O₃₁PS



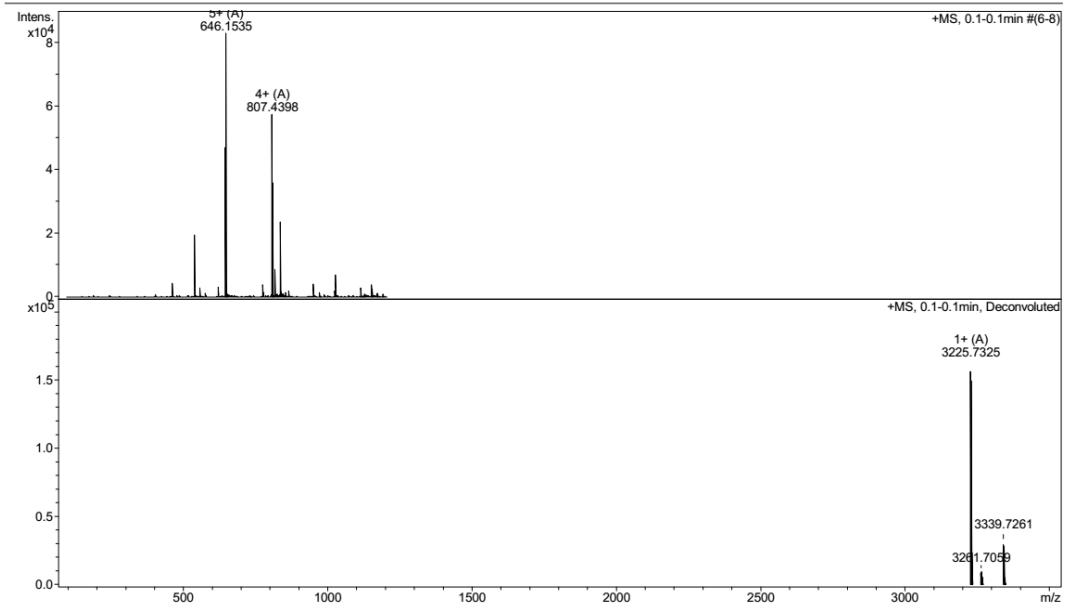
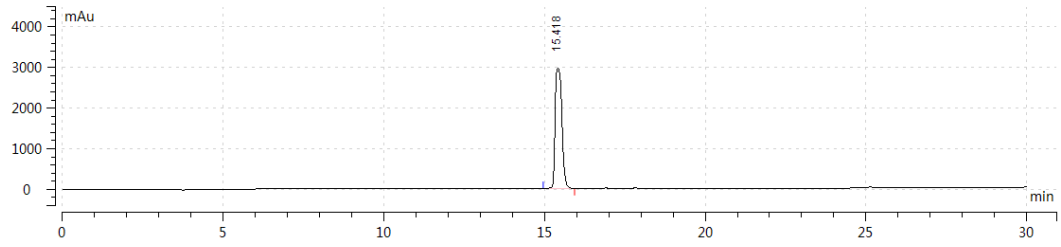


FITC labelling B4: Staple FITC-AcpYGRAS₅RRQS₅RR-AcpAGpTALF-

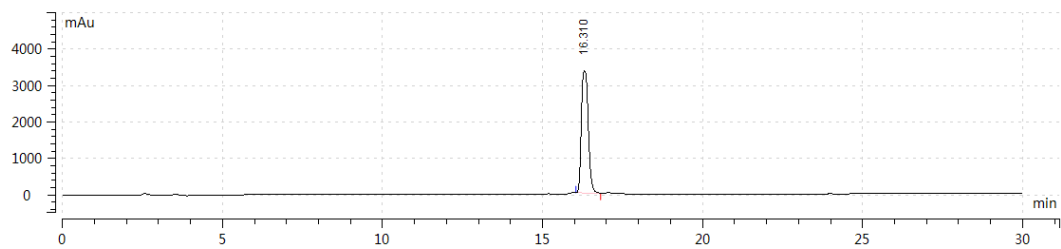
NH₂ C₁₂₃H₁₈₃N₃₆O₃₁PS

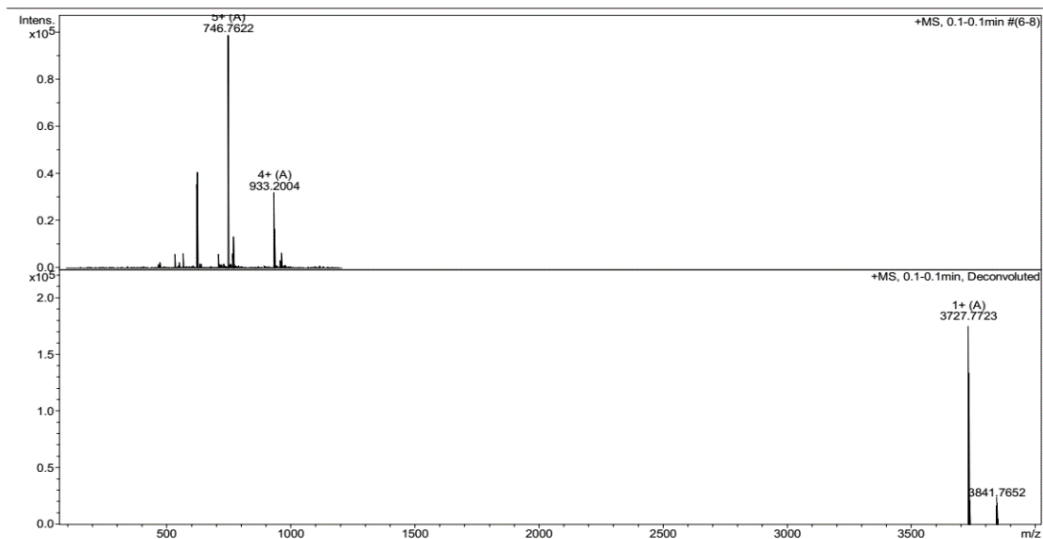


C1: YGRKKRRQRRRG C-(S-S)-CGTALDWSWLQTE C₁₃₆H₂₂₁N₅₁O₃₇S₂

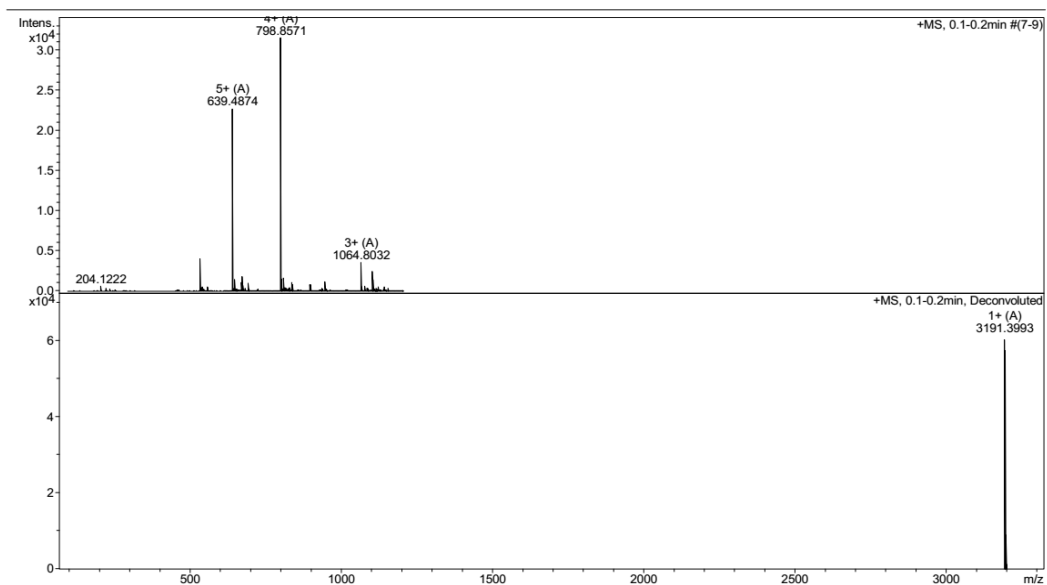
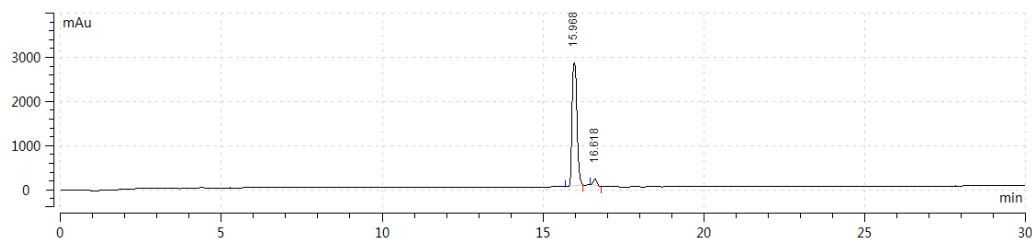


FITC labelling C1: FITC-AcpYGRKKRRQRRRGC-(S-S)-
CGTALDWSWLQTE, C₁₆₃H₂₄₃N₅₃O₄₃S₃



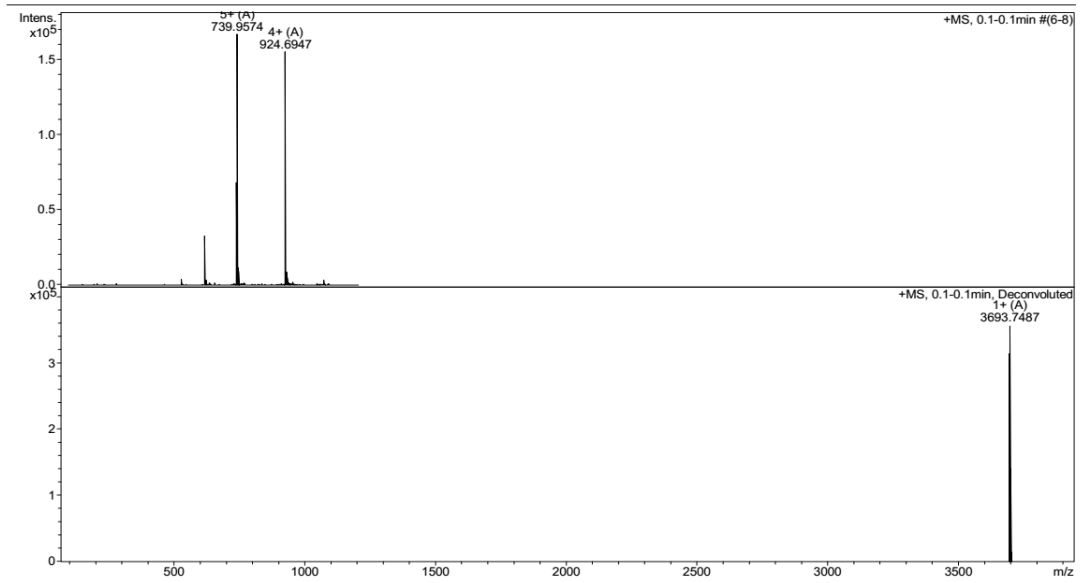
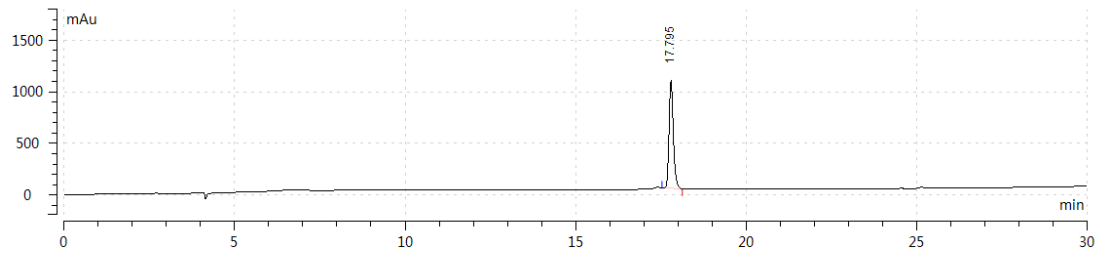


C2: Stapled YGRKS₅RRQS₅RRGC-(S-S)-CGTALDWSWLQTE,

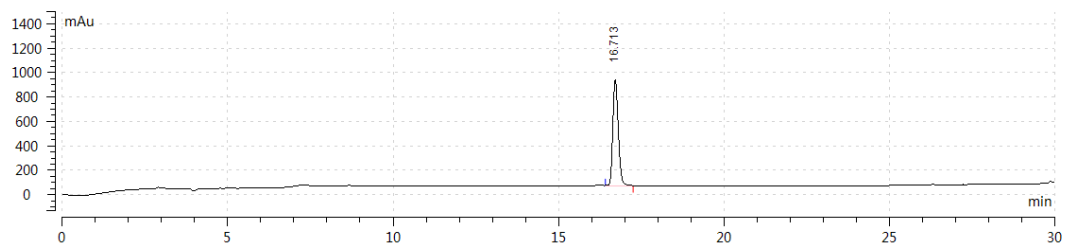
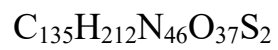


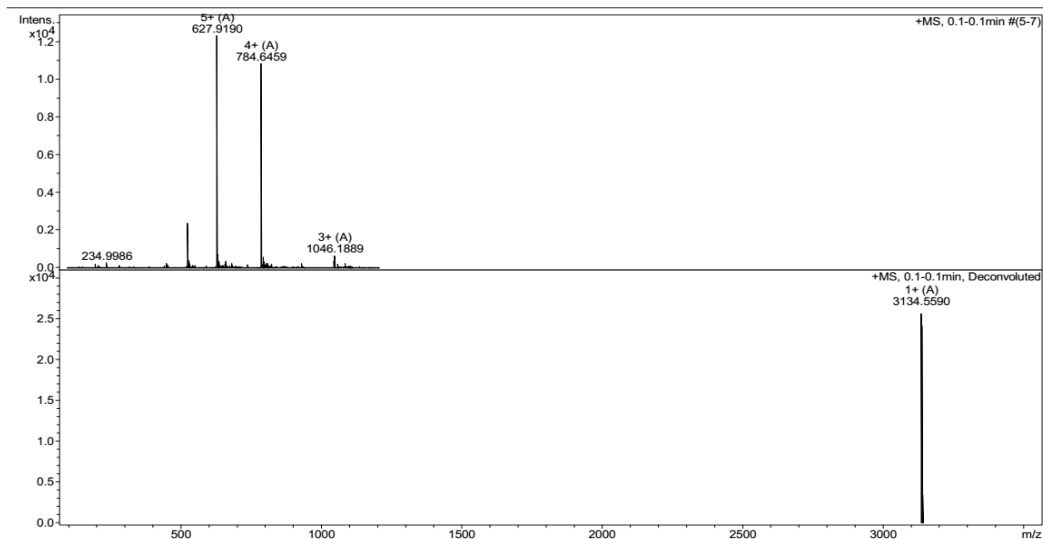
FITC labelling C2: Stapled FITC-AcpYGRKS₅RRQS₅RRGC-(S-S)-



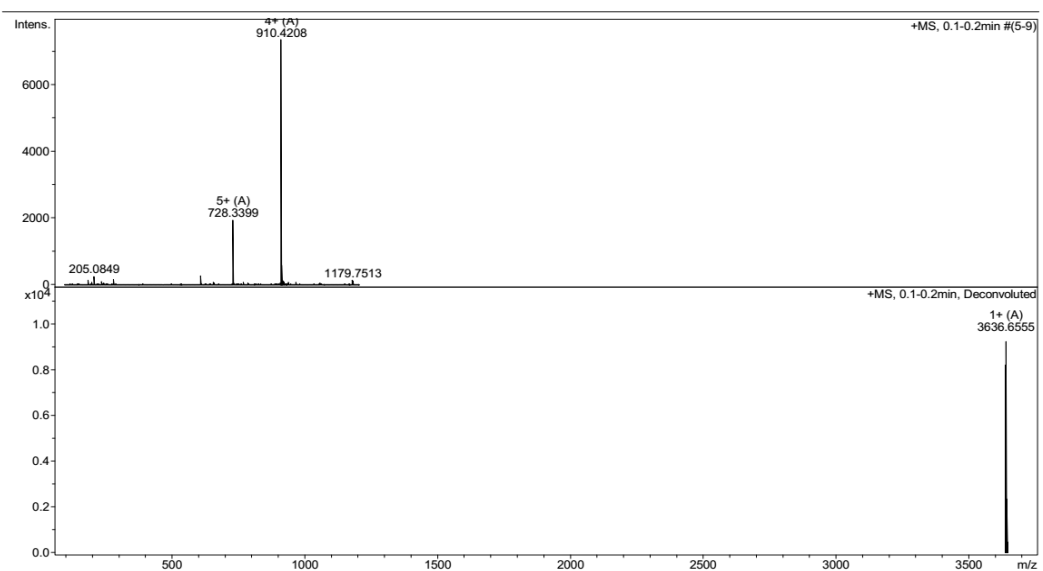
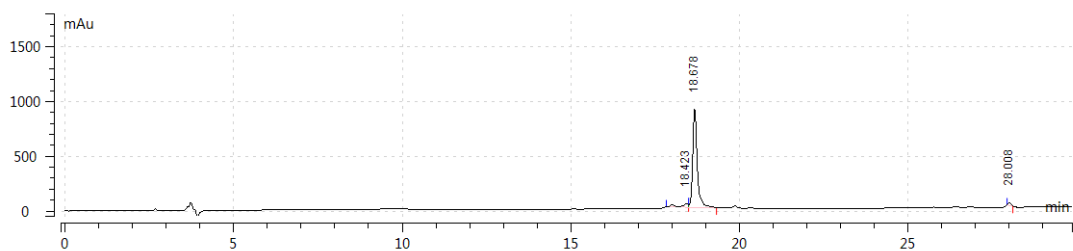


C3: Stapled YGRAS₅RRQS₅RRGC-(S-S)-CGTALDWSWLQTE,

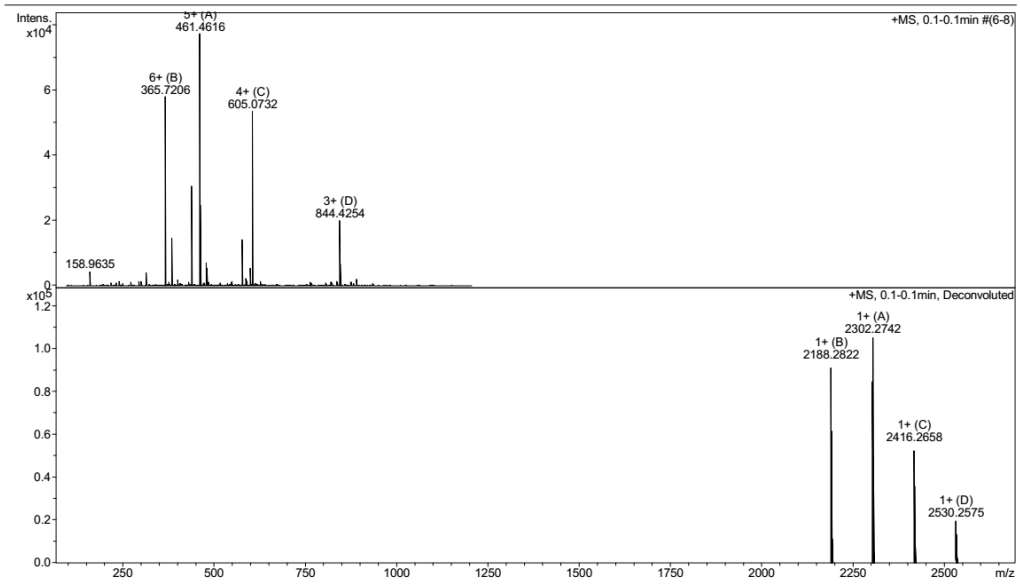
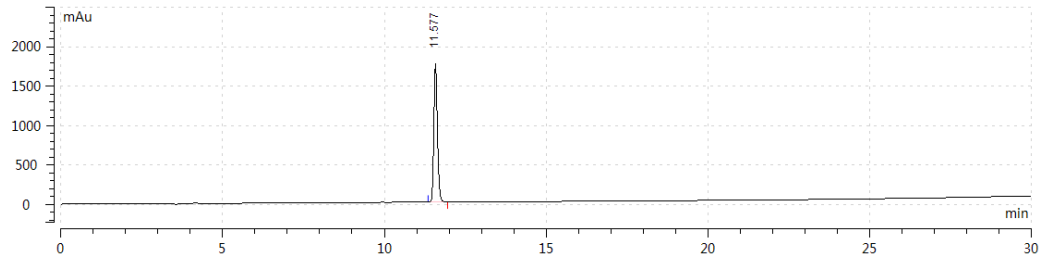




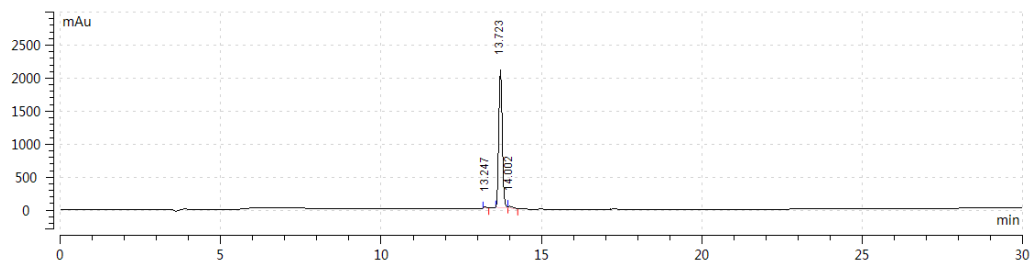
FITC labelling C3: Stapled FITC-AcpYGRAS₅RRQS₅RRGC-(S-S)-CGTALDWSWLQTE, C₁₆₂H₂₃₄N₄₈O₄₃S₃

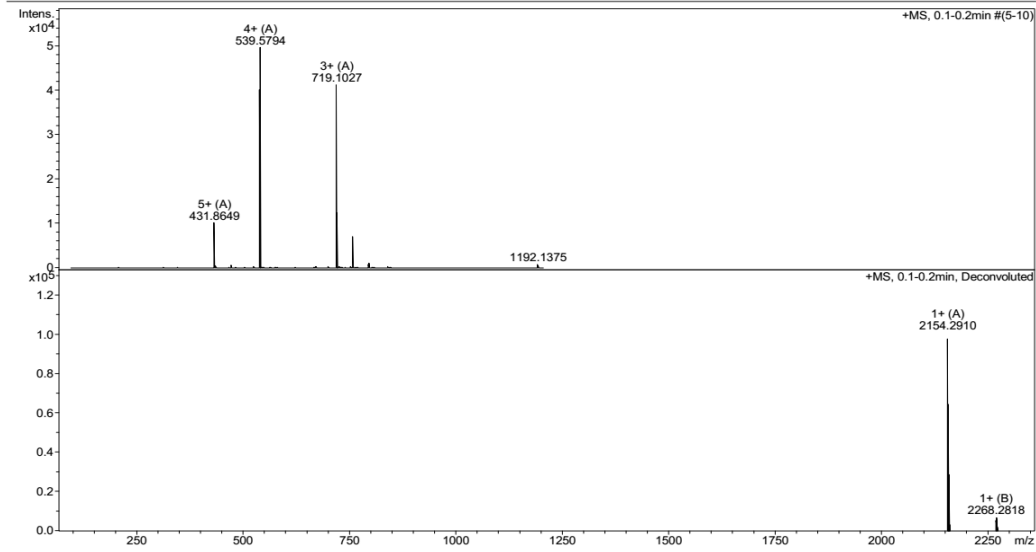


D1: Biotin-miniPEG₂-Acp-YGRKKRRQRRR-NH₂, C₉₂H₁₆₆N₃₈O₂₂

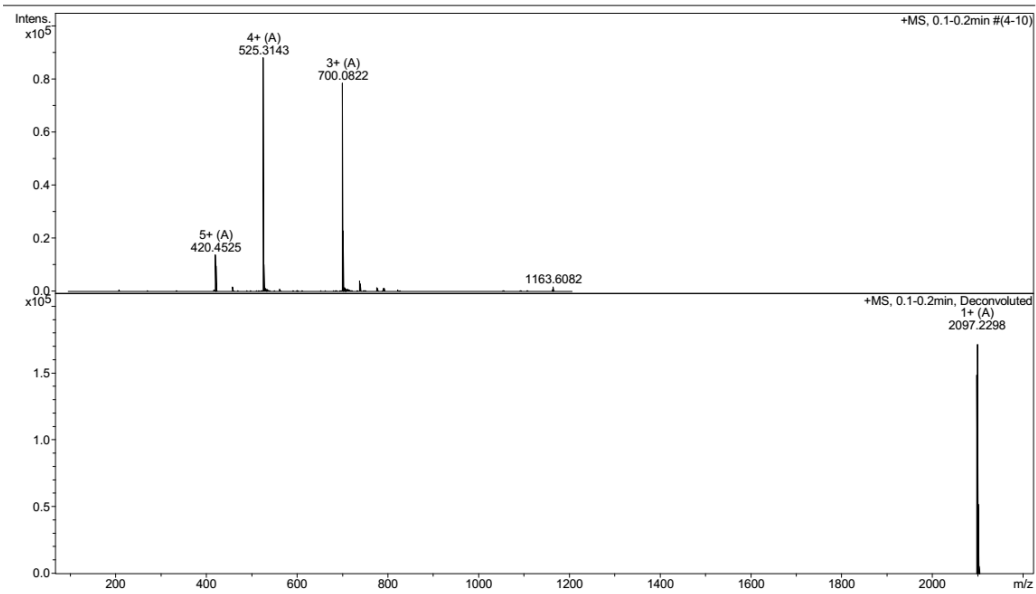
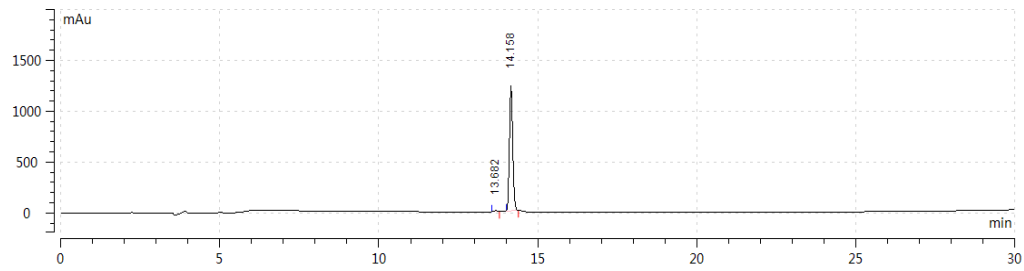


D2: Stapled Biotin-miniPEG₂-Acp-YGRKS₅RRQS₅RR-NH₂,

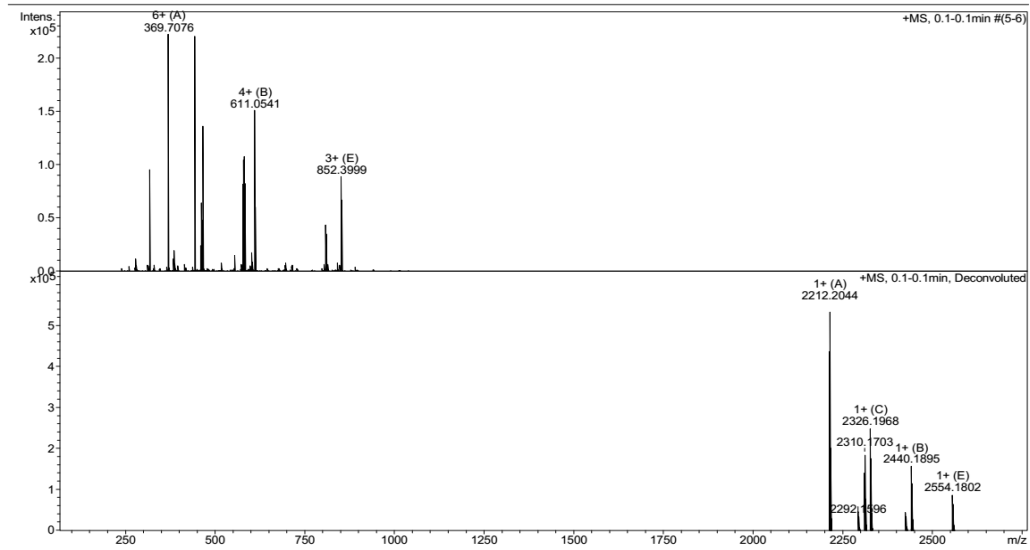
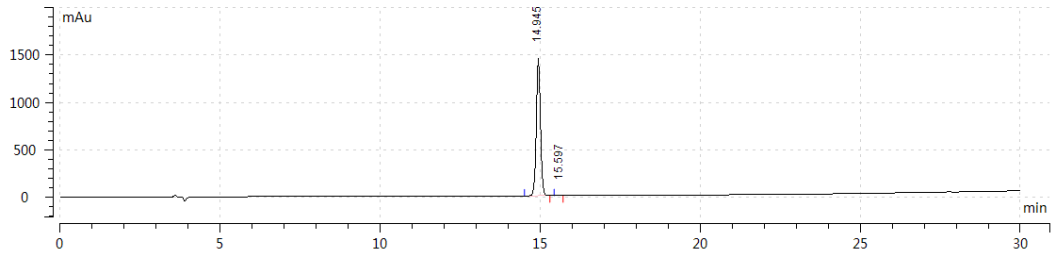




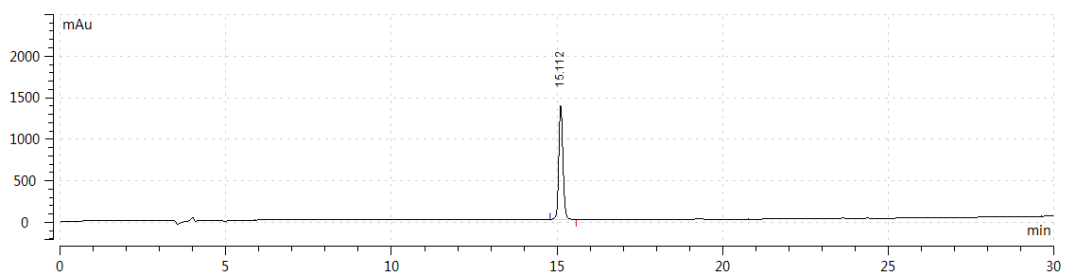
D3: Stapled Biotin-miniPEG₂-Acp-YGRAS₅RRQS₅RR-NH₂,

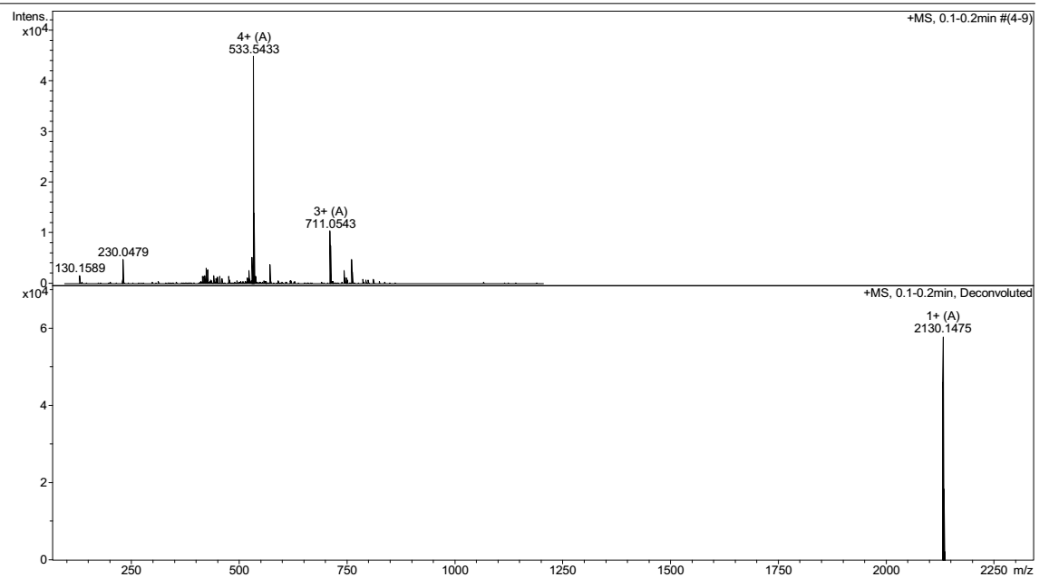


Rho labelling A1: Rho-AcpYGRKKRRQRRR-NH₂, $C_{97}H_{158}N_{36}O_{20}S_2$

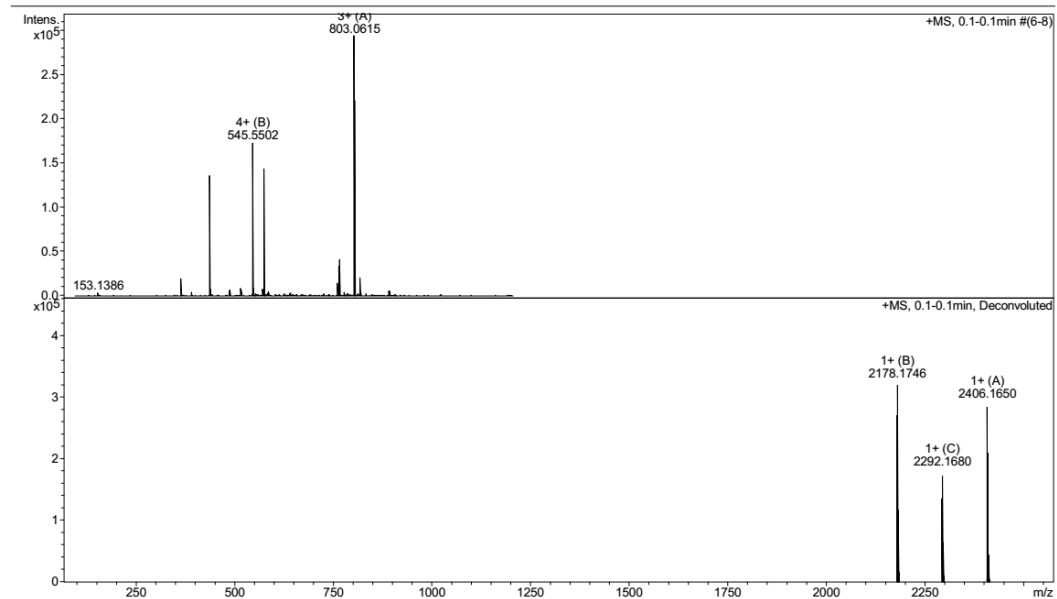
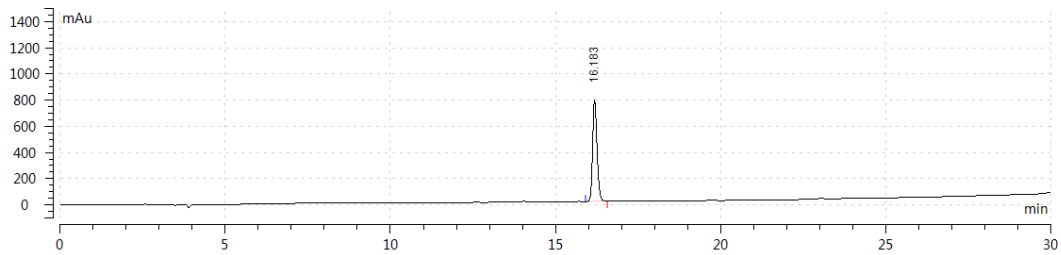


NF labelling A1: NF- AcpYGRKKRRQRRR-NH₂, C₉₉H₁₄₄N₃₄O₂₀

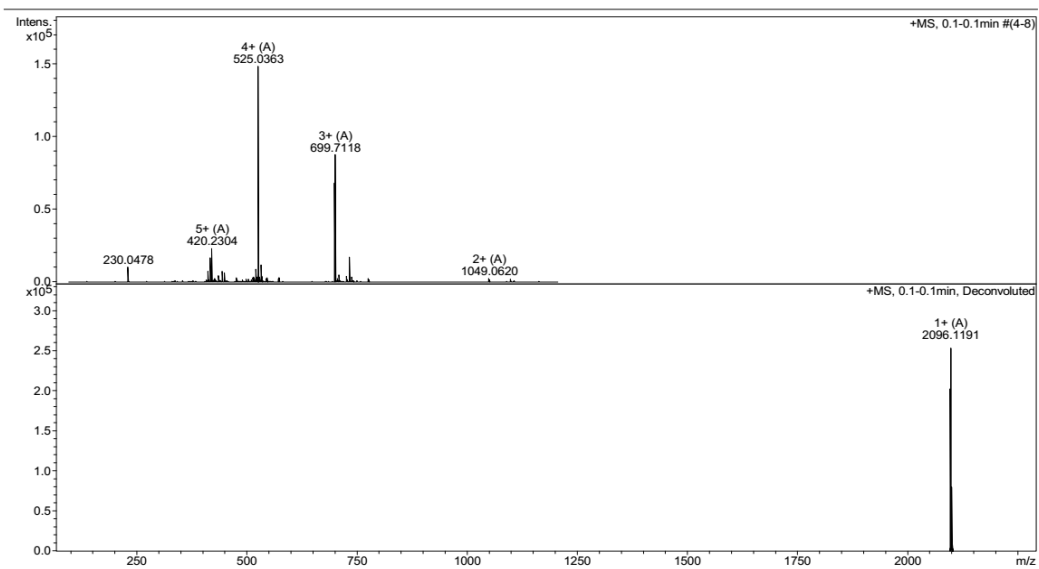
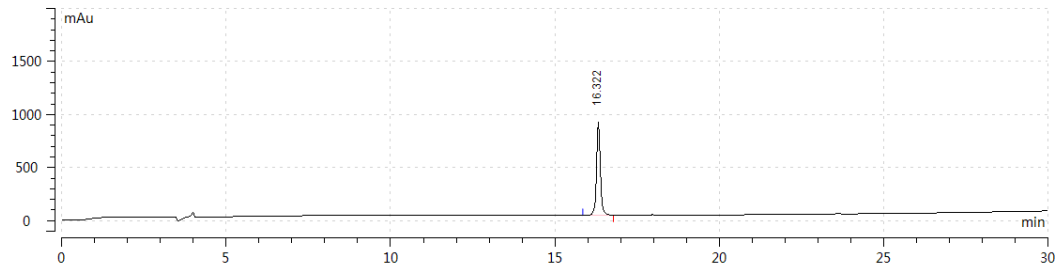
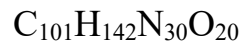




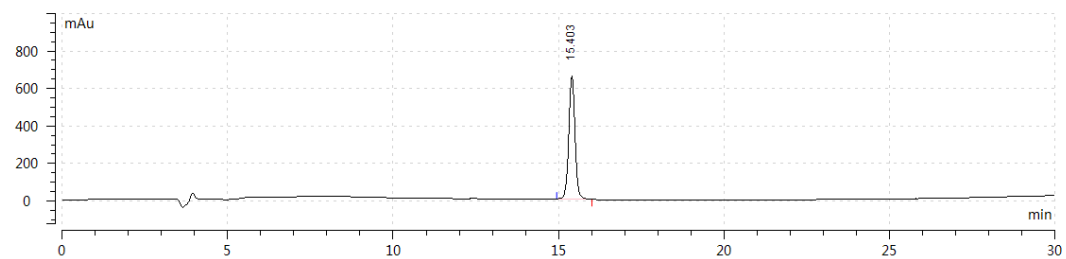
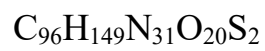
Rho labelling A4: Stapled Rho-AcpYGRKS₅RRQS₅RR-NH₂,
 C₉₉H₁₅₆N₃₂O₂₀S₂

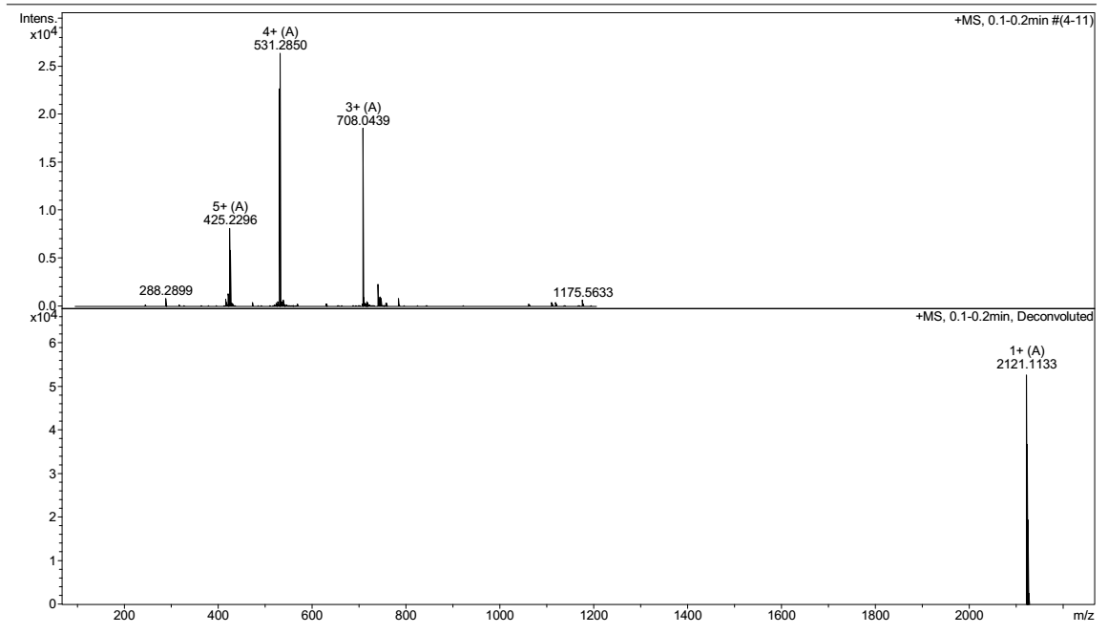


NF labelling A4: Stapled NF-AcpYGRKS₅RRQS₅RR-NH₂,

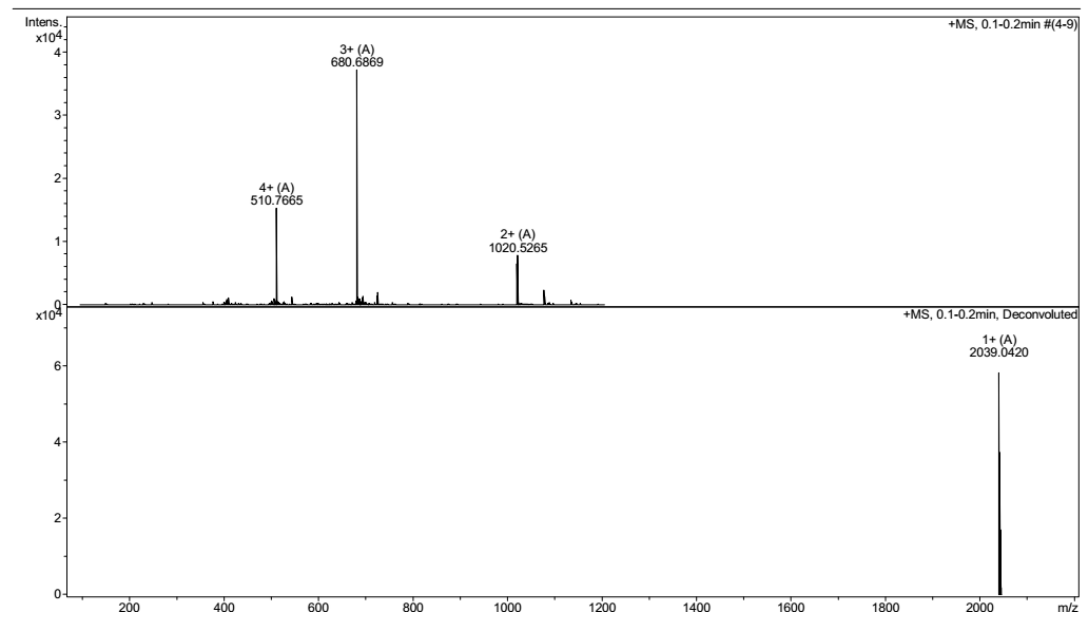
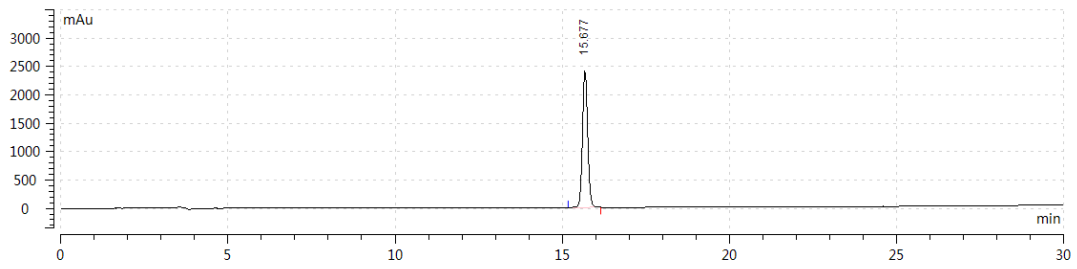


Rho labelling A6: Stapled Rho- AcpYGRAS₅RRQS₅RR-NH₂,

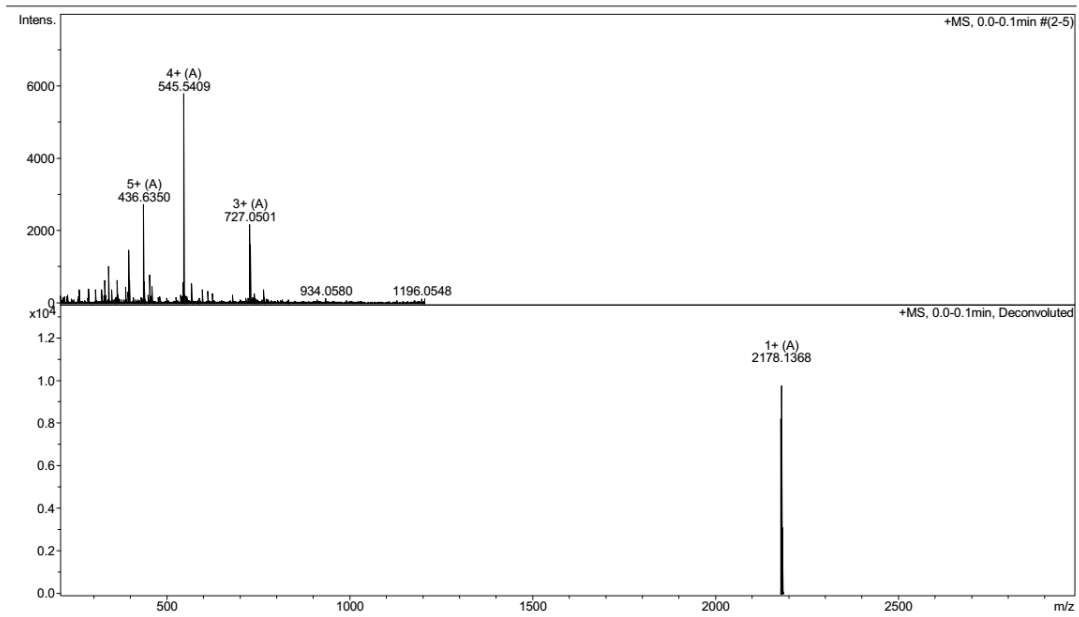
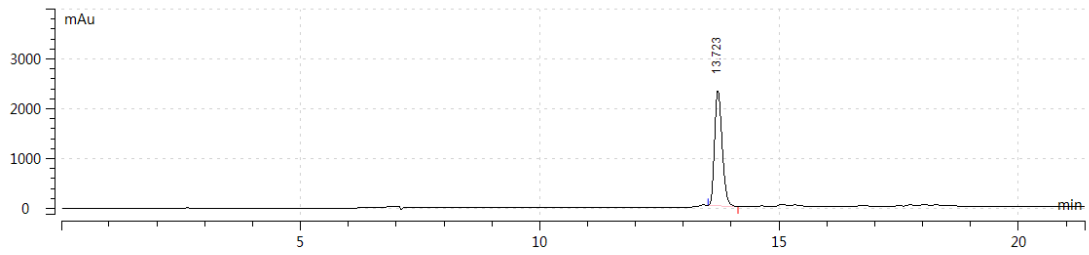




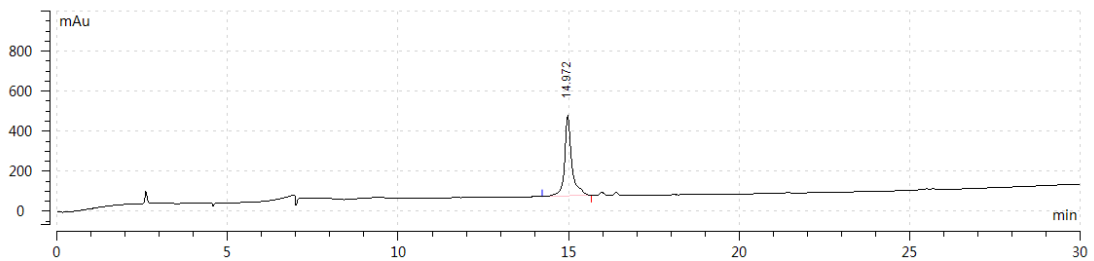
NF labelling A6: Stapled NF- AcpYGRAS₅RRQS₅RR-NH₂, C₉₈H₁₃₅N₂₉O₂₀

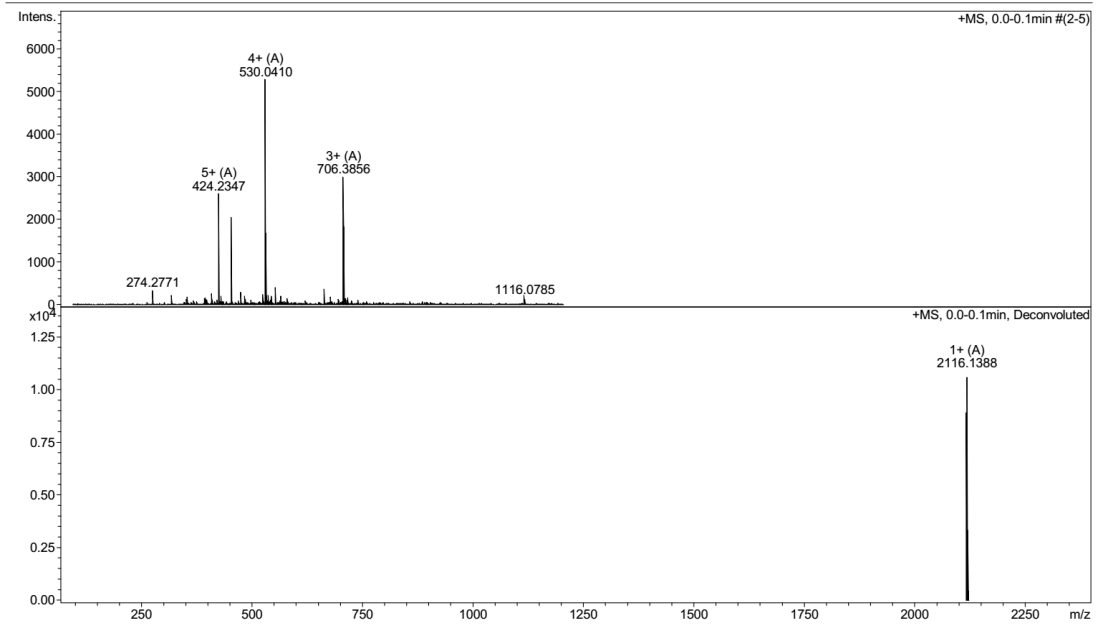


FITC labelling Tat₄₈₋₆₀ FITC-βA-GRKKRRQRRRPPQ

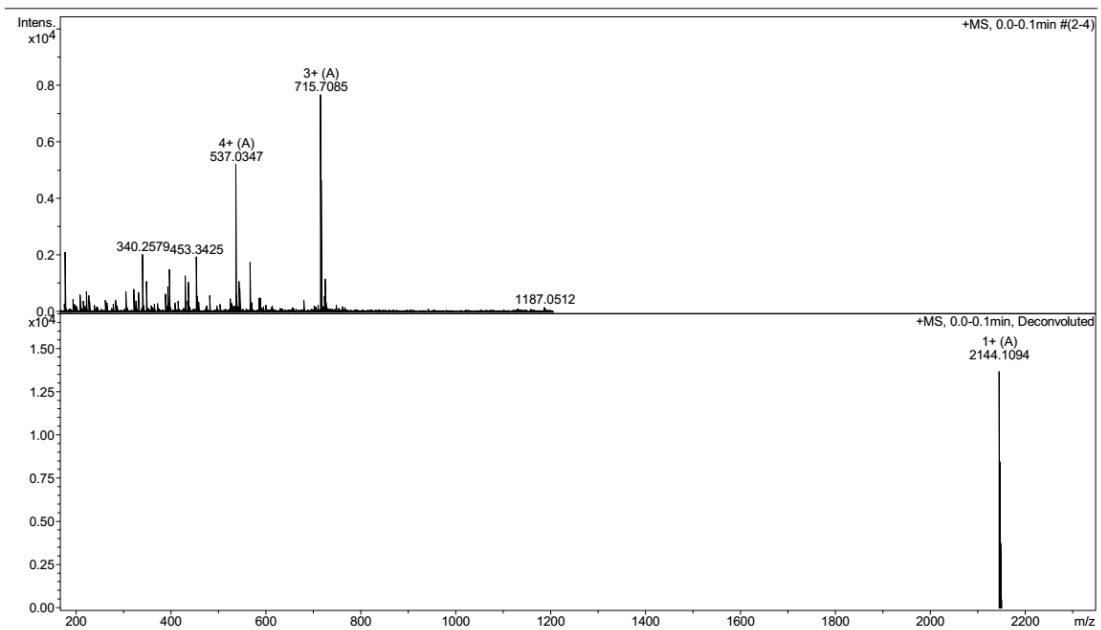
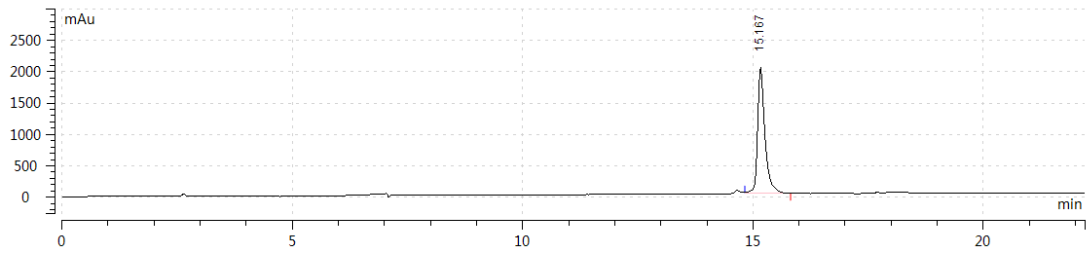


FITC labelling SAH-Tat-1 : Stapled FITC-βA-GRKKKS₅RQRS₅RPPQ





FITC labelling SAH-Tat-2 : Stapled FITC- β A-GRK S₅RRQ S₅RRPPQ



1. Y. W. Kim, T. N. Grossmann and G. L. Verdine, *Nat. Protoc.*, 2011, **6**, 761.
2. J. P. Christian E. Schafmeister, and Gregory L. Verdine, *J. Am. Chem. Soc.*, 2000, **122**, 5891.
3. C. I. Bayly, P. Cieplak, W. Cornell and P. A. Kollman, *J. Phys. Chem.*, 1993, **97**, 10269.
4. C. Simmerling, B. Strockbine and A. E. Roitberg, *J. Am. Chem. Soc.*, 2002, **124**, 11258.
5. M. Feig, P. Rotkiewicz, A. Kolinski, J. Skolnick and C. L. Brooks, *Proteins-Structure Function and Bioinformatics*, 2000, **41**, 86.
6. G. Ozer, E. F. Valeev, S. Quirk and R. Hernandez, *J. Chem. Theory. Comput.*, 2010, **6**, 3026.
7. Y. Zhuang, H. R. Bureau, S. Quirk and R. Hernandez, *Mol. Simulat.*, 2020, DOI: 10.1080/08927022.2020.1807542.
8. A. Andres, M. Roses, C. Rafols, E. Bosch, S. Espinosa, V. Segarra and J. M. Huerta, *Eur. J. Pharm. Sci.*, 2015, **76**, 181.
9. Z. Qian, A. Martyna, R. L. Hard, J. Wang, G. Appiah-Kubi, C. Coss, M. A. Phelps, J. S. Rossman and D. Pei, *Biochemistry*, 2016, **55**, 2601.
10. H. Traboulsi, H. Larkin, M. A. Bonin, L. Volkov, C. L. Lavoie and E. Marsault, *Bioconjugate Chem.*, 2015, **26**, 405.
11. Z. Qian, J. R. LaRochelle, B. Jiang, W. Lian, R. L. Hard, N. G. Selner, R. Luechapanichkul, A. M. Barrios and D. Pei, *Biochemistry*, 2014, **53**, 4034.
12. X. C. H. Ruan , C. Xie , B. Li , M. Ying , Y. Liu , M. Zhang , X. Zhang , C. Zhan , W. Lu and W. Lu *ACS Appl. Mater. Interfaces*, 2017, **9**, 17745.
13. W. P. Verdurmen, P. H. Bovee-Geurts, P. Wadhvani, A. S. Ulrich, M. Hallbrink, T. H. van Kuppevelt and R. Brock, *Chem. Biol*, 2011, **18**, 1000.
14. D. P. . A. Iñiguez-Lluhí, *Mol. Cell. Biol.*, 2000, **20**, 6040.